

A QUANTITATIVE EXAMINATION OF THE BUOYANT BEHAVIOR
OF MACROMOLECULES OF KNOWN MOLECULAR WEIGHT IN A DENSITY
GRADIENT AT EQUILIBRIUM IN THE ULTRACENTRIFUGE

Thesis by
James Brown Ifft

In Partial Fulfillment of the Requirements
For the Degree of
Doctor of Philosophy

California Institute of Technology
Pasadena, California

1962

ACKNOWLEDGMENTS

I have been fortunate to have had the opportunity to work with Dr. Robert [Name] during my graduate work. I would like to thank him for his interest in my work and for his suggestions and criticisms during my thesis studies. His tremendous reputation for scholarship and research has been a great inspiration to me.

I would like to thank John [Name] for his many helpful and pleasant discussions during our four-year association in these laboratories. My years of graduate study have been greatly enriched by his generosity of his time and talent.

to

Evelyn

I am indebted to the National Institutes of Health for support during the last two years of this research and to the Sloan Foundation for two summer fellowships.

I owe a great deal to my parents whose understanding and love have guided me through the several phases of my life.

I can scarcely express what my wife Evelyn has meant to me through these years of study. Her faith in me has made this thesis possible; her love for me has made these last few years of my life. For this, and for this typing, a humble and grateful husband says thank you.

Acknowledgements

I have been indeed fortunate in working with Dr. Jerome Vinograd throughout my graduate work. I would like to thank him for his interest in this research and for his suggestions and guidance in carrying out these studies. His tremendous enthusiasm for scholarship and research has been a great stimulation to me.

I would like to thank John Hearst for our many stimulating and pleasant discussions during our four-year association in these laboratories. My years of graduate study have been deeply enriched by his generosity of his time and talent.

I am indebted to the National Institutes of Health for support during the last two years of this research and to the Sloan Foundation for two Summer Fellowships.

I owe a great deal to my parents whose understanding and love have guided me through the several phases of my life.

I can scarcely express what my wife Evelyn has meant to me through these years of study. Her faith in me has made this thesis possible; her love for me has made these the happiest years of my life. For this, and for this typing, a humble and grateful husband says thank you.

Abstract

Table of Contents

The quantitative aspects of the method of sedimentation equilibrium in a density gradient with a purified protein of known molecular weight have been examined.

In order to quantitatively evaluate the results of density gradient experiments, the density distribution and the density gradient in the salt solution at equilibrium in the ultracentrifuge must be known. Calculations based on thermodynamic data were made to determine these quantities.

The results of this work are given in Part I.

Because of the large hydrostatic pressures encountered during centrifugation, it was necessary to evaluate the effects of pressure on the results. In Part II, an experimental investigation of the changes in banding position of deoxyribonucleic acid (DNA) and tobacco mosaic virus (TMV) with pressure was made. A useful quantity involving the compressibilities of the solution and of the solvated macromolecule was obtained. The results agree with the thermodynamic theory presented.

An experimental investigation of bovine serum mercaptalbumin (BMA) in a variety of salt solutions was carried out. Part III presents the experimental techniques and the methods of calculation for such experiments. The net hydration of BMA was determined solely from the ultracentrifuge results. The extent of anion binding was independently determined to obtain the net hydration of the protein-salt complex and the density gradient required to calculate the solvated molecular weight.

Table of Contents

Part I - The Determination of Density Distributions and Density Gradients in Binary Solutions at Equilibrium in the Ultracentrifuge	1
Part II - The Effects of Pressure on the Buoyant Behavior of Deoxyribonucleic Acid and Tobacco Mosaic Virus in a Density Gradient at Equilibrium in the Ultracentrifuge	10
Part III - The Behavior of Bovine Serum Mercaptalbumin in a Density Gradient at Equilibrium in the Ultracentrifuge	22
A. <u>The Behavior of BMA in a CsCl Density Gradient</u>	26
1. Experimental	31
a. Materials	31
b. Examination of materials	32
(1) Sedimentation velocity	32
(2) Two component sedimentation equilibrium	32
c. Procedures for density gradient experiments	39
(1) Selection of centerpiece and filling technique	39
Single-sector centerpiece	39
Non-grooved double-sector centerpiece	41
Grooved double-sector centerpiece	42
(2) General run conditions	44
(3) Preparation of solutions	45
(4) Measurement of plates	45
d. Determination of apparent specific volume of bovine serum albumin	50
(1) In water	51
(2) In concentrated CsCl solution	51

2.	Calculations	54
a.	Evaluation of r_0 , ρ_0 , $(d\rho/dr)_{\text{phys},0}$, σ	54
3.	Results and discussion	59
a.	Comparison of different methods of evaluating σ	59
b.	Effect of non-constant gradient on results	64
c.	Table of results and discussion	68
B.	<u>The Behavior of BMA in Various Salt Gradients</u>	70
1.	Experimental	71
a.	Materials	71
b.	Procedures	73
2.	Calculations	77
a.	Evaluation of K for each buoyant solution	77
b.	Derivation of buoyancy density gradient expression	78
c.	Relation between hydration parameters and water activity	81
3.	Results	83
a.	Refractive index versus density relations	83
b.	Tables of results and discussion	84
C.	<u>Determination of Anion Binding of BMA</u>	90
1.	Experimental	92
a.	Materials	92
b.	Procedures	93
2.	Calculations	95
3.	Results and discussion	96

D. <u>Effect of Anion Binding on Results of Density Gradient Experiments</u>	98
1. Net hydration of BMA-salt complex	99
a. Comparison with data from other studies	104
2. Derived buoyant densities	110
3. Effective density gradients	112
4. Solvated and anhydrous molecular weights	118
5. Conclusions	122
E. Appendix	123
1. Effect of non-constant refractive index increment	124
2. Protocol sheet for density gradient experiments	128
3. Effect of neglecting cubic term in original derivation	131
Part I	
F. References	133
The Determination of Density Distributions	
Propositions Density Gradients in Binary Solutions at	137
References for Propositions Ultracentrifuge	169

THE DETERMINATION OF DENSITY DISTRIBUTIONS AND DENSITY GRADIENTS IN BINARY SOLUTIONS AT EQUILIBRIUM IN THE ULTRACENTRIFUGE¹

BY JAMES B. IFFT,² DONALD H. VOET³ AND JEROME VINOGRAD

Gates and Crellin Laboratories of Chemistry,⁴ California Institute of Technology, Pasadena, California

Received December 14, 1960

The calculation of density gradients and density distributions in binary solutions at sedimentation equilibrium in an ultracentrifuge is presented. The differential equation describing sedimentation equilibrium is $\beta(\rho)d\rho = \omega^2 r dr$ where β is a function of the temperature and the activity, molecular weight, and partial specific volume of the solute at a density ρ . Values of β have been calculated from published data for density and activity over the entire concentration range for CsCl, KBr, RbBr, RbCl, LiBr and sucrose at 25.0°. For each binary system $\beta(\rho)$ has been expressed as a cubic polynomial in ρ . The integral form of the above equation was then solved for the integration constants using a digital computer for the first four salts mentioned above. The integration constant is the radial distance at which the initial density of the solution occurs. This is the isoconcentration position. Experimental confirmation of the density gradient and of a density distribution for CsCl are presented.

Introduction

The analysis of results obtained with the recently developed procedures for sedimentation equilibrium of macromolecules in a density gradient in the ultracentrifuge⁵ requires a knowledge of the density and the gradient of density in the liquid column. For a single dilute species, the apparent molecular weight⁶ of the macromolecule is given by the relation

$$M_{app} = \frac{RT\rho_0}{\sigma^2(d\rho/dr)_0\omega^2 r_0} \quad (1)$$

where ρ_0 is the buoyant density of the solvated species of molecular weight, M_{app} , σ is the standard deviation of the Gaussian concentration distribution of the macromolecule, $(d\rho/dr)_0$ is the density gradient at the position r_0 , the center of the Gaussian band, and ω is the angular velocity.

In previous work, the buoyant density has been evaluated by asserting that the isoconcentration distance, r_e , and the corresponding original density, ρ_e , are to be found at the radial center of the liquid column. For bands near the center of the liquid column, to a good approximation

$$\rho_0 = \rho_e + (d\rho/dr)_e \Delta r \quad (2)$$

where Δr is the displacement of the mode from the center of the liquid column.

The density gradient is evaluated by one of two alternative methods.⁷ The optical method makes use of the relation

(1) (a) This investigation was supported in part by Research Grant H-3394 from the National Institutes of Health, U. S. Public Health Service; (b) this work was presented in part before the 33rd National Colloid Symposium, Division of Colloid Chemistry, American Chemical Society, Minneapolis, Minnesota, June 18 to 20, 1959.

(2) U. S. Public Health Service Research Fellow of the National Cancer Institute, 1959-1960; Division of General Medical Sciences, 1960-1961.

(3) Supported for one summer by the National Science Foundation Undergraduate Research Participation Program, N.S.F.-G7954.

(4) Contribution No. 2653.

(5) M. Meselson, F. W. Stahl and J. Vinograd, *Proc. Natl. Acad. Sci.*, **43**, 581 (1957).

(6) R. L. Baldwin, *ibid.*, **45**, 939 (1959).

(7) M. Meselson, Ph.D. Dissertation, California Institute of Technology, 1957.

$$\frac{d\rho}{dr} = \frac{dn}{dr} \times \frac{d\rho}{dn} \quad (3)$$

where dn/dr is the measured refractive index gradient in the schlieren optical system and $d\rho/dn$ is obtained experimentally by refractometry of solutions of known composition. In the physical chemical method, the density gradient is calculated from the relation for sedimentation equilibrium in a two-component system

$$\frac{d\rho}{dr} = \frac{d \ln a}{d \ln a} (1 - \bar{v}\rho) \frac{M\omega^2 r}{RT} \quad (4)$$

where M , a and \bar{v} are the molecular weight, activity and partial specific volume of the solute species.

In this paper a method is presented for evaluating r_e . The method is based upon integrating a form of equation 4, using the conservation condition to obtain the integration constant. As a part of the procedure, it has been necessary to tabulate the values of the $d\rho/dr$ as a function of ρ and to express these as polynomials. The results for a series of solutes in water are first presented. The results of the integrations are given in the latter portion with some experimental confirmation of the results.

Results and Discussion

The Calculation of the Density Gradient.—For any binary solution, equation 4 may be written

$$\beta(\rho) \frac{d\rho}{dr} = \omega^2 r \quad (5)$$

where

$$\beta(\rho) = \frac{d \ln a}{d\rho} \frac{RT}{(1 - \bar{v}\rho)M}$$

The quantity β was evaluated by graphical methods from published data of densities^{8,9} and activity coefficients.¹⁰ The partial specific volume, \bar{v} , was

(8) "International Critical Tables," Vol. 3, McGraw-Hill Book Co., New York, N. Y., 1928.

(9) F. Bates and Associates, "Polarimetry, Saccharimetry and the Sugars," Circular 440, National Bureau of Standards, Washington, D. C., 1942, p. 626.

(10) R. A. Robinson and R. H. Stokes, "Electrolyte Solutions," Butterworths, London, England, 1955.

evaluated by the chord method on a large scale plot of $1/\rho$ vs. Z_2 , the weight fraction of the solute. Thus a graph of \bar{v} vs. ρ was obtained. Activities were calculated from data relating mean ion activity coefficient and molality. Corresponding density data were derived from the almost linear weight fraction vs. density plot. The variation of $d\rho/d \ln a$ with ρ was evaluated graphically by determining tangents to the ρ vs. $\ln a$ curve. The values of $d\rho/d \ln a$ and \bar{v} at corresponding densities were tabulated and $\beta(\rho)$ calculated. The results for CsCl^{10a}, RbBr, RbCl, KBr and sucrose are given in Table I. The data for LiBr are given separately in Fig. 1. These results may be used directly to evaluate the density gradient in a phase of density ρ at equilibrium in the ultracentrifuge.

TABLE I
VARIATION OF $\beta \times 10^{-3}$ WITH SOLUTION DENSITY

ρ	Sucrose	KBr	RbBr	RbCl	CsCl
1.02	8.091				
1.03	6.789				
1.04	5.605				
1.05	4.643		6.729	9.817	
1.06	4.019				
1.075		7.496			
1.08	3.449				
1.10	3.237	6.121	3.643	5.532	
1.12	3.121				
1.125		5.229			
1.14	3.091				
1.15		4.594	2.536	4.109	2.491
1.175		4.151			
1.20		3.848	2.122	3.445	1.984
1.225		3.637			
1.250		3.469	1.772	3.172	1.715
1.275		3.330			
1.30		3.213	1.635	3.083	1.546
1.325		3.112			
1.35			1.528	2.777	1.430
1.40			1.434	2.334	1.346
1.45			1.372		1.286
1.50					1.245
1.55					1.216
1.60					1.197
1.65					1.190
1.70					1.190
1.75					1.199
1.80					1.215
1.85					1.236

In this treatment, the effects of pressure have been neglected. Neglecting these effects is equivalent to stating that the solution is incompressible and that $\beta(\rho)$ is the same at atmospheric pressure and at the pressures in the rotating liquid column. The solution, however, is not incompressible. The compression gradient at density ρ is $K\rho^2\omega^2r$, where K is the compressibility coefficient. At the center of the sectorial cell for CsCl solutions, this compression gradient is of the order of 10% of the density gradient due to salt redistribution. The effects of pressure in density gradient systems are to be presented in a future publication.

(10a) The reciprocals of $\beta(\rho)$ for CsCl have been calculated by R. Trautman, *Arch. Biochem. Biophys.*, **87**, 289 (1960), by a somewhat different procedure. The data for CsCl in Table I have been compared with Trautman's data and differ by less than 1%.

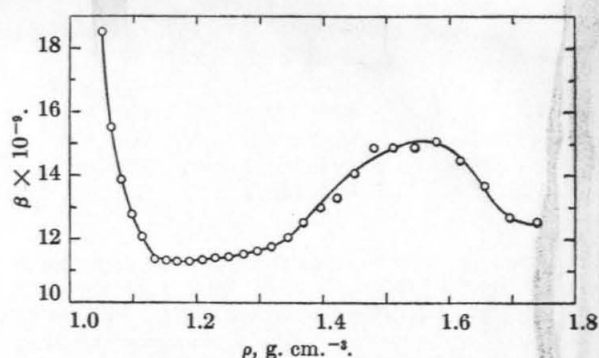


Fig. 1.—Variation of β with solution density, LiBr.

The latter statement regarding the effect of pressure on $\beta(\rho)$ appears to be valid, as is demonstrated in the experimental section, at the center of a 1.287 g. cm.⁻³ CsCl solution (2.57 molal) in a sector cell at 56,100 r.p.m. The density gradient calculated from equation 5 agrees with the gradient determined by schlieren optical methods to within 0.7%. In this experiment, the density gradient due to the redistribution of CsCl and H₂O at equilibrium is evaluated by subtracting the schlieren elevation photographed just after reaching full speed from the elevation obtained at equilibrium. This procedure substantially eliminates the effects of pressure on the liquid, the cell windows and the centerpiece.

The density distributions in CsCl and RbBr solutions and in KBr and RbCl solutions should be similar in the density region, 1.15 to 1.30. In addition, the former two salts produce higher density gradients than the latter two in their common density regions.

The Construction of the Polynomials $\beta(\rho)$.—In order to use the tabulated values of $\beta(\rho)$ most effectively, a polynomial $\text{ave}(y_i) = \sum_{j=0}^k a_j \xi_j^i$ was fitted to each set of data by the method of least squares. The polynomials were constructed by orthogonalizing the linearly independent functions $1, x, x^2, \dots, x^k$ by the Gram-Schmidt orthogonalization procedure. This method of curve fitting is described in Bennett and Franklin.¹¹ Tables of the numerical values of the ξ 's are given by Fisher and Yates.¹² Thus, polynomials of the form

$$\beta(\rho) = \beta_0 + \beta_1\rho + \beta_2\rho^2 + \dots + \beta_k\rho^k \quad (6)$$

were obtained for the solutes previously mentioned. The values of the first four β coefficients are given in Table II.

The accuracy with which the polynomial $\beta(\rho)$ gives the curve represented by the original β vs. ρ data depends upon k , the degree of the polynomial and upon n , the number of points used to calculate the polynomial. In this work, third degree polynomials were used. In the case of CsCl, a fifth degree polynomial reduced the maximum deviation of the β values calculated from the polynomial equation from the β values originally derived from

(11) C. A. Bennett and N. L. Franklin, "Statistical Analysis in Chemistry and the Chemical Industry," John Wiley and Sons, New York, N. Y., 1954, pp. 255-264.

(12) R. A. Fisher and F. Yates, "Statistical Tables," Oliver and Boyd, London, 1957, pp. 90-100.

TABLE II

Salt	Density range	POLYNOMIAL COEFFICIENTS ^a			
		$\beta_0 \times 10^{-9}$	$\beta_1 \times 10^{-9}$	$\beta_2 \times 10^{-9}$	$\beta_3 \times 10^{-9}$
CsCl	1.15 -1.85	47.9726	-85.3724	51.7764	-10.4312
RbBr	1.05 -1.45	620.9619	-1,416.8024	1,079.2080	-273.7280
RbCl	1.05 -1.40	1,222.1450	-2,878.2225	2,264.0729	-593.3408
KBr	1.075-1.325	966.7593	-2,280.4334	1,802.8082	-475.9704
Sucrose	1.02 -1.14	860.6168	-2,320.1077	2,085.6993	-625.0000

^a See text for polynomial equation.

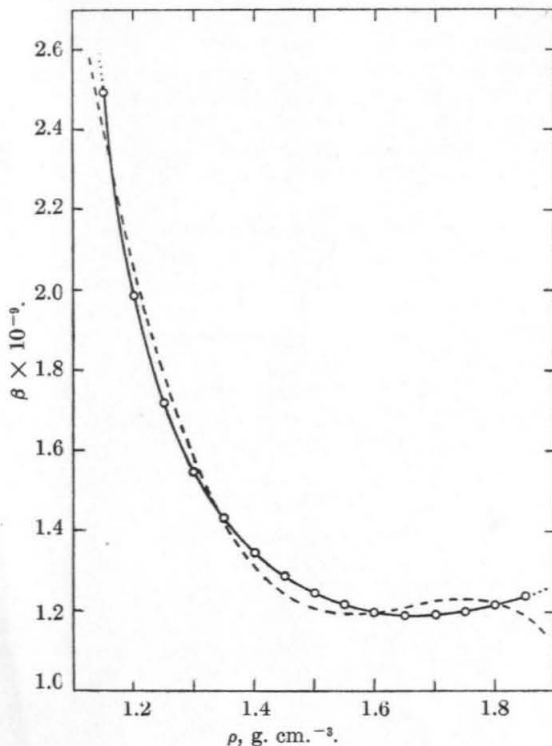


Fig. 2.—Comparison of polynomial $\beta(\rho)$ curve and original $\beta(\rho)$ curve, CsCl. Solid line, original $\beta(\rho)$ curve; dashed line, polynomial $\beta(\rho)$ curve.

activity and density data from 3% in β to 1%. The third degree polynomial was adequate to give the values of the isoconcentration points, r_e , to within 0.1%, except for RbBr. The value of n used depended on the shape of the $\beta(\rho)$ curve and varied from 15 to 21.

The maximum deviation of the β values calculated from the third degree polynomial from the corresponding original β values was $\pm 1\%$ for KBr, $\pm 3\%$ for CsCl and sucrose, $\pm 6\%$ for RbCl, and $\pm 12\%$ for RbBr. The agreement between the derived relations and the original data is illustrated in Fig. 2 for CsCl.

Integration of the Polynomial Expansion of the Sedimentation Equilibrium Equation.—Equation 5 represented as a third degree polynomial may be integrated to give a fourth degree polynomial.

$$\alpha_4(\rho^4 - \rho_e^4) + \alpha_3(\rho^3 - \rho_e^3) + \alpha_2(\rho^2 - \rho_e^2) + \alpha_1(\rho - \rho_e) + \omega^2(r_e^2 - r^2)/2 = 0 \quad (7)$$

where the α 's are constants. The integration constant, r_e , was evaluated using the outside condition of conservation of mass of the solute

$$c_e = \frac{\int_0^V c \, dv}{V} \quad (8)$$

where c is the concentration at $v(r)$, c_e the initial concentration, and V is the total liquid volume in the cell. Since these concentrations are in units of mass/volume

$$c = Z_2 \rho \quad (9)$$

Examination of the relation between Z_2 and $1/\rho$ shows that these quantities are linearly related over the maximum density increments of 0.1 to 0.2 g. cm.⁻³ encountered in a gradient column. Combining this linear relation

$$Z_2 = k_1(1/\rho) + k_2 \quad (10)$$

where k_1 and k_2 are constants, with equation 9 and with the conservation relation 8, we obtain

$$\rho_e = \frac{\int_0^V \rho \, dv}{V} \quad (11)$$

For sector and cylindrical cells, equation 11 takes the forms

$$\rho_e = \frac{2 \int_{r_a}^{r_b} \rho r \, dr}{(r_b^2 - r_a^2)} \quad (11a)$$

and

$$\rho_e = \frac{\int_{r_a}^{r_b} \rho \, dr}{(r_b - r_a)} \quad (11b)$$

respectively, where r_a and r_b are the radii at the top and bottom of the cell.

The solution of equation 7 incorporating the conservation conditions 11a or 11b was performed with a Burroughs 205 digital computer. Input data for the computer are the constants α_1 , α_2 , α_3 , α_4 , ρ_e , ω , r_a , r_b , n , the number of evenly spaced intervals in the liquid column, either 4 or 6, and $R_e(1)$ and $R_e(2)$, two bracketing estimates for r_e .

Equation 7 rewritten for a specific ρ_i and r_i is

$$\alpha_4 \rho_i^4 + \alpha_3 \rho_i^3 + \alpha_2 \rho_i^2 + \alpha_1 \rho_i = \frac{\omega^2}{2} (r_i^2 - r_e^2) + \alpha_4 \rho_e^4 + \alpha_3 \rho_e^3 + \alpha_2 \rho_e^2 + \alpha_1 \rho_e = -\alpha_0$$

The constant, α_0 , is computed using $R_e(1)$ and one of the values of r_i . Then the quartic polynomial is solved for the corresponding ρ_i . Each of the $n + 1$ points (r_i , ρ_i) is computed similarly and Simpson's rule used to compute the integral $I_1 = \int \rho r \, dr$, in the case of the sector. The procedure is repeated for $R_e(2)$. A linear interpolation is used to find $R_e(3)$. I_3 is calculated and compared with $I_0 = \rho_e(r_b^2 - r_a^2)/2$. The procedure is continued with parabolic interpolations until satisfactory agreement is reached between I_m and I_0 , whereupon the last set of values of ρ_i and r_i and the final value of r_e are printed out.

The program was operated for aqueous solutions

of CsCl, RbCl, RbBr and KBr for both sector cells and cylindrical cells containing 2, 3 and 5 ml. of solution over a range of solution densities and for several angular velocities. The limiting radii were chosen to correspond to a 0.70-ml. liquid volume in a 12-mm. 4° sector in the analytical ultracentrifuge or to the above volumes in 5 ml. plastic tubes in the SW-39 swinging bucket rotor in the preparative ultracentrifuge.

Representative density distribution data are given as follows: Fig. 3 presents the data for CsCl in cylinders of varying length and initial density. The distributions are as expected in that they become more linear as the cell lengths decrease and they are steeper for the higher ρ_e 's reflecting the higher gradients. The maximum density difference which can be obtained for CsCl is seen to be about 0.4 g. cm. $^{-3}$.

Figure 4 gives the distributions for the four salts in 3-ml. cylinders at varying angular velocities. The slope of the curves increases with increasing velocity as required by the density gradient expression. The isoconcentration point is not invariant with changes in ω as is suggested by the small scale plots, Fig. 4, but varies as shown in Figs. 6 and 7.

The numerical values for the CsCl density distribution in sectors are given in Table III.

TABLE III
DENSITY DISTRIBUTIONS
Cs Cl Sector

ρ_e	ω , r.p.m.	Density at				
		$r_a = 6.0$	$r = 6.3$	$r = 6.6$	$r = 6.9$	$r_b = 7.2$
1.2	56,100	1.137	1.164	1.195	1.231	1.273
1.3	56,100	1.217	1.252	1.293	1.340	1.394
1.45	56,100	1.343	1.390	1.443	1.502	1.564
1.6	56,100	1.484	1.538	1.595	1.654	1.715
1.7	56,100	1.585	1.639	1.695	1.753	1.814
1.2	44,770	1.160	1.177	1.197	1.219	1.244
1.45	44,770	1.382	1.413	1.446	1.482	1.521
1.7	44,770	1.629	1.662	1.697	1.733	1.771
1.7	33,450	1.660	1.679	1.698	1.719	1.740

The remainder of the density data can be calculated from the isoconcentration point data given below. This data provides ρ_e and r_e in equation 7 which can then be solved for the density distribution noting that $\alpha_n = \beta_{n-1}/n$. Also, a stepwise integration can be performed using the isoconcentration point and $\beta(\rho)$ data. Alternatively, approximate density distributions for intermediate values of the parameters can be evaluated by interpolation.

The order of magnitude of the errors in the above distributions can be evaluated by considering the areas between the polynomial and actual $\beta(\rho)$ curves. To a good approximation, the point ρ_e, r_e is the same for both the polynomial calculation and for the actual distribution. This will be demonstrated in a later section. We then can use equation 5 to estimate the deviations at other points in the distribution.

The area under the polynomial curve between ρ_e and ρ is equal to $\int_{\rho_e}^{\rho} \beta(\rho)_p d\rho$. A similar integral can be written for the area under the real curve.

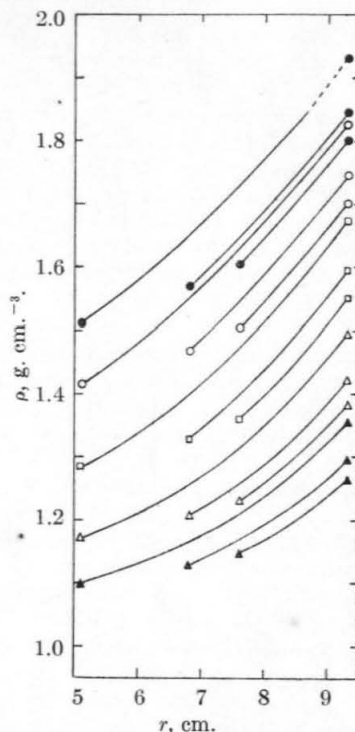


Fig. 3.—Density distributions in cylinders: CsCl; 39,000 r.p.m. ●, $\rho_e = 1.7$; ○, $\rho_e = 1.6$; □, $\rho_e = 1.45$; △, $\rho_e = 1.3$; ▲, $\rho_e = 1.2$.

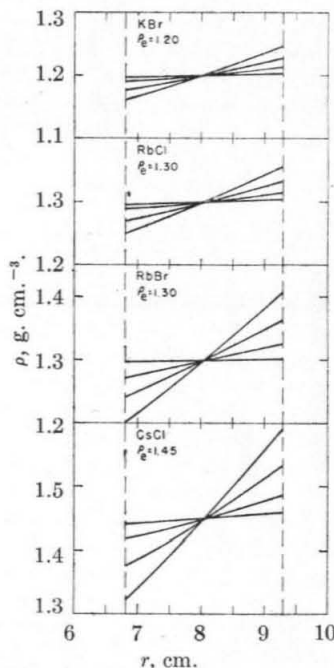


Fig. 4.—Density distributions for four salts in 3 ml. cylinders at varying speeds. In the order of increasing slope, the curves are for 10,000, 20,000, 30,000 and 39,000 r.p.m.

The area between the two curves from ρ_e to ρ is given by

$$\int_{\rho_e}^{\rho} \beta(\rho)_p d\rho - \int_{\rho_e}^{\rho} \beta(\rho)_r d\rho = \frac{\omega^2}{2} (r_p^2 - r_r^2)$$

From a measurement of this area, the real value of r at ρ, r_r , can be calculated. The value for ρ as given by the polynomial is obtained from the

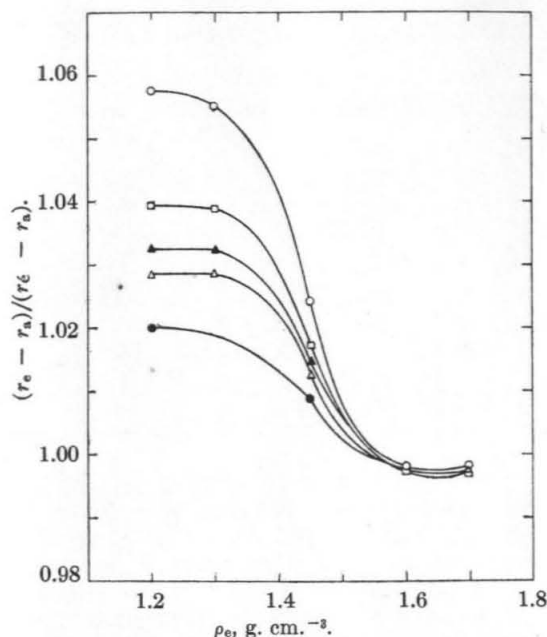


Fig. 5.—Variation of normalized isoconcentration point with original solution density, CsCl: O, 5-ml. cylinder, 39,000 r.p.m.; □, 3-ml. cylinder, 39,000 r.p.m.; △, 2-ml. cylinder, 39,000 r.p.m.; ▲, sector, 56,100 r.p.m.; ●, sector, 44,770 r.p.m.

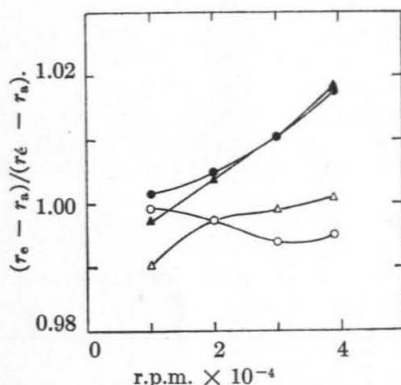


Fig. 6.—Variation of normalized isoconcentration point with angular velocity, 3-ml. cylinders. ●, CsCl, $\rho_e = 1.45$; ○, RbBr, $\rho_e = 1.3$; ▲, KBr, $\rho_e = 1.2$; △, RbCl, $\rho_e = 1.3$.

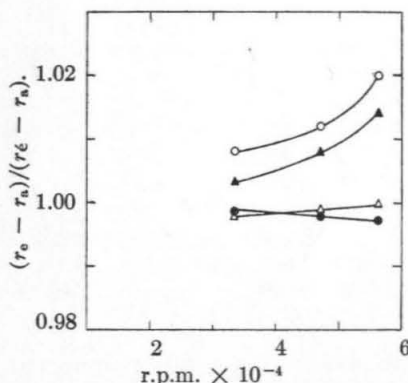


Fig. 7.—Variation of normalized isoconcentration point with angular velocity, sectors: ●, CsCl, $\rho_e = 1.7$; ○, RbBr, $\rho_e = 1.3$; ▲, KBr, $\rho_e = 1.3$; △, RbCl, $\rho_e = 1.3$.

density distribution plots. For the case of CsCl of $\rho_e = 1.7$ and 56,100 r.p.m. in a sector integration from r_e to the cell bottom showed that the

difference in r for which both distributions had a density of 1.81 was 0.012 cm. This corresponds to a density difference of 0.002 g. cm.⁻³ The differences in ρ are successively less as the distances from r_e decrease. The density differences between the real and computer distributions will be approximately the same in the cylindrical cases since the area in the example discussed was nearly maximal. Also the values of r in the cylindrical case are larger and hence, for a given area between the curves, the difference in r_p and r_r will be smaller. Thus the maximum deviation which can be attached to each of the densities in the CsCl distributions reported is 0.002 g. cm.⁻³. Inspection of the areas between the curves for the other salts indicates that the maximum deviations in density for KBr will be smaller than 0.002 g. cm.⁻³ and for RbCl and RbBr will be less than the accuracy with which Fig. 4 can be read.

To be of greatest use, the isoconcentration points obtained in the above program were normalized in two ways. Since the actual values obtained for r_e depend on the r_a and r_b used in the program, they were first normalized by dividing the difference between r_e and r_a by the length of the liquid column to yield $(r_e - r_a)/(r_b - r_a)$. The isoconcentration positions were further normalized by dividing this fraction by another fraction, $(r_e' - r_a)/(r_b - r_a)$, where r_e' is a limiting value for r_e , to give $(r_e - r_a)/(r_e' - r_a)$.

Under the assumption that $\beta(\rho)$ is constant, the integrated form of equation 5 and the conservation equations 11 may be combined to give values for the limiting isoconcentration points in sectors, equation 12a, and in cylinders 12b

$$r_e' = \sqrt{\frac{r_b^2 + r_a^2}{2}} \quad (12a)$$

$$r_e' = \sqrt{\frac{r_b^2 + r_a r_b + r_a^2}{3}} \quad (12b)$$

Equation 12a was derived earlier by Rinde¹³ under the assumption that $M(1 - \bar{v}\rho)\omega^2(r_b^2 - r_a^2)/2RT \ll 1$. We will now expect that the actual values of r_e in a real situation will converge on r_e' when β approaches a constant value. This is the case, for example, for CsCl solutions in the density range 1.65 to 1.75 g. cm.⁻³. Within this range are the buoyant densities for cesium deoxyribonucleates. For any system, of course, the change in β from the top to the bottom of the liquid column becomes smaller as the angular velocity or the length of the liquid column is decreased.

The normalized isoconcentration points are presented in Figs. 5-7 and in Table IV. In the density range 1.6-1.7, the β curve for CsCl, Fig. 2, goes through a broad minimum. Thus it would be expected that the value of the normalized isoconcentration point should approach 1.000 in this region which it does as shown in Fig. 5. Also to be noted is the increasing divergence of r_e from r_e' as either the cell length or the angular velocity increases. As previously discussed, this is to be expected since either variation reduces the constancy of β . In Figs. 6 and 7, it is seen that r_e does vary slightly with angular velocity and, as

expected, tends toward r_e' as ω is reduced to zero.

TABLE IV
NORMALIZED ISOCONCENTRATION POINTS

	ω , r.p.m.	Volume, ml.	ρ_e	RbBr	RbCl	KBr
A. Sectors	56,100	0.7	1.1	1.049	1.033	1.025
	56,100	0.7	1.2	1.036	1.016	1.015
	44,770	0.7	1.1	1.032	1.021	1.016
	44,770	0.7	1.2	1.024	...	1.009
B. Cylinders	39,000	5	1.1	1.093	1.059	1.044
	39,000	5	1.2	1.084	1.027	1.026
	39,000	5	1.3	...	1.006	...
	39,000	3	1.1	1.063	1.040	1.030
	39,000	3	1.2	1.064	1.019	1.018
	39,000	3	1.3	0.995	1.001	1.018

The graphs may be viewed as describing the errors which arise when the readily available limiting values of r_e are employed. The error in r_e , if r_e' is used, is given adequately by the approximate expression, $(r_e - r_e')/r_e = \delta \cdot (r_b - r_a)/(r_b + r_a)$ where δ is the variation from 1.000 in the $(r_e - r_a)/(r_e' - r_a)$ plot. The error in ρ_0 encountered on using r_e' for r_e may be found approximately by multiplying $\delta \cdot (r_b - r_a)/2$ by the density gradient. In general, ρ_0 is desired to within 0.001 g. cm.⁻³, which in the case of a 0.15 g. cm.⁻⁴ gradient corresponds to specifying the band position to 67 μ . Under these conditions, r_e' may be used in place of r_e for any sector run in CsCl where $\delta < 0.011$ or equivalently, for $\rho_e > 1.5$. The maximum δ allowable, if the same accuracy in determining ρ_0 is to be achieved in cylinders, decreases with increasing length to a value of 0.003 for a 5-ml. CsCl cylinder.

Generally, the practice to date has been to use the radial center of the cell for r_e . For CsCl of $\rho_e = 1.7$ in a 12 mm. cell where $r_m = (r_b + r_a)/2 = 6.60$, multiplication of $d\rho/dr$ at r_e by $(r_e - r_m)$ yields the following errors in computing ρ_0 : 0.005 at 56,100 r.p.m., 0.003 at 44,770 r.p.m., and 0.002 at 33,450 r.p.m. Thus depending on the conditions of the experiment, rather serious errors may occur in determining ρ_0 if the center of the cell is used for r_e .

Comparison of Figs. 2 and 5 indicates that there is a close correlation between the slope of the $\beta(\rho)$ curve and the value of r_e obtained. It was further noted that a straight line represents the $\beta(\rho)$ curve better than the polynomial over short regions of the curve pertinent to an experiment. Thus an expression for r_e in closed form was sought by solving equation 5 in linear form using the conservation condition, equation 11, as before.

Using $\beta = \beta_0 + \beta_1\rho$, equation 5 was integrated and solved for $(\rho - \rho_e)$. This variable was substituted into $\int_{r_a}^{r_b} (\rho - \rho_e)r dr = 0$, which is another form of the conservation equation 11a for sectors. This equation was integrated to give an expression for r_e using two approximations. The first involved a good expansion in powers of $(r_e')^2 - (r_e)^2$. The second expansion is accurate to within $\pm 1\%$ in $(r_e')^2 - (r_e)^2$ if $D = \beta_1\omega^2/\beta^2$ is less than 0.05, which is the case for the maximum centrifuge velocities attainable except for the lowest density regions of

each salt. The expression obtained is

$$(r_e')^2 - (r_e)^2 = D(r_b^2 - r_a^2)/48 \quad (13)$$

Using this equation, values of r_e were computed for three points on each of the $\beta(\rho)$ curves. These points in general corresponded to portions of the curves where either the slope of the polynomial had a different sign than the actual curve, the deviation between the curves was a maximum, or the slopes were large. In all cases examined, the use of the slope of the tangent to the polynomial curve yielded values within 0.004 cm. of the computer value. This demonstrates not only the validity of this equation but also the fact that a tangential line yields satisfactory values compared with the computer value which is the exact solution for the polynomial curve. This is important because, under the restriction noted, the isoconcentration points can be obtained by the tangent method given above and thus without recourse to a computer. The same results were obtained through the use of the straight line through the points corresponding to the densities at the cell ends as given by the computer.

Typical values for r_e were calculated for each of the salts using the tangents to the actual β curve. In all cases, except under conditions where the expansion is poor, the agreement of this value with the computer r_e for CsCl, RbCl and KBr was within 0.005 cm. This corresponds, for a large gradient, to the acceptable error of 0.001 d.u. The numbers for RbBr differ by as much as 0.016 cm. This is due primarily to the large error noted previously in the polynomial fit. The isoconcentration points for RbBr given in Figs. 6 and 7 and Table IV were obtained by the use of equation 13.

An expression for r_e in closed form in the cylindrical case using a linear β equation as above could not be obtained. Thus, all of the isoconcentration point data for cylinders are those obtained by the computer. By analogy, we assume that the values for RbCl, CsCl and KBr are accurate; the RbBr data probably are good only on the average to 0.01 cm.

The Resolving Power of the Density Gradient Method for Macromolecules of Different Buoyant Densities.—With the availability of information regarding the density gradient formation for various salt solutions, it is of interest to consider the effect of the selection of the salt on the resolution obtainable between substances separated in the gradient column.

We will define resolution, Λ , for two homogeneous macromolecular species in a density gradient as

$$\Lambda = \frac{\Delta r}{(\sigma_1 + \sigma_2)} \quad (14)$$

the distance between the modes, Δr , divided by the sum of the standard deviations of the bands. For small distances, equation 5 is $\Delta r = \Delta\rho(\beta/\omega^2 r)$. Substituting this expression and equation 1 for σ into equation 14 under the simplifying assumptions of a constant density gradient and $\Delta\rho \ll \rho_0$ and $\Delta r \ll r_0$, the resolution equation becomes

$$\Lambda = \Delta\rho \left(\frac{1}{RT} \right)^{1/2} \left[\frac{(M_1 M_2)^{1/2}}{(M_1)^{1/2} + (M_2)^{1/2}} \right] \left(\frac{\beta}{\rho} \right)^{1/2} \quad (15a)$$

where $\Delta\rho$ is the difference in buoyant densities

of the macromolecular solutes of molecular weights M_1 and M_2 and both β and ρ are evaluated at the mean banding position \bar{r}_0 . For two solutes of nearly the same molecular weight M , but different buoyant densities, the resolution equation becomes

$$\Lambda = \frac{\Delta\rho}{2} \left[\left(\frac{M}{RT} \right)^{1/2} \right] \left(\frac{\beta}{\rho} \right)_{\bar{r}_0}^{1/2} \quad (15b)$$

This equation is further simplified by recalling that β , cf. equation 5, is proportional to RT . Introducing $\beta' = \beta/RT$, equation 15b can be written

$$\Lambda = \frac{\Delta\rho}{2} \left(\frac{M\beta'}{\rho} \right)^{1/2} \quad (15c)$$

Thus Λ does not depend as strongly on temperature as is indicated in equations 15a and 15b. It is independent of T except for the small effects of temperature on the activity coefficients.

For a given pair of macromolecules in a given salt gradient, the resolution is independent of angular acceleration. This is to be expected since both Δr , for a given $\Delta\rho$, and σ are proportional to $(\omega^2 r)^{-1}$. As the bands become narrower, they approach each other. Resolution is therefore not affected by changes in velocity.

On the other hand, resolution is improved by carrying out experiments in solvents having the largest β values. For the aqueous salt solutions previously discussed, these are the solutions containing salts of low molecular weights. At a density of 1.3, potassium bromide and rubidium chloride solutions resolve better than cesium chloride solutions by factors of 1.45 and 1.41, respectively, even though the gradients achieved at a particular angular velocity are smaller.

A value of $\Lambda = 1$ will lead to such overlap that only one maximum will be evident in the concentration profile. At $\Lambda = 2$, concentration profiles will intersect such that 5% of the material will be intermixed. At $\Lambda = 3$, almost complete separation is achieved.

Alternately, the resolution can be measured by the elevation midway between the modes. On a plot normalized by dividing c by c_0 , this elevation is given by $y = 2e^{-\Lambda^2/2}$ if the initial concentrations and σ 's are identical. If the initial concentrations are unequal, both the degree of mixing and the elevation y will be increased.

An experimental test of the resolution equation has been afforded in the experiments of Meselson and Stahl.¹⁴ They observed a density separation of 0.014 density unit for the DNA's containing ¹⁴N and ¹⁵N isotopes. Using their molecular weight and buoyant densities to calculate Δr and the standard deviations, a Λ of 3.6 is obtained. Substitution in equation 15b yields the same density separation as observed indicating the internal consistency of the resolution equation. The elevation of the trough between the concentration distributions presented in this paper appears to be considerably higher than would be the case for two Gaussian distributions having a $\Lambda = 3.6$. This is due in part to the unequal initial concentrations and possibly due to not having reached equilibrium or to the presence of a small amount of impurity.

(14) M. Meselson and F. W. Stahl, *Proc. Natl. Acad. Sci.*, **44**, 671 (1958).

For proteins of $M = 10^5$ and $\rho = 1.3$, $\Lambda = 35 \Delta\rho$ for CsCl solutions and $50 \Delta\rho$ for KBr solutions. Therefore to obtain a resolution of 2, $\Delta\rho$ must be 0.058 and 0.040 in CsCl and KBr, respectively. Thus appropriate macromolecules in the size range of proteins may be segregated in a single density gradient column. Such a segregation recently has been reported by Bock.¹⁵ for β -galactosidase and ¹⁵N,D- β -galactosidase.

Experimental

Preparation of Solutions.—The CsCl solutions were prepared from CsCl obtained from the Maywood Chemical Co., Maywood, N. J. Solution densities were determined with a Zeiss refractometer utilizing the linear relation¹⁶ between ρ and n , $\rho^{25.0} = 10.8601n^{25.0D} - 13.4974$. The N-43 fluorochemical was supplied by the Minnesota Mining and Manufacturing Co., Fluorochemical Department.

A. Measurement of $d\rho/dr$.—A CsCl solution of $\rho_e = 1.287$ was centrifuged to equilibrium at 56,100 r.p.m. in a Spinco Model E analytical ultracentrifuge and schlieren photographs made.

The density gradient was determined experimentally from equation 3. The refractive index gradient was measured from the relation $dn/dr = y \tan \theta / LTm$ where y is the vertical distance on the schlieren curve between the baseline, photographed immediately at velocity, and the equilibrium curve, θ is the diaphragm angle, L the optical lever arm, T the cell thickness, and m the cylindrical lens magnification. The value of dn/dr was determined at the isoconcentration point and, after correction for dispersion,¹⁷ found to be 0.0136. Multiplication by the slope of the ρ vs. n relation given above yields $d\rho/dr = 0.147$. The value for the gradient derived theoretically from the β curve is 0.146. The 0.7% discrepancy can be accounted for in the uncertainties both in the experimental parameters and in the accuracy of β .

B. Measurement of the Density Distribution in a CsCl Solution in a Preparative Centrifuge Cell.—Fluorocarbon (0.33 ml.) was used to place the false bottom 0.5 cm. from the bottom of the plastic cell. Two ml. of CsCl solution of $\rho_e = 1.700$ was added, and then a layer of mineral oil to prevent evaporation and cell collapse. The SW-39 rotor then was spun 24 hr. to equilibrium at 39,000 r.p.m. in a Spinco Model L preparative centrifuge. After braking to a halt, the cell was immediately sampled dropwise into previously weighed vials. This was done by making a small hole in the bottom of the tube with a pin and controlling the drop rate with a syringe attached to the tube. The vials then were reweighed and the refractive index of each sample measured.

From these data, calculations yielded a plot of ρ vs. r which is presented in Fig. 8 together with the theoretical distribution. The experimental curve, representative of a number of such runs, differs significantly from the theoretical distribution. Identical runs made with no braking and runs of 48 hr. yielded similar results, indicating that these differences were not due to rapid braking or failure to attain equilibrium.

The small but consistent elevation of the experimental curve suggests that some evaporation occurred during sampling and analysis. The significant departure of the curve at the ends of the cell could be due to back diffusion, which therefore was further investigated.

(15) Private communication from R. M. Bock.

(16) This relationship is the least squares line through data abstracted from "International Critical Tables" and confirming data obtained in this Laboratory.

(17) The schlieren photographs were made with light from an AH-6 mercury lamp filtered through an Eastman number 16 wratten filter and registered on Eastman metallographic plates. The effective wave length in these photographs is a pressure-broadened 5460 Å. Hg line. Since $(dn/dr) = (dn/dc)(dc/dr)$, the dispersion factor desired is $(dn/dr)_{5460} / (dn/dr)_{5460} = (dn/dc)_{5460} / (dn/dc)_{5460}$. Data for the calculation of the latter ratio are given by A. Heydweiller, *Physik. Z.*, **26**, 526 (1925). Several reasonable interpolations lead to a value of 0.990 for the dispersion factor for solutions of CsCl in the range 2 to 4 molar. The measured elevation is multiplied by the dispersion factor to give $(dn/dr)_{5460}$.

C. Measurement of the Rate of Back Diffusion.—An analytical centrifuge cell was filled with CsCl of $\rho_0 = 1.700$ and the cell brought to 39,460 r.p.m. at maximum acceleration. Using a pulse counter as a guide, baseline photographs were obtained at 9,945 r.p.m. and just at full speed. After equilibrium was achieved, as determined by a series of schlieren patterns, the angular velocity was reduced to 9,945 r.p.m. in 6 minutes. Schlieren photographs then were made at suitable intervals to determine the rate of back diffusion.

At various radii, the distances y_i between the curves and their corresponding baselines were measured on enlarged tracings of the photographic plates. The resulting plots were integrated numerically using the meniscus as the origin. The integrals evaluated up to two points, r_1 and r_2 , 0.26 and 0.56 mm. from the top and bottom of the liquid column, respectively, were combined with the densities at these positions, as determined from the computer data, to give the following relation between ρ and the summations

$$\rho_r = \alpha \left(\sum_{r_a}^r y_i - \sum_{r_a}^{r_2} y_i \right) + \rho_{r_2}$$

where

$$\alpha = \frac{\rho_{r_1} - \rho_{r_2}}{\left(\sum_{r_a}^{r_1} y_i - \sum_{r_a}^{r_2} y_i \right)}$$

It is thus unnecessary to know either $d\rho/dn$ or the machine constant in the relation between the measured elevations and the refractive index gradient. Only the exptl. distribution curve at 39,460 r.p.m. is shown in Fig. 9 since it agrees so closely with the computer distribution. The distributions are superimposed at the cell ends as required by this treatment. The exptl. distribution deviates slightly downward in the central region to a maximum difference of $0.0005 \text{ g. cm.}^{-3}$.

The schlieren data obtained after reduction of speed were converted to density distributions by essentially the procedure described above with the additional assumption that the position of the isoconcentration point did not change in the expt. This assumption is justified as indicated in Fig. 7. The value of r_0 changes only very slightly if the curve is extrapolated to an ordinate of 1.000 at zero speed.

As is to be expected, the first effect observed on lowering the speed is the Archibald effect. That is, the concentration profile remains approximately the same throughout the center portion of the liquid column but changes very abruptly at the ends. Thus even at 12 min. after reduction of speed, there are significant deviations at the top and the bottom about 2 mm. in from the ends, but no deviation in the middle portion. At 29 min., there are deviations of 0.015 and 0.021 g. cm.^{-3} at the top and bottom of the cell, respectively. The deviations from the theoretical curve noted on sampling a 1.7 cm. preparative cell at 30 min. after braking are correspondingly 0.034 and 0.023 g. cm.^{-3} . The deviations at the bottom are expected to be in closer agreement since the sampling procedure examines this portion of the liquid column first. The deviations in the preparative cell are necessarily larger since the cell is longer and also since the analytical centrifuge expt. could not be performed at rest. We conclude that the major portion of the deviations noted at the ends of the liquid column in the preparative run is due to back diffusion.

NOTE ADDED IN PROOF:—In subsequent publications (Hearst and Vinograd and Hearst, Ifft and Vinograd, *Proc. Natl. Acad. Sci.*, July (1961)), it is shown that the effective density gradient which must be used in dealing with buoyant

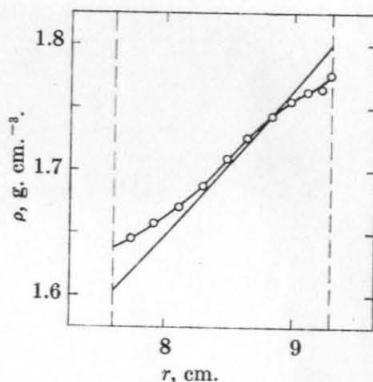


Fig. 8.—Density distributions in the preparative centrifuge; 2 ml. cylinder; CsCl; 39,000 r.p.m.; solid line, theoretical distribution; O, exptl. distribution.

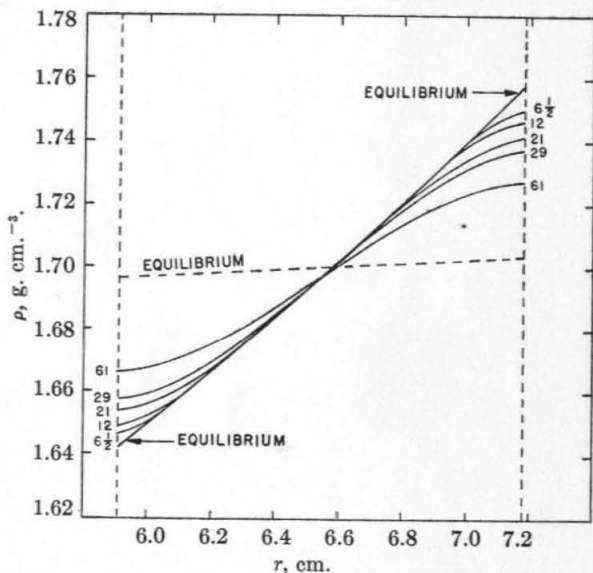


Fig. 9.—Exptl. density distributions in the analytical ultracentrifuge at equilibrium at 39,460 r.p.m. and after reducing velocity to 9945 r.p.m.: dashed line, theoretical distribution at 9945.

macromolecules, is the sum of the composition density gradient and density gradient terms associated with the effects of pressure and solvation. In this paper, the term density gradient is used to describe only the composition gradient. The density gradient employed in equations 1 and 15 should properly be the effective density gradient.

Acknowledgment.—The authors wish to thank Mr. Eugene Robkin and Prof. Matthew Meselson for their contributions in the early stages of this work; and Mr. John E. Hearst for many helpful and illuminating discussions. We also wish to thank Mr. Arthur Robinson who calculated the LiBr data.

Part II

The Effects of Pressure on the Buoyant Behavior
of Deoxyribonucleic Acid and Tobacco Mosaic Virus in a
Density Gradient at Equilibrium in the Ultracentrifuge

THE EFFECTS OF PRESSURE ON THE BUOYANT BEHAVIOR OF
DEOXYRIBONUCLEIC ACID AND TOBACCO MOSAIC VIRUS IN A
DENSITY GRADIENT AT EQUILIBRIUM IN THE ULTRACENTRIFUGE*

BY JOHN E. HEARST,† JAMES B. IFFT,‡ AND JEROME VINOGRAD

GATES AND CRELLIN LABORATORIES OF CHEMISTRY** AND NORMAN W. CHURCH LABORATORY OF
CHEMICAL BIOLOGY, CALIFORNIA INSTITUTE OF TECHNOLOGY

Communicated by Linus Pauling, May 29, 1961

In the original analysis¹ of the behavior of macromolecules and viruses in a buoyant density gradient at equilibrium in the ultracentrifuge, all components were assumed to be incompressible. As a few hundred atmospheres are normally generated in the liquid, it is to be expected that previous results based on the assumption of incompressibility require re-examination.

Several consequences arise on consideration of previously ignored pressure-dependent terms. It is shown below that these may be separately considered.

- (a) There is a redistribution of solute with respect to solvent in the binary medium.
- (b) The solution is compressed with no change in molality in each of the thin layers perpendicular to the centrifugal field in the liquid column. This compression adds a *compression density gradient* to the *composition density gradient*.
- (c) The banding macromolecular species is compressed and moves to a new neutrally buoyant solution. A change in band shape occurs.

It is shown in the analysis below that changes in salt molality in response to pressure are small and may be neglected. The combined effects of compressing the solution and the macromolecular species are significant and affect the band shape, band position, and buoyant density.

Theory.—Although the effects of pressure in two- and multicomponent sedimentation equilibrium experiments²⁻⁴ have been considered by previous workers, the problem is examined here with special reference to the formation of the density gradient and the behavior of neutrally buoyant macromolecules. For a two-component system at equilibrium in a centrifugal field at constant temperature, the thermodynamic relation,

$$M_2(1 - \bar{v}_{2,P}\rho)\omega^2 r dr = \left(\frac{\partial\mu_2}{\partial m_2}\right)_P dm_2, \quad (1)$$

is valid.⁵ This expression remains valid for free solute⁶ in the three-component system at low polymer concentration. In equation (1), M_2 is the molecular weight, $\bar{v}_{2,P}$ the anhydrous partial specific volume, $\mu_2(P, m_2)$ the chemical potential, and m_2 the molality of the solute. The density of the solution, the radial distance, and the angular velocity are $\rho(P, m_2)$, r , and ω , respectively. In equation (1) \bar{v}_2 , $(\partial\mu_2/\partial m_2)$, and ρ are pressure-dependent variables.

The first two variables are expressed in terms of first-order expansions in pressure about a pressure of 1 atm by Taylor's theorem. Higher-order terms in these expansions are small and therefore neglected. Throughout this paper P will refer to the pressure above atmospheric pressure.

$$\left(\frac{\partial\mu_2}{\partial m_2}\right)_P = \left(\frac{\partial\mu_2}{\partial m_2}\right)_{P=0} + \left(\frac{\partial^2\mu_2}{\partial P\partial m_2}\right)P$$

Substituting the relation $(\partial\mu_2/\partial P)_{m_2} = M_2\bar{v}_2$ into the above equation gives a relation in terms of experimentally accessible variables,

$$\left(\frac{\partial\mu_2}{\partial m_2}\right)_P = \left(\frac{\partial\mu_2}{\partial m_2}\right)_{P=0} + M_2\left(\frac{\partial\bar{v}_2}{\partial m_2}\right)_{P=0} P. \quad (2)$$

Similarly,

$$\bar{v}_{2,P} = \bar{v}_{2,P=0} + \left(\frac{\partial\bar{v}_2}{\partial P}\right)_{P=0} P.$$

Introducing the relation for the partial specific isothermal compressibility of the solute, $\kappa_2 \equiv -[1/\bar{v}_2(d\bar{v}_2/dP)]_{P=0,m_2}$

$$\bar{v}_{2,P} = \bar{v}_{2,P=0}(1 - \kappa_2 P). \quad (3)$$

By a similar Taylor's expansion, the density of the solution may be expressed in terms of the isothermal compressibility coefficient of the solution, κ , at $P = 0$, and the density, $\rho^0(m_2)$,⁷ of the solution of molality, m_2 , at atmospheric pressure.

$$\rho = \rho^0/(1 - \kappa P) \quad (4)$$

Upon substitution of the effects of pressure, equations (2), (3), and (4), the differential equation (1) becomes

$$\frac{dm_2}{dr} = \frac{M_2 \left[1 - \frac{(1 - \kappa_2 P)}{(1 - \kappa P)} \bar{v}_2^0 \rho^0 \right] \omega^2 r}{\left(\frac{\partial\mu_2}{\partial m_2}\right)^0 + M_2 \left(\frac{\partial\bar{v}_2}{\partial m_2}\right)^0 P}, \quad (5)$$

Equation (5) provides a means of calculating the composition density gradient,

$$\left(\frac{d\rho}{dr}\right)^0 = \frac{dm_2}{dr} \left(\frac{d\rho}{dm_2}\right)^0 = \left(\frac{d\rho}{dm_2}\right)^0 \frac{M_2 \left[1 - \frac{(1 - \kappa_2 P)}{(1 - \kappa P)} \bar{v}_2^0 \rho^0 \right] \omega^2 r}{\left(\frac{\partial\mu_2}{\partial m_2}\right)^0 + M_2 \left(\frac{\partial\bar{v}_2}{\partial m_2}\right)^0 P}, \quad (6)$$

and by comparison with the comparable equation at atmospheric pressure,

$$\left(\frac{d\rho}{dr}\right)^0 = \left(\frac{d\rho}{dm_2}\right)^0 \frac{M_2 [1 - \bar{v}_2^0 \rho^0] \omega^2 r}{(\partial\mu_2/\partial m_2)^0} \equiv \frac{\omega^2 r}{\beta^0}, \quad (7)$$

we can estimate the effect of pressure on salt distribution. Equation (7) defines β^0 , a parameter previously calculated by Ifft, Voet, and Vinograd⁸ and designated by them as β . Because the pressure correction terms are small, equation (6) may be simplified by expansion, retaining only first-order terms in the corrections. Incorporating the definition of β^0 expressed by equation (7),

$$\left(\frac{d\rho}{dr}\right)^0 = \frac{\omega^2 r}{\beta^0} \left\{ 1 - \left[\frac{\bar{v}_2^0 \rho^0 (\kappa - \kappa_2)}{1 - \bar{v}_2^0 \rho^0} + \frac{M_2 \left(\frac{\partial \bar{v}_2}{\partial m_2}\right)^0}{\left(\frac{\partial \mu_2}{\partial m_2}\right)^0} \right] P \right\} \quad (8)$$

$$\left(\frac{d\rho}{dr}\right)^0 \equiv \frac{\omega^2 r}{\beta^0} \{1 - \phi P\}.$$

The quantity ϕ has been evaluated for CsCl solutions, Table 1. Pohl's compressibility data,⁹ and data for ρ^0 and \bar{v}_2^0 used in reference 8 were employed in the calculations.¹⁰

TABLE 1
PRESSURE CORRECTION TERMS FOR THE COMPOSITION DENSITY GRADIENT, CsCl 25°C

ρ^0	$\kappa \text{ atm}^{-1},$ $\times 10^6$	$\kappa_2 \text{ atm}^{-1},$ $\times 10^6$	$\bar{v}_2^0 \rho^0$	$M_2 \left(\frac{\partial \bar{v}_2}{\partial m_2}\right)^0 / \left(\frac{\partial \mu_2}{\partial m_2}\right)^0$ $\times 10^6$	$\phi \text{ atm}^{-1},$ $\times 10^6$
1.3	34.2	-33.4	0.342	42.4	77.5
1.5	29.5	-15.9	0.405	26.8	57.7
1.7	25.8	-5.9	0.464	21.8	49.2

As the pressure at the center of a 1.1 cm CsCl column, $\rho^0 = 1.7 \text{ gm cm}^{-3}$, at 44,770 rpm is approximately 130 atm,¹¹ the ϕP correction terms will generally be less than 0.01 and are therefore neglected. The corrections become smaller if shorter CsCl columns are used. The advantage of neglecting the pressure correction to the salt distribution is that ρ^0 may then be calculated with the equation,

$$\rho^0 = \rho_e^0 + \int_{r_e}^r \left(\frac{d\rho}{dr}\right)^0 dr = \rho_e^0 + \int_{r_e}^r \frac{\omega^2 r}{\beta^0} dr, \quad (9)$$

where r_e is the radius at which the molality of CsCl is that of the initial homogeneous solution, and ρ_e^0 is the initial density at atmospheric pressure. The iso-concentration distance, r_e , has been determined⁸ for different salts as a function of ρ_e^0 and ω^2 . Since the effect of pressure on salt redistribution is small, these data remain valid.

Having established that significant salt redistribution is not caused by the pressures encountered during density gradient analyses, we obtain the *physical density gradient* by differentiating equation (4) with respect to r ,

$$\frac{d\rho}{dr} = \frac{1}{1 - \kappa P} \left(\frac{d\rho}{dr}\right)^0 + \frac{\rho^0(m)}{(1 - \kappa P)^2} \frac{d(\kappa P)}{dr}. \quad (10)$$

Introducing $dP/dr = \rho \omega^2 r$, equation (10) for the case of constant compressibility coefficient becomes

$$\frac{d\rho}{dr} = \frac{1}{1 - \kappa P} \left[\left(\frac{d\rho}{dr}\right)^0 + \frac{\kappa \rho^0 \omega^2 r}{(1 - \kappa P)^2} \right]. \quad (11)$$

Neglecting pressure-correction terms of the order of 1% of $d\rho/dr$, the above equation is

$$\frac{d\rho}{dr} = \left[\left(\frac{1}{\beta^0}\right) + \kappa \rho^0 \right] \omega^2 r \equiv \frac{\omega^2 r}{\beta}. \quad (12)$$

The second term in equation (12) is the significant compression term and is tabulated with $1/\beta^0$ in Table 2 for CsCl solutions. The values for the compressibility coefficient κ are interpolated from the data of Pohl.⁹ His data are extrapolated linearly from $\rho = 1.4$ to $\rho = 1.8$ gm cm⁻³.

With the aid of equation (12) it has been demonstrated¹² in the case that \bar{v}_s is a function only of solute activity and pressure that the buoyancy condition in a density gradient experiment is¹³

$$\rho_0^0 = \frac{1}{\bar{v}_s^0} \left\{ 1 - \frac{(\kappa - \kappa_s)P_0}{1 - \left(\frac{\partial \rho_0^0}{\partial a_1^0}\right)_P \left(\frac{da_1^0}{d\rho^0}\right)} \right\} \quad (13)$$

The slope of the ρ_0^0 versus P_0 relation is $-\psi/\bar{v}_s^0$, where ψ is $\kappa - \kappa_s/[1 - (\partial \rho_0^0/\partial a_1^0)_P (da_1^0/d\rho^0)]$. In the following experiments, a study of the dependence of ρ_0^0 on pressure is made. This dependence is found to be linear.

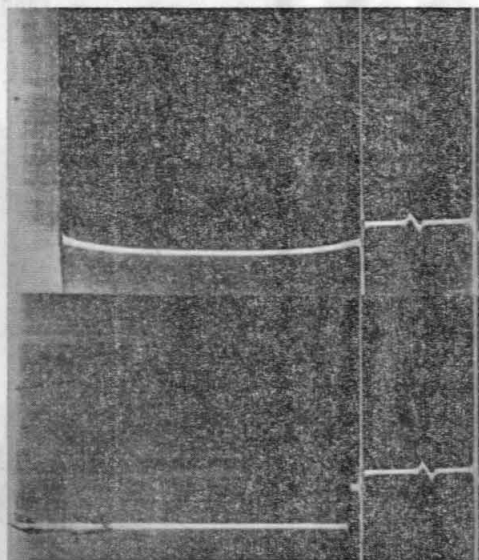


FIG. 1.—The effect of pressure on band position of T-4 DNA in CsCl solution $\rho_c^0 = 1.699$ g. cm.⁻³ at 25°C at 44,770 rpm. The pressure at band center in the lower part of the photograph is 54.5 atm. and in the upper part is 170.7 atm.

The Determination of ψ .—The value of ψ may be measured with adequate accuracy by noting the displacements of equilibrium bands upon changing the pressure. This was accomplished in two ways: An immiscible oil was layered in successive increments on a short column of CsCl solution containing a buoyant macromolecular species and rotated after each increment until equilibrium was attained. The cell containing a band was rotated to equilibrium at varying angular velocities.

Experimental.—Materials: The CsCl was obtained from Maywood Chemical Co., Maywood, N. J., and recrystallized three times. Emission spectroscopic analyses performed in the Department of Geology showed less than 0.03% metallic impurities. The silicone oil was Dow Corning 550 fluid, Lot No. 88-161. According to the manufacturer, it is a methyl- and phenyl-substituted polysiloxane containing less than 10 parts per million of metal salt impurity. The FC-43 fluoro-chemical

was obtained from the Minnesota Mining and Manufacturing Co. and is stated to be triperfluorobutylamine. The tobacco mosaic virus strain U 1 (TMV) was kindly supplied by Professor S. Wildman, University of California at Los Angeles. The stock solution contained 5.47 mg/ml TMV in 0.001 versene, pH 7.5. The preparation of the T-4 bacteriophage DNA has been described.¹⁴ All other chemicals used were reagent grade materials.

Procedure.—The effect of pressure on band position: The oil column experiments were performed with both TMV and DNA solutions. The speed-variation experiments were performed only with DNA solutions. The solutions delivered into the standard 4°, 12-mm, Kel-F center-piece cell assembly had densities, ρ^0 , of 1.325 and 1.704 g cm.⁻³ for TMV and DNA respectively. The first solution contained 46 μ g cm.⁻³ of TMV and was buffered with 0.01 M tris at pH 7.0. The second solution was buffered with 0.02 M tris at pH 9. The DNA concentration in terms of E_{1}^{260} cm was 0.085. All experiments were begun by filling cells with 0.02 ml of fluorocarbon, 0.18

ml of CsCl solution, and 0.02 ml of silicone oil. Both the fluorocarbon and the silicone oil were included to provide accurate means of recording the top and bottom menisci of the CsCl column. This column was about one-fourth the length attainable in the standard centerpiece.

The solutions were centrifuged at 25.0°C. and photographed with the schlieren optical system after equilibrium had been established. The actual speeds were evaluated from odometer readings made at the beginning and end of the run. These agreed with the nominal values within $\pm 0.02\%$. In these short columns at 44,770 rpm, the DNA runs required 14 hours and the TMV runs about 90 minutes to reach equilibrium. A typical pair of exposures is shown in Figure 1. The top and bottom CsCl menisci and the silicone oil meniscus were taken to be the centers of the symmetrical meniscus images. These, as well as the counter balance reference edges and the positive and negative peaks, associated with the inflections in the polymer concentration distributions, were

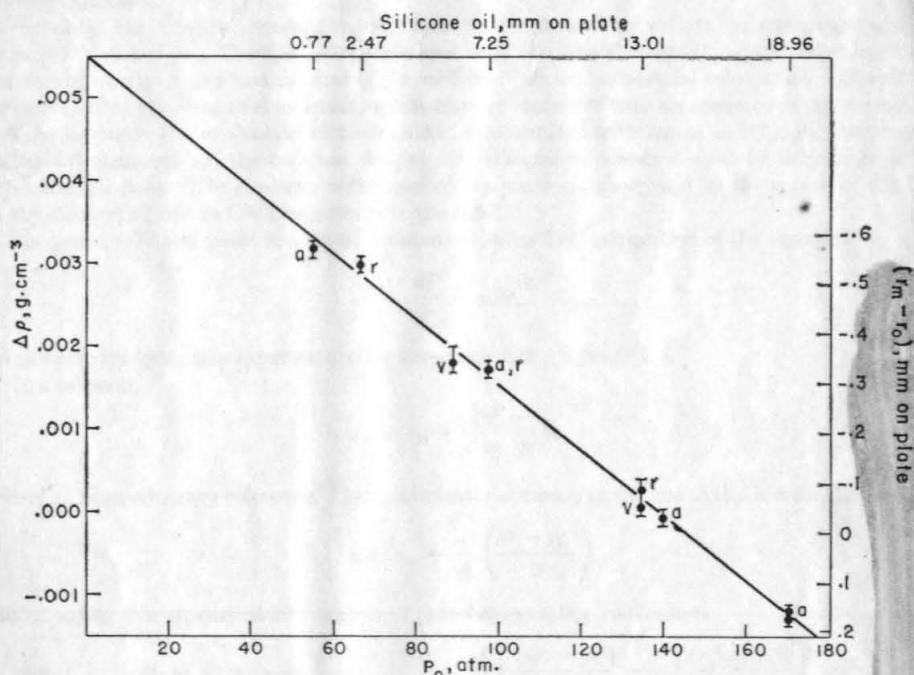


FIG. 2.—Buoyant density increments for T-4 DNA in CsCl solution at various pressures, $\rho_c^0 = 1.699 \text{ g. cm.}^{-3}$ at 25°C at 44,770 rpm. Expt. no. 1. *a*, addition of oil; *r*, removal of oil; *v*, points obtained at 31,410 rpm and 39,460 rpm. The coordinates at the top and right-hand side indicate the original data. Slope = $-3.94 \times 10^{-3} \text{ g. cm.}^{-3}/\text{atm}$. The maximum error intervals are indicated.

measured with a coordinate plate and film Comparator Model M 2001-P, Gaertner Scientific Co. Chicago, Illinois. Reading accuracy was $\pm 0.01 \text{ mm}$, which corresponds to ± 5 microns in the cell. The band position was taken to be the average of the distances associated with the positive and negative peaks.

In the oil column experiments, the cells were reopened at the filling hole after the first equilibration and 0.16 ml silicone oil added. The solutions were again run to equilibrium. The procedure was repeated twice again. Silicone oil was similarly removed with a 24-gauge needle in two or three stages.

In one of the DNA runs, after the cell was filled with silicone oil and centrifuged to equilibrium, the angular speed was dropped to 31,410 rpm, then raised to 39,460 rpm, and again raised to 44,770 rpm. Thirty-five hours were required for equilibrium at 39,460 rpm and 65 hours at 31,410 rpm. The slow step in these experiments was band motion. The band width became constant after 22 hours at both speeds. After 5 days continuous running, the band returned to its original position at 44,770 rpm as indicated by the double point at 170 atm (Fig. 2).

The density of the silicone oil at 25°C. was measured in a calibrated 0.3 ml micropipet. The density was $1.067 \pm 0.001 \text{ g cm}^{-3}$.

The Effect of Pressure on the Composition Density Gradient.—In the theoretical part of this paper, it was noted that the composition density gradient is insensitive to pressure. To check this conclusion, the effect of pressure on the refractive index gradient was measured. The 4° Kel-F, 12-mm standard cell was filled with 0.02 ml of fluorocarbon, 0.34 ml of CsCl solution, $\rho^0 = 1.339 \text{ gm cm}^{-3}$ and 0.02 ml of silicone oil. The rotor was brought to 44,770 rpm as rapidly as possible, and schlieren images at a bar angle of 55° were photographed immediately upon reaching this speed and again after 10 hours, at equilibrium. The experiment was repeated after thorough homogenizing of the CsCl solution and the addition of 0.34 ml of silicone oil. The composition density gradient was obtained at r_e from the difference in elevations between the early and equilibrium exposures.

For these experiments, tracings were made of 20-fold cell to vellum enlargements with an Omega D-2 enlarger. The CsCl meniscus was used for lateral orientation and the image of a horizontal wire mounted just in front of the schlieren camera for vertical orientation. Elevations proportional to the compression density gradient were measured with an accuracy of 0.4 per cent.

Calculations.—For evaluation of the results in accordance with equation (13), P_0 , the pressure at band center, and ρ_0^0 , the buoyant density at atmospheric pressure, must be derived from the experimental data. The pressure is the sum of the pressures generated by the action of the field in the silicone oil and in CsCl solution over the band.

The pressure at any point in a liquid volume is obtained by integration of the equation

$$\frac{dP}{dr} = \rho\omega^2 r. \quad (14)$$

In order to integrate this expression, the r dependence of ρ is needed.

In a solution,

$$\rho = \rho_\alpha + \int_{r_\alpha}^r \frac{\omega^2 r}{\beta} dr, \quad (15)$$

where r_α is an arbitrary reference. It is sufficiently accurate to assume that β is a constant.

$$\rho = \rho_\alpha + \frac{\omega^2}{\beta} \left(\frac{r^2 - r_\alpha^2}{2} \right) \quad (16)$$

Substituting this expression into equation (1) and integrating from r_1 to r_2 ,

$$P_2 - P_1 = \rho_\alpha \omega^2 \left(\frac{r_2^2 - r_1^2}{2} \right) + \frac{\omega^4}{2\beta} \left[\frac{(r_2^4 - r_1^4)}{4} - r_\alpha^2 \frac{(r_2^2 - r_1^2)}{2} \right]. \quad (17)$$

To simplify computation, r_α is so selected that the term in the brackets in equation (17) vanishes. For this condition, r_α is the root mean square between r_1 and r_2 . In all cases the use of the arithmetic mean for r_α did not introduce a significant error.

$$r_\alpha = \sqrt{\frac{r_2^2 + r_1^2}{2}} = \frac{r_2 + r_1}{2} + \frac{1}{8} \frac{(r_2 - r_1)^2}{r_2} \dots$$

The pressure at band center caused by the CsCl solution was evaluated as follows: The quantity r_α is the root mean square radius between band center, r_0 , and the CsCl meniscus, r_{cm} . The density ρ_α is obtained with sufficient accuracy with equation (9), assuming β^0 constant, the limits of integration being r_e and r_α . This neglects the effect of pressure on ρ_α . Substitution into equation (5) yields

$$P_{r_0, \text{CsCl}} = \frac{\rho_\alpha \omega^2}{1.013 \times 10^6} \frac{(r_0^2 - r_{cm}^2)}{2}. \quad (18)$$

The numerical coefficient is introduced in order to express pressure in atmospheres. ρ_α was found to vary only 0.12% in a given series over the entire range of oil column lengths and was therefore considered constant.

In the oil column treated as a one-component system, $1/\beta^0 = 0$, and $1/\beta = \kappa' \rho^0$, equation (12), where κ' is the isothermal compressibility of the oil. The same arguments used for the CsCl column apply here. In this case, however, the compressibility and the pressure contribution of the oil are larger; the effect of pressure on ρ_α is therefore taken into account. For a good estimate of the pressure P_α , equation (14) is integrated between the oil meniscus, r_{om} , and r_α , under the assumption that the density is constant.

$$P_\alpha = \frac{\rho^0 \omega^2}{1.013 \times 10^6} \frac{(r_\alpha^2 - r_{om}^2)}{2} = \frac{\rho^0 \omega^2}{1.013 \times 10^6} \frac{(r_{cm}^2 - r_{om}^2)}{4} \quad (19)$$

The r_α was eliminated with the definition of r_α . Upon substituting $\rho_\alpha = \rho^0(1 + \kappa' P_\alpha)$ and equation (19) into equation (17), and letting r_2 be the cesium chloride meniscus, r_{cm} , and r_1 be the oil meniscus, r_{om} ,

$$P_{cm} = \rho^0 \left\{ 1 + \kappa' \left[\frac{\rho^0 \omega^2}{1.013 \times 10^6} \frac{(r_{cm}^2 - r_{om}^2)}{4} \right] \right\} \left(\frac{r_{cm}^2 - r_{om}^2}{2} \right). \quad (20)$$

The pressure at band center is the sum of the pressures given by equations (18) and (20).

Now the shifts in band position must be expressed in density units. The buoyant density at atmospheric pressure, ρ_0^0 , is calculated with equation (9). In order to express the dependence of β^0 on r , β^0 is expanded:

$$\beta^0 = \beta_\gamma^0 + \left(\frac{d\beta^0}{dr} \right)_\gamma (r - r_\gamma)$$

where r_γ is again an arbitrary reference radius. Integrating and evaluating r_γ so that the $(d\beta^0/dr)_\gamma$ term equals zero as before, the following equations are obtained,

$$r_\gamma = \frac{r_2 + r_1}{2} + \frac{(r_2 - r_1)^2}{12 r_2} \dots$$

and

$$\rho_2^0 - \rho_1^0 = \frac{\omega^2}{\beta_\gamma^0} \left(\frac{r_2^2 - r_1^2}{2} \right).$$

As in the previous case, the selection of β^0 at the arithmetic mean rather than at r_γ will not introduce a significant error.

Since the density shifts due to the pressure variation are very small, the quantity $\Delta\rho = \rho_0^0 - \rho_e^0$ was evaluated and not ρ_0^0 itself. The desired expression is

$$\Delta\rho = \rho_0^0 - \rho_e^0 = \frac{\omega^2}{\beta_e^0} \left(\frac{r_0^2 - r_e^2}{2} \right). \quad (21)$$

The following relation utilizing the original comparator data (capital R 's) and the magnification factor, MF , was used,

$$(r_0^2 - r_e^2) = \frac{2 \times 5.725}{MF} \left(R_0 - \frac{R_{cm} + R_{fm}}{2} \right) + \frac{1}{(MF)^2} \left(R_0^2 - \frac{R_{cm}^2 + R_{fm}^2}{2} \right), \quad (22)$$

where R_{fm} is the radius of the fluorocarbon meniscus.

According to theory, a plot of $\Delta\rho$ versus P_0 should yield a straight line of slope $-\psi/\bar{v}_{s,0}^0$ and intercept $(1/\bar{v}_{s,0}^0 - \rho_e^0)$. Figures 2 and 3 present the data obtained for one series each of DNA and TMV. The value of $\bar{v}_{s,0}^0$ was determined from the intercept. From the intercept and the slope, values for ψ were obtained. Duplicate experiments in each case were performed.

In the measurements, the radii were located with a precision of 0.01 mm on the plate. The values of P_0 were calculated with no significant error. The values of $\Delta\rho$ are very sensitive to the accuracy of measurement because these values are derived from the difference of the squares of two numbers of comparable magnitudes. The maximum error in each of the $\Delta\rho$ values was

TABLE 2

THE EFFECT OF COMPRESSION ON THE PHYSICAL DENSITY GRADIENT IN CsCl SOLUTIONS AT EQUILIBRIUM IN THE ULTRACENTRIFUGE AT 25°C

ρ^0	$1/\beta^0 \times 10^{-10}$	$\kappa\rho_0^2 \times 10^{-13}$	$\frac{1/\beta^0 + \kappa\rho_0^2}{1/\beta^0} = \frac{1/\beta}{1/\beta^0}$
1.2	5.042	0.543	1.108
1.3	6.468	0.586	1.091
1.4	7.429	0.629	1.085
1.5	8.034	0.673	1.084
1.6	8.351	0.714	1.085
1.7	8.400	0.757	1.090
1.8	8.231	0.797	1.097

evaluated in a short CsCl column with and without a layer of silicone oil. The effect on the net refractive index gradient at the root mean square position in the cell due to this layer of oil, which corresponded to a pressure increment of 72.1 atmospheres, was -1.3% . This result is within the experimental measuring errors and the effect predicted by the theory, Table 1. It is consistent with the previously obtained agreement⁸ between the composition density gradient obtained optically at the pressure in the cell and calculated from physical chemical data obtained at atmospheric pressure. Three approaches now show that the CsCl-water distribution is not significantly changed by compression, even though the solution is compressed and the physical density gradient increased.

In density gradient experiments the macromolecular species does not respond only to the physical density gradient. Of importance is the *effective density gradient*, which is shown in the preceding paper¹² to be

$$\left(\frac{d\rho}{dr}\right)_{\text{eff}} = \left[\frac{1}{\beta^0} + \psi\rho_0^{02}\right] (1 - \alpha)\omega^2r \quad (23)$$

where

$$\alpha = \left(\frac{\partial\rho_0^0}{\partial a_1^0}\right)_P \left(\frac{da_1^0}{d\rho^0}\right).$$

The quantity ψ must therefore be known in order to evaluate correctly the effective density gradient and the molecular weight of either the anhydrous or the hydrated species.

The values of ψ and $\bar{v}_{s,0}^0$ obtained from the oil column experiments are given in Table 3. The numbers in the fifth column, $1/\bar{v}_{s,0}^0$ are the values of the composition variable ρ_0^0 when the band is at atmospheric pressure. The values listed as ρ_0^0 are values calculated for the pressure at the middle of a 1.1 cm column of CsCl solution at 44,770 rpm. Thus significant deviations in ρ_0^0 will be encountered by workers banding the same material at different radii in the cell.

If proper experimental data are available, ψ can be used to calculate the apparent compressibility of the solvated polymer. A more complete discussion of this matter

TABLE 3

EFFECT OF PRESSURE ON BUOYANT MOLECULES IN A DENSITY GRADIENT

Material	Expt. No.	$\psi \times 10^6$ atm ⁻¹	$\frac{1}{\bar{v}_{s,0}^0}$	$\frac{1}{\bar{v}_{s,0}^0}$	ρ_0^0
T-4 Bacteriophage	1	23.1	0.587	1.704	1.699
DNA	2	23.5	0.587	1.703	1.698
Tobacco mosaic	3	21.8	0.756	1.322	1.319
virus, strain U 1	4	21.5	0.757	1.321	1.318

is presented in the preceding article.¹⁶ If the effects of solvation are neglected, the value of κ_s for *TMV* obtained from ψ and from Pohl's compressibility data is $12.9 \times 10^{-6} \text{ atm}^{-1}$. This value agrees favorably with the value $10 \times 10^{-6} \text{ atm}^{-1}$ which Jacobson¹⁷ obtained for various proteins in dilute salt solutions. The agreement may be the result of coincidence, because the effects of solvation have been neglected.

For *T-4 DNA* ψ was found to be $23.3 \times 10^{-6} \text{ atm}^{-1}$. The parameter α for *DNA* in *CsCl* is 0.24.¹⁶ These numbers may now be used to calculate the difference in compressibility, $\kappa - \kappa_s = 17.7 \times 10^{-6} \text{ atm}^{-1}$. From this difference κ_s is found to equal $8.7 \times 10^{-6} \text{ atm}^{-1}$. It should be stressed that κ_s is an apparent compressibility. It not only includes the compression of the solvated species, but also a pressure dependence of the amount of hydrated water.

The use of an insoluble marker material, such as a thin film of plastic, has been suggested by Szybalski.¹⁸ Solvation effects for such a material should be negligible

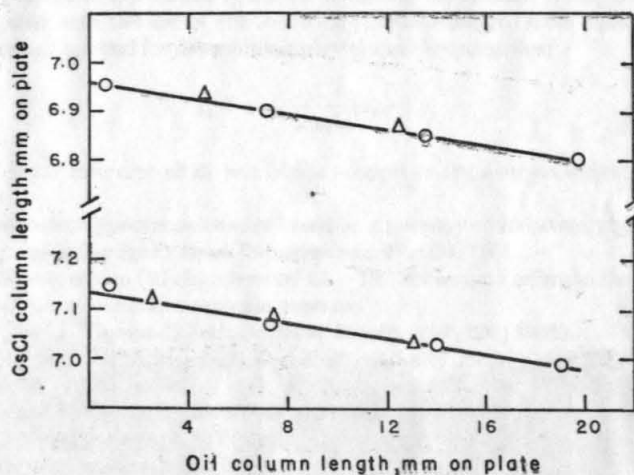


FIG. 4.—The effect of pressure on *CsCl* solution column length. O, addition of oil; Δ , removal of oil. The lower line is from expt. no. 1 and the upper line is from expt. no. 2.

because surface areas are relatively small. Large pressure effects on marker positions are to be expected and have been observed.¹⁸

DNA samples, denatured, isotopically substituted, or of differing composition, can be used as density markers, providing that the dependence of ψ and α on pressure for the marker is the same as the sample under investigation. The effective density gradient, equation (23), is used to calculate density differences in such experiments.

Cell Distortion.—The *CsCl* column length was found to change in a characteristic manner with the level of the supernatant silicone oil (Fig. 4). The two sets of points correspond to two independent experiments. In these, the cell was disassembled and reassembled with a solution of slightly different density. The linear and elastic response reflects the behavior of a cell assembly with a Kel-F centerpiece and quartz windows. The observed decrease in *CsCl* column length of 2.1% is 10.8 times larger than that attributable to the compression of the solution.

* This investigation was supported in part by Research Grant H-3394 from the National Institutes of Health, U.S. Public Health Service.

† Predoctoral Fellow of the National Science Foundation.

‡ U.S. Public Health Service Research Fellow of the Division of General Medical Sciences.

** Contribution No. 2701.

¹ Meselson, M., F. W. Stahl, and J. Vinograd, these PROCEEDINGS, **43**, 581 (1957). Their treatment also neglects the small pressure dependence of $(\partial\mu_2/\partial m_2)_P$, equation (2).

² Young, T. F., K. A. Kraus, and J. S. Johnson, *J. Chem. Phys.*, **22**, 878 (1954).

³ Williams, J. W., K. E. Van Holde, R. L. Baldwin, and H. Fujita, *Chem. Revs.*, **58**, 715 (1958).

⁴ Baldwin, R. L., these PROCEEDINGS, **45**, 939 (1959).

⁵ Goldberg, R. J., *J. Phys. Chem.*, **57**, 194 (1953).

⁶ Refer to reference 12 for the definition of the term "free solute."

⁷ The superscript zero is used throughout this paper to designate variables at atmospheric pressure. The density $\rho^0(m_2)$ is a function only of m_2 and should be thought of as a composition variable. The actual density ρ is a measure of physical density and is a function of m_2 and pressure.

⁸ Ifft, J. B., D. H. Voet, and J. Vinograd, *J. Phys. Chem.* (in press).

⁹ Pohl, F., Dissertation, Rheinische Friedrich Wilhelms Universität, Bonn, Germany (1906).

¹⁰ κ_2 was evaluated with the aid of the following equation derived from equation (4) and with the aid of the intercept method for determining partial specific quantities:

$$\kappa_2 = \kappa + \frac{1}{\rho^0 v_2^0} (\kappa_i - \kappa)$$

The quantity κ_i is the intercept at $Z_2 = 1$ of the tangent to the κ versus weight fraction of CsCl Z_2 , curve.

¹¹ All subsequent error approximations are based on a pressure of 130 atmospheres.

¹² Hearst, J. E., and J. Vinograd, these PROCEEDINGS, **47**, 000 (1961).

¹³ Equation (13) is equation (22) in reference 12. The subscript s refers to the solvated species; a_1^0 is the activity of the solute at atmospheric pressure.

¹⁴ Hearst, J. E., and J. Vinograd, *Arch. Biochem. Biophys.*, **92**, 206 (1961).

¹⁵ Margenau, H., and G. M. Murphy, *The Mathematics of Physics and Chemistry* (Princeton: D. Van Nostrand Co., 1956), p. 515.

¹⁶ Hearst, J. E., and J. Vinograd, these PROCEEDINGS, **47**, 000 (1961).

¹⁷ Jacobson, B., *Arkiv för Kemi*, **2**, 177 (1951).

¹⁸ Szybalski, W. (private communication).

INTRODUCTION

The ultracentrifuge has been an important tool in the development of our understanding of macromolecules. To the two classical techniques of two-component sedimentation equilibrium and sedimentation velocity, Weeselsen, Stahl, and Vinograd (1) have added a third technique, that of sedimentation equilibrium in a density gradient. This technique provides the density and molecular weight of the sedimented macromolecular species from the position and standard deviation of the **Part III** concentration distribution which is formed in a buoyant density gradient.

The Behavior of Bovine Serum Mercaptalbumin in a Density Gradient at Equilibrium in the Ultracentrifuge (2,3,4) provides the examination of the behavior of nucleic acids. In addition, numerous investigations of viruses using this technique in preparative ultracentrifuges have been made (5,6,7). There have been a few investigations of proteins in density gradients (8,9,10) and there has been no careful attempt to study the behavior of a soluble protein of known molecular weight. The purpose of this research has been to carry out such an investigation.

The protein selected for study was bovine serum mercaptalbumin (BSA). An excellent preparative technique which provides a homogeneous material has recently been developed (11). BSA has a well-characterized molecular weight and partial specific volume, it is soluble in

INTRODUCTION

The ultracentrifuge has been an important tool in the development of our understanding of macromolecules. To the two classical techniques of two-component sedimentation equilibrium and sedimentation velocity, Meselson, Stahl, and Vinograd (1) have added a third technique, that of sedimentation equilibrium in a density gradient. This technique provides the density and molecular weight of the solvated macromolecular species from the position and standard deviation of the Gaussian concentration distribution which is formed in a buoyant density gradient.

The initial work and most of the subsequent studies (2,3,4) involved the examination of the behavior of nucleic acids. In addition, numerous investigations of viruses using this technique in preparative ultracentrifuges have been made (5,6,7). There have been a few investigations of proteins in density gradients (8,9,10) but there has been no careful attempt to study the behavior of a soluble protein of known molecular weight. The purpose of this research has been to carry out such an investigation.

The protein selected for study was bovine serum mercaptalbumin (BMA). An excellent preparative technique which provides a homogeneous material has recently been developed (11). BMA has a well-characterized molecular weight and partial specific volume, it is soluble in

concentrated salt solutions, and is stable at room temperature for extended periods of time.

A serious problem in this investigation is the width of the concentration distribution of the BMA. The upper limit of the maximum centrifugal force available (250,000 g) and the molecular weight of BMA ($M_w = 69,000$) combine to produce a band width of about 2 mm. in the salt gradients normally employed. Because the gradient departs significantly from constancy over this distance, problems arise both in experimental methods and analyses.

After considering several factors, the schlieren optical system was chosen to record the results of the density gradient experiments instead of the absorption optical system employed in studies of nucleic acids. Because the bands are wide, the usual method of interpolating the baseline is not reliable and a separate run to record the baseline is required if absorption optics are used. Preliminary runs showed that the absorption baselines were curved, were not reproducible, and could not be satisfactorily subtracted from the BMA concentration curve. Procedures are available whereby the refractive index gradient distribution of the solution and a satisfactory baseline can be simultaneously recorded if schlieren optics are used. The principal advantage of the absorption optical system with nucleic acids is the 100 fold increase in sensitivity associated with the high extinc-

tion coefficient of the nucleic acids at $260 \text{ m}\mu$. In the case of bovine albumin, only a two fold increase in sensitivity occurs at $280 \text{ m}\mu$.

The original formulation of Horelson, Stein and Ingram (1) for the evaluation of a molecular weight from serum albumin using absorption optics and concluded that satisfactory methods were not available for the analysis of soluble proteins of relatively low molecular weight.

The quantity ρ_0 is the physical density at the radial center r_0 of the Gaussian concentration distribution of standard deviation, σ . The angular velocity is ω and $(d\rho/dr)_{\text{phys},0}$ is the physical density gradient at r_0 . The quantity $(d\rho/dr)_{\text{phys},0}$ is evaluated as the sum of the expansion and compression density gradient terms (cf. equation 14 of Part II). The product ρ_0 has its usual significance. This equation was derived for a two-component system, a macromolecule and a density gradient forming solvent, in which there is no interaction of the macromolecule with the solvent.

Part III (14) has considered the case for which not only ρ but also \bar{v}_1 , \bar{v}_2 , and \bar{v}^M are functions of position in the liquid column. The quantities \bar{v}_1 and \bar{v}_2 are the partial specific volumes of the salt and macromolecule respectively and \bar{v}^M is the net hydration in terms of gms. water/gm. macromolecule. He obtained a rigorously correct expression of η which involved six terms; only

SECTION A

THE BEHAVIOR OF BMA IN A CsCl DENSITY GRADIENT

The original formulation of Meselson, Stahl and Vinograd (1) for the evaluation of a molecular weight from a density gradient experiment is given by equation 1.

$$M = \frac{RT\rho_0}{\sigma^2 \omega^2 r_0 (d\rho/dr)_{\text{phys},0}} \quad (1)$$

The quantity ρ_0 is the physical density at the radial center r_0 of the Gaussian concentration distribution of standard deviation, σ . The angular velocity is ω and $(d\rho/dr)_{\text{phys},0}$ is the physical density gradient at r_0 . The quantity $(d\rho/dr)_{\text{phys},0}$ is evaluated as the sum of the composition and compression density gradient terms (cf. equation 12 of Part II). The product RT has its usual significance. This equation was derived for a two-component system, a macromolecule and a density gradient forming solvent, in which there is no interaction of the macromolecule with the solvent.

Baldwin (12) has considered the case for which not only ρ but also \bar{v}_1 , \bar{v}_3 , and Γ' are functions of position in the liquid column. The quantities \bar{v}_1 and \bar{v}_3 are the partial specific volumes of the salt and macromolecule respectively and Γ' is the net hydration in terms of gms. water/gm. macromolecule. He obtained a rigorously correct expression of M which involved six terms, only

two of which are experimentally available. Also, the macromolecule concentration is given in weight per kilogram of water whereas the centrifuge records concentration or the gradient of concentration on a weight per volume scale. He calculated the distribution on a weight per volume concentration scale under the assumptions that $d\bar{v}_1/dr$ and $d\bar{v}_3/dr$ were negligible. This assumes that the relevant species are incompressible. The resulting expression for σ^2 (equation 17a in reference 12) is identical with equation 1 if two correction terms involving the change in the macromolecular solvation with salt concentration are neglected. The derivation clearly indicates that the approximate molecular weight obtained under these assumptions is that of the solvated species.

In this section, we shall calculate molecular weights using the physical density gradient in equation 1. It must be stressed that the derived value for the apparent molecular weight of the solvated species which we will designate as $M_{app,0}$ is only an approximation at best and may be considerably in error if $d\bar{v}_3/dr$ and $d\Gamma'/dr$ are not small. This assumption is examined in considerable detail in subsequent sections.

Hydration parameters can be evaluated from the buoyant densities without using molecular weights. Williams (13) was the first to show that the hydration of a macromolecule in terms of gm. water/gm. protein can be

determined from its buoyant density and partial specific volume in the buoyant solvent. We will designate this hydration value as Γ'_a .

$$\rho_0 = \frac{1 + \Gamma'_a}{\bar{v}_3 + \Gamma'_a \bar{v}_1} \quad (2)$$

The \bar{v}_1 and \bar{v}_3 are the partial specific volumes of the solute which is selectively bound and of the anhydrous macromolecular species respectively.

The density gradient technique also provides a second method for the calculation of Γ' . If the correct value of the solvated molecular weight M_s and that of the anhydrous molecular weight, M_a , are available, the solvation can be determined from their difference. We will denote the solvation parameter calculated by this method as Γ'_b .

$$\Gamma'_b = \frac{M_s - M_a}{M_a} \quad (3)$$

These two methods of determining Γ' yield the proper value for the hydration if the buoyant species can be defined by a single solvation parameter and the anhydrous molecular weight. The situation is more complicated in the case of BMA because it binds anions voraciously. As discussed in Section D, the species that is measured is the solvated protein molecule plus neutral salt molecules corresponding in number to the number of anions bound. Thus the \bar{v}_3 in equation 2 is

the partial specific volume of the protein-salt complex and the hydration parameter obtained is the net hydration per gram of this complex.

The values of $\bar{\Gamma}'_b$ should reflect the correct amount of both hydration and salt binding. However the recent work of Hearst and Vinograd (14) suggests that equation 1 is incorrect and the solvated molecular weight and $\bar{\Gamma}'_b$ may be in error. For the case of DNA, the derivative of \bar{v}_s with distance, where \bar{v}_s is the partial specific volume of the solvated species, was found to contribute significantly to the effective density gradient. A procedure for determining the correct density gradient taking into account the non-zero value of this derivative for BMA in density gradients is discussed in subsequent sections.

The purpose of the present section is to discuss satisfactory procedures and methods of analysis whereby density gradient experiments can be conducted and quantitative results can be obtained for a material such as bovine mercaptalbumin. The results for the molecular weight and hydration parameters are presented principally to demonstrate the precision of the method. The meaning of these data will be discussed in Section D.

For this examination of procedures, cesium chloride was selected as the salt to provide the density gradient. It possesses the highest density gradient among the salts for which composition density gradients have been

evaluated (see Part I). A number of experiments using a variety of experimental techniques are reported below.

Materials

The materials used in all of the experiments reported

EXPERIMENTAL

Materials

The albumin used in all of the density gradient centrifugal methods for purity and to obtain the anhydrous experiments was bovine serum mercaptalbumin (BMA).

The purified material was kindly supplied by Dr. D. Ridgeway of this laboratory. It was prepared from lyophilized Fraction V powder (Armour Lot No. T-94,101). It was crystallized three times as the mercury dimer and purified on a mixed-bed ion-exchange column according to the method of Dintzis (11). The colorless, 5% isoionic (pH 4.92) solution was stored at -20°C . and slowly thawed at 4°C as needed.

The albumin used in the apparent specific volume measurements was crystallized bovine plasma albumin, Armour Lot No. T-68,204.

The CsCl and fluorochemical described in Part II were used for all density gradient experiments. The CsCl employed in the apparent specific volume measurements was used as supplied by the Maywood Chemical Co. This material is known to be free of rubidium. The acetate buffer solutions were prepared from reagent-grade materials.

Examination of Materials

The BMA described above and used in all subsequent density gradient experiments was examined by two other centrifugal methods for purity and to obtain its anhydrous z-average molecular weight.

Sedimentation velocity experiments were performed at various times during the investigation. The same results as described below were consistently obtained. The solution sedimented was 1% protein in 0.1 M acetate buffer at pH 5.32. These solutions and also those used in the two-component sedimentation equilibrium experiments described below were prepared by mixing appropriate volumes of the 5% BMA stock solution with 0.2 M NaAc buffer, pH 5.5, and water. As shown in figure 1, the sedimenting peak was symmetrical. Less than about 3% aggregated material was present as indicated by the small, fast peak. The position of the maximum of the refractive index gradient distribution was used to measure \bar{r} , the position corresponding to the actual movement of the molecule in the homogeneous solution. A value of $S_{20,w}$ of 4.35 S was obtained. This number compares favorably with that of 4.27 S obtained from the precise data of Baldwin (15) by interpolation to this concentration and correction to 20°C.

In more sensitive tests for the homogeneity of the protein sample, several two-component sedimentation

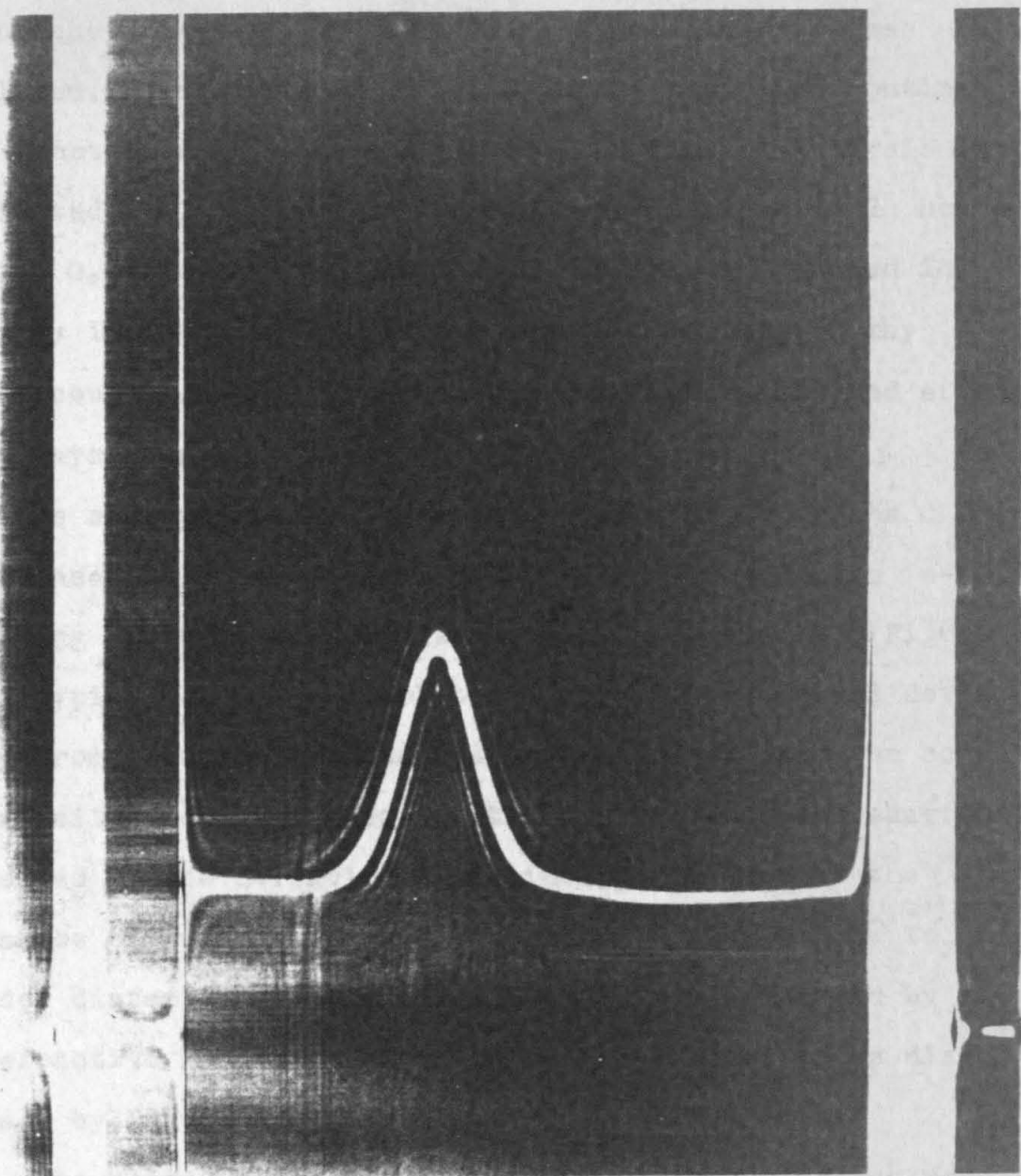
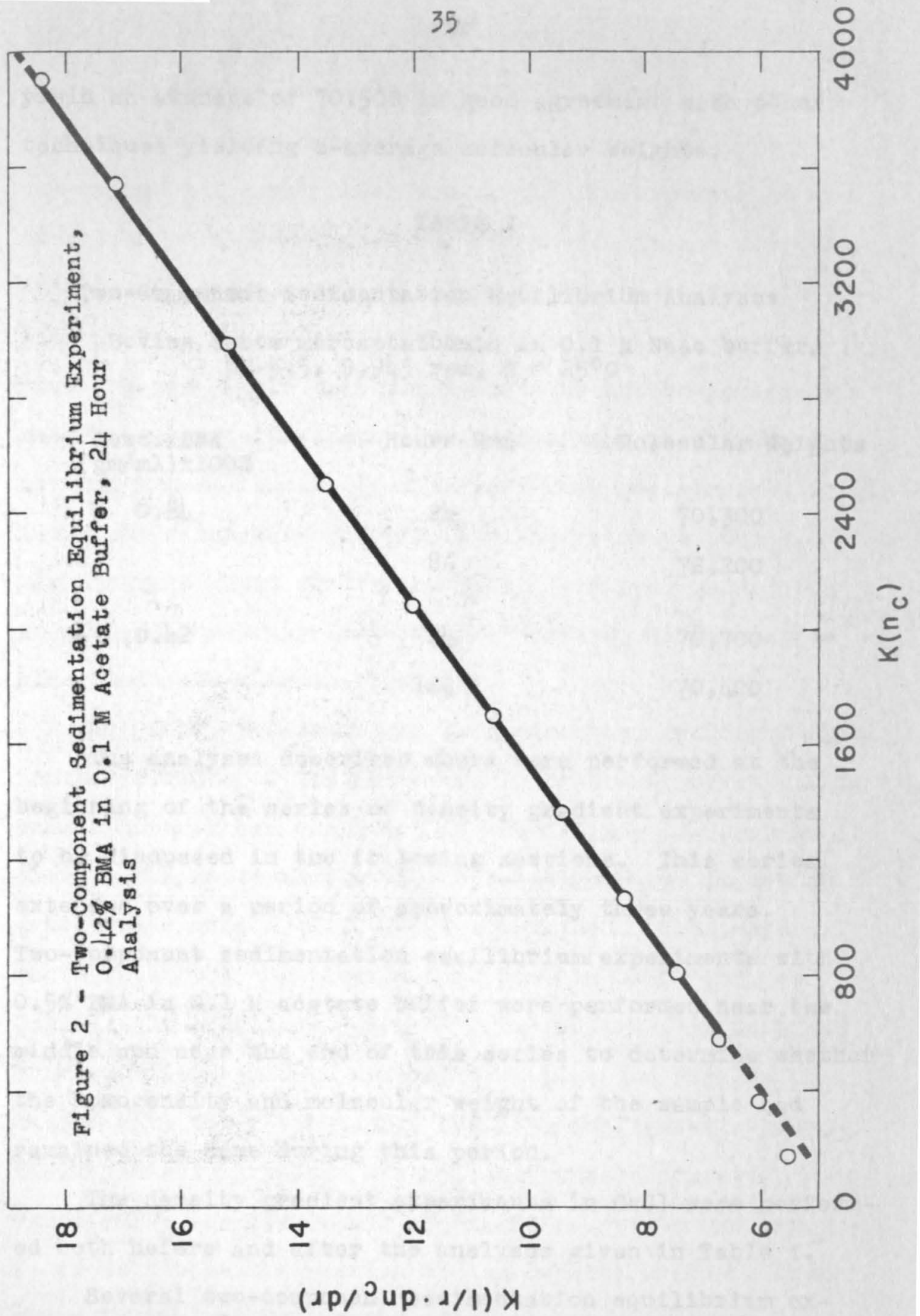


Figure 1 - Distribution of BMA during sedimentation velocity experiment, 0.94 % BMA in 0.1M acetate buffer, pH 5.5, 56,100 rpm, 21.86° C

equilibrium runs were performed at different protein concentrations in 0.1 M acetate buffer. The short-column technique suggested by Van Holde and Baldwin (16) was employed. Each run with 3 mm. liquid columns was continued for about five days at 9,945 rpm. The time of analysis is indicated in Table I. Equilibrium was attained in 24 hours in the 0.42% solution. After equilibrium was reached in one day in the 0.84% solution, a slow dimerization may have occurred as indicated by the high value obtained after five days running time.

As shown in figure 2, a plot of $(dn/dr)/r$ versus n was linear over the central 80% of the column length indicating substantial molecular weight homogeneity. Figure 2 is typical of all such plots. There is a downward deviation from linearity at the bottom of the cell and the converse situation at the top. This is the opposite behavior expected if the deviation from linearity is due to the presence of some aggregated material. It may be due to window distortion in this region or it may be caused by a refractive artifact occurring near the menisci as discussed by Trautman (17).

The slope of the linear portion of this plot was used to calculate the molecular weights given in Table I. The value for \bar{v}_3 of 0.734 ml./gm. reported by Dayhoff, et al (18) and confirmed in this study was used in the calculation. Excluding the 72,200 value, the remaining values



yield an average of 70,500 in good agreement with other techniques yielding z-average molecular weights.

TABLE I

Two-Component Sedimentation Equilibrium Analyses

Bovine serum mercaptalbumin in 0.1 M NaAc buffer,
pH 5.5, 9,945 rpm, T = 25°C

Conc. BMA (gm/ml) x 100%	Hours Run	Molecular Weights
0.84	24	70,300
	86	72,200
0.42	24	70,700
	120	70,400

The analyses described above were performed at the beginning of the series of density gradient experiments to be discussed in the following sections. This series extended over a period of approximately three years. Two-component sedimentation equilibrium experiments with 0.5% BMA in 0.1 M acetate buffer were performed near the middle and near the end of this series to determine whether the homogeneity and molecular weight of the sample had remained the same during this period.

The density gradient experiments in CsCl were performed both before and after the analyses given in Table I.

Several two-component sedimentation equilibrium experiments in KBr and RbBr can be directly compared with the

periments were performed following the density gradient experiments in KBr and RbBr, about two years after the sample had originally been prepared. The experiments yielded values of 66,200 and 66,800 for the z-average molecular weight with average deviations for each analysis of less than 1,000. This result indicated that the sample may have changed during this period of time and had possibly undergone partial decomposition. Another possibility may be that a small amount of dimer may have been present originally and dissociated during this long storage period. A high voltage paper electrophoresis experiment showed that no ninhydrin positive material was present in the sample other than the albumin itself.

The final two-component experiment was performed with another portion of the BMA prepared by Dr. Ridgeway. This sample however had been kept at -20°C since its preparation whereas the above sample was repeatedly thawed as needed. A molecular weight of 70,100 was obtained. This material was used in the experiments conducted in CsBr, CsI, and Cs_2SO_4 salt solutions. Density gradient runs in CsCl and RbBr were performed to determine whether the results obtained with the first sample could be duplicated. Essentially identical values for ρ_0 and σ were achieved. Thus, while the low result of 66,500 cannot be understood, it is felt that the results of the density gradient experiments in KBr and RbBr can be directly compared with the

results in other salt solutions.

Procedures for Density Gradient Experiments

The most serious problem encountered in density gradient experiments with BMA is that of the correct selection of the baseline, i. e. the refractive index gradient distribution due to the solvent alone. The baseline is tilted and curved not only because of bulging of the windows but also because of the non-constant density gradient. Experience has shown that it is very difficult to obtain an accurate value of σ unless the baseline is experimentally available. Extrapolation between the ends of the sigmoidal curve due to the Gaussian protein distribution is at best a crude approximation. Even the midpoint of the sigmoidal curve, which is used to determine the buoyant density of the macromolecular species, cannot be obtained with adequate precision unless an experimental baseline is used.

To obtain the correct baseline, it is essential that the initial solution densities of the solvent and BMA solution be equal and that the liquid column lengths be identical. The first requirement can be met by careful refractometry (see Proposition 1 for a more accurate technique). A solution of the second problem was obtained after numerous experiments with a variety of procedures.

Selection of Centerpiece and Filling Technique

Method 1. Single-sector centerpiece. One method used to insure identical column lengths was to assemble a cell

with a single sector, 40° , metal centerpiece using a molybdenum disulfide grease. The cell was filled with ca. 0.7 ml. CsCl. solution of the appropriate density and was accurately weighed. After centrifuging to equilibrium, schlieren photographs were taken and the cell was reweighed. Losses of 3-4 mg. were generally observed. After withdrawal of the cell contents, the cell was refilled to the same weight with the BMA in CsCl solution. This was done without disassembling the cell. The cell was again centrifuged and equilibrium photographs obtained. Exact superposition of these photographs was then required. The menisci were used for horizontal alignment. A fine copper wire, 0.003 in. diameter, was inserted horizontally in front of the schlieren camera to provide a reference line on the plate for accurate vertical alignment. This procedure was found to be the least satisfactory of the three techniques investigated. It is difficult to insert the identical weight of BMA solution. Frequently, in the course of adjusting the weight, some solution is lost between the shell and the centerpiece and reproducible column lengths were not obtained. Also, inherent in this procedure are several problems associated with performing duplicate centrifuge runs. The cell windows may distort differently. Operating conditions must be held constant and the time for performing an experiment is more than

doubled.

Method 2. Non-grooved double-sector centerpiece.

Another method examined was the use of a double-sector, $2\frac{1}{2}^{\circ}$ epoxy resin centerpiece. The use of such a centerpiece requires the insertion of identical volumes of baseline and protein solution into each side of the cell. Also, the two sectors must have identical dimensions and must deform in identical ways.

A syringe holder with a micrometer head and Agla brand, micrometer, all-glass 1 ml. syringes supplied by Burroughs Wellcome and Co., London, were used. In several of the first experiments 25 λ of fluorochemical was inserted into each sector in order to accurately locate the cell bottom (17). In later experiments, fluorocarbon was not added because of occasional filling difficulties and because the position of the cell bottom need be determined with only moderate accuracy. About 0.4 ml. of CsCl solution which corresponded to an 800 division advance of the micrometer was then inserted into each side of the centerpiece. Number 27 gauge needles were used. The ends of the needles had been ground flat. The needles were bent at right angles near the center of the shaft. They were wiped with a solution of stearic acid in benzene to avoid wetting problems.

This procedure was successful in achieving identical column lengths in only about half of the dozen or so experiments in which it was used. The failures were due to uneven

cell distortion, wetting at the filling hole, or problems associated with the solution delivery.

Numerous attempts were made using either water or NaCl solutions to calibrate the above two methods. Consistent and reproducible results could not be obtained with either technique.

Method 3. Grooved double-sector centerpiece. The most consistently successful technique involved the use of a double-sector, $2\frac{1}{2}^{\circ}$, epoxy centerpiece with two small grooves connecting the two sectors. One groove is located at the top of the centerpiece to permit equilibration of air pressure. The other groove is near the center of the column. About 0.40 ml. of baseline solution is placed in one side and 0.38 ml. of protein solution in the other. Upon reaching ca. 7,000 rpm, the baseline solution is transferred into the BMA solution through this central groove until the column lengths are exactly equalized.

The procedure provides a rapid method of filling the cell and identical column lengths are assured. The disadvantages are minor. If the center of the band is near the groove, some macromolecular material may pass through the groove and form a band of low concentration there. Although this introduces some difficulty in drawing the baseline, it does not affect the results because the subtraction of the gradient of one Gaussian distribution from another of the same σ yields the correct standard deviation.

The gradient of a Gaussian concentration distribution is proportional to the concentration at that point. Thus the subtraction of two such gradients of the same σ is equivalent to the subtraction of two Gaussian distributions. The standard deviation of such a distribution is clearly independent of c_0 . Another problem occasionally encountered toward the end of this work was that on deceleration, the solution in one sector would transfer into the other sector. This is caused by a failure of the polyethylene gasket seal on one side. It does not cause any serious problem other than to obviate the possibility of checking the solution refractive indices at the conclusion of the run. This was a routine part of each experiment to insure that no evaporation had occurred.

No firm conclusion was reached as to the requirements of a particular combination of windows and centerpiece time, which would distort uniformly and reproducibly. Although one particular double-sector centerpiece was used for much of the work, the quartz discs were randomly changed. Thus it is believed that satisfactory results can be obtained with almost any parts supplied by Spinco.

Unless otherwise indicated, all of the experiments described below were performed with such a grooved double-sector centerpiece.

General Run Conditions

All experiments were performed in a standard Spinco Model E analytical ultracentrifuge equipped with an RTIC unit. All measurements were made at an angular velocity of 56,100 rpm and a temperature of 25.0°C. The results were recorded on Eastman Kodak metallographic plates using a phase plate in the schlieren optical system. All centerpieces employed were 12 mm. thick. The angular velocity used in the calculations was determined from the time interval between odometer readings made at the beginning and end of each run.

The time necessary for equilibrium to be established was determined by tracing photographs taken at successive time intervals. The center of the band and the position and height of the maximum and minimum were measured. When no further change was noted after a suitable length of time, the distribution of protein in the CsCl gradient was considered to be at equilibrium.

An irregularly shaped band is formed between 6 and 7 hours. Depending on how close ρ_e^0 is to ρ_0^0 , a symmetrical band is formed at about 8-9 hours at essentially the correct banding position. This distribution is not the equilibrium one however in that the band narrows with a corresponding increase in height of the inflection points until no further change is noted after 15 hours. Several runs were continued for about 45 hours and measurements of photographs obtained

at 6-8 hour intervals showed no detectable change in band position or shape. This demonstrates not only that equilibrium was established but also the fact that BMA is stable for extended periods of time at room temperature in this high salt concentration.

Most experiments were run for 24-30 hours. The minimum running time was 22 hours.

Preparation of Solutions

Solutions were prepared by mixing appropriate volumes of concentrated CsCl solution of density ca. 1.8 gm./ml., OD^{260} 0.025, and pH 7.1, 0.1 M NaAc buffer pH 5.5, 5% BMA solution and/or H_2O . The ratio of the volumes of water and stock CsCl solution were calculated with a non-additive volume relationship and the relation between density and weight fraction of CsCl (14). The solution densities were then adjusted if necessary by means of a Zeiss refractometer using the relation between refractive index $n_D^{25^\circ C}$ and $\rho^{25^\circ C}$ given in Table VII such that $n_{BSA\ soln} = n_{baseline} + 0.0018 \times C$ where C is the protein concentration in gm./ml.%. All solutions contained 0.01 M acetate buffer and were ca. 0.10% in BMA unless otherwise indicated. The pH of the solutions varied between 5.5 and 5.6.

Measurement of Plates

As shown below, an accurate evaluation of σ requires an integration under the sigmoidal curve shown in figure 3.

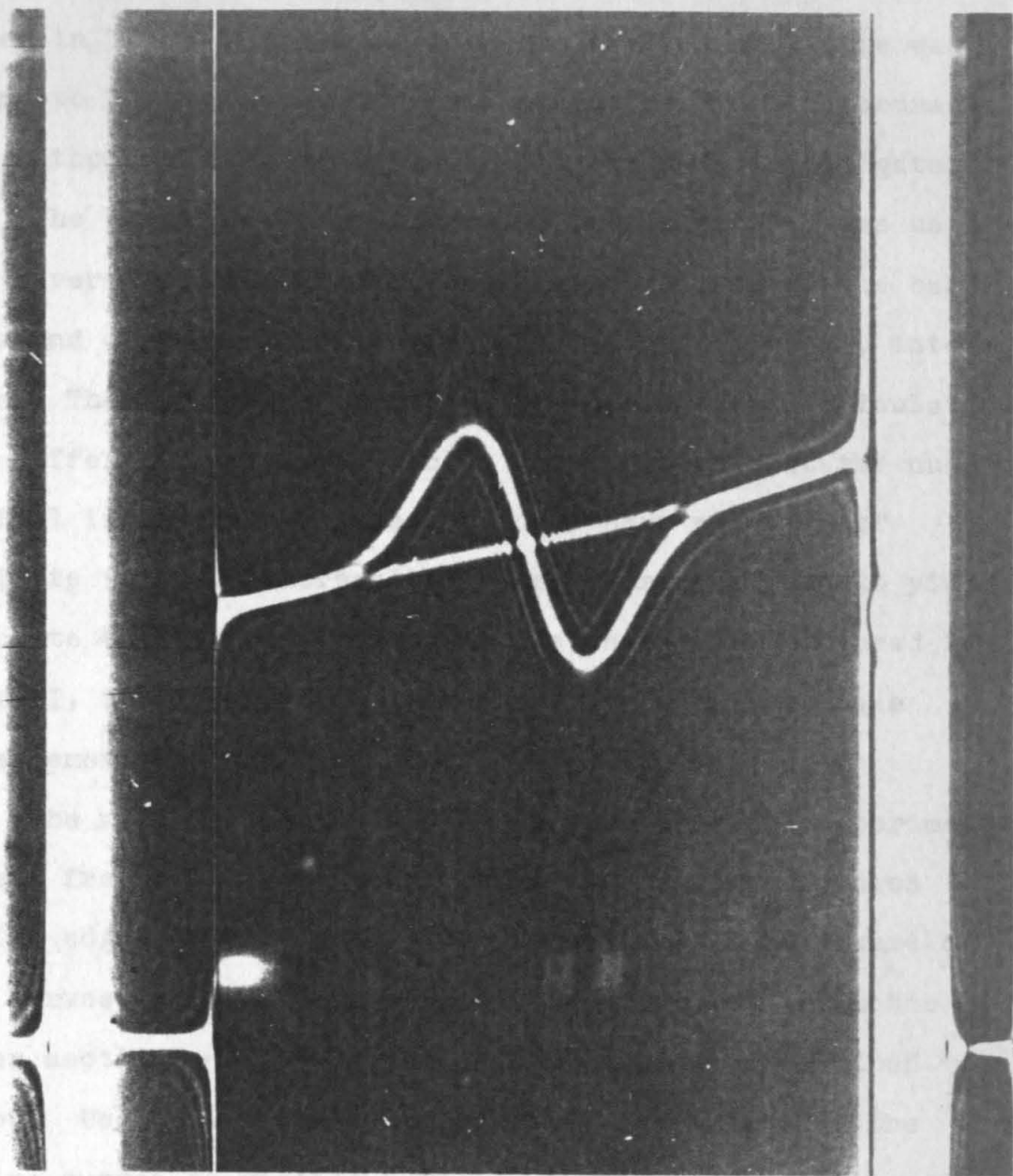


Figure 3 - Schlieren photograph of 0.1% BMA
in 2.59 molal CsCl and of baseline at equilibrium,

This is the equilibrium photograph of experiment no. 3 given in Table IV. A numerical integration procedure was found to be the simplest and to yield the desired accuracy. Two methods of performing this analysis were investigated. The Gaertner comparator described in Part II was used for several analyses. The vertical coordinates of the baseline and of the protein curve were measured at 5 mm. intervals. These numbers were recorded on a printing calculator. The differences were carried as subtotals so that the numerical integration was performed without re-entry of ordinate values. Whereas the comparator was found to yield accurate values when horizontal distances were measured in Part II, it was not found to be satisfactory for these measurements. The main problem in analyzing double sector experiments arises from the overlapping of the interference fringes at the edges and at the center of the band. The nature of the curves in these regions can be interpolated from the other sections of the curves in the procedure described below. Use of a comparator, however, requires that the entire curves be visible. The comparator was used to measure several plates that were also measured by the procedure described below. The precision as judged by a comparison of the area under each lobe and by the nature of the log plots was found to be considerably less when using the comparator.

More satisfactory results could have been obtained perhaps with the comparator if the data measured in the clearly visible regions had been plotted and the curves interpolated from these points. Because this requires an additional step, it was decided that the following procedure was the more satisfactory.

The analysis procedure used throughout was that of tracing 10-fold enlargements of the schlieren plates on large vellum sheets. An Omega II-D enlarger was used. The position of the curves was transferred to the paper by careful placement of a series of dots which locate the center of the bright central fringe. The shading of the first order dark fringes is helpful in placing the dots. This procedure can be performed accurately and rapidly. Smooth curves were drawn through the dots. The positions of the top and bottom reference edges, the menisci and the cell bottom were accurately located. The area under the sigmoidal curve was numerically integrated using lines drawn parallel to the menisci at 5 mm. intervals and measured with a precision ruler. The mid-point heights of the 5 mm. wide trapezoids were recorded with a printing calculator as above.

A necessary criterion for a successful experiment is that the areas under the two lobes of the curves be equal. If the areas are widely divergent, either the baseline has been drawn incorrectly or the solution densities were not

equal. This area requirement is not a sufficient condition for a satisfactory analysis. This was shown for one experiment for which a satisfactory baseline was not available. Several baselines were drawn at different elevations and numerical integrations performed until the areas differed by less than 1%. The resulting log plots were not linear to 1σ indicating that the curvature of the baseline selected was incorrect. This again points to the necessity of having the correct experimental baseline.

The precision of this method of numerical integration was determined by making duplicate tracings of the same plate. This was done for several experiments. In all cases, the area under one lobe was determined with a precision of $\pm 1.0\%$. Another check on the precision of this method was to compare the ratio of the areas to the ratio of the cotangents of the bar angles in successive photographs. The elevation on the plate should be directly proportional to the cotangent of the bar angle. The comparison was made with the 55° and 80° photographs of experiment no. 2 listed in Table IV. The ratio of the cotangents is 3.97. The ratios for top and bottom lobes were 3.88 and 3.94 respectively.

The distance between the reference edges of the counterbalance used was measured with an optical comparator and found to be 1.595 cm. as opposed to 1.600 cm. The top reference edge was assumed to be 5.730 cm. from the axis of rotation at 56,100 rpm.

Determination of apparent specific volume of BSA
in water and in concentrated CsCl solution

The apparent specific volumes (φ) of serum albumin in water and in a 2.47 molal CsCl solution, a composition corresponding to the buoyant density*, were measured by pycnometric procedures (cf. for instance "Methods in Enzymology" (19)).

The protein solution was prepared by dissolving 4.0 gm. of albumin in 80 ml. of twice distilled water at 5°C. Twenty grams of Amberlite MB-3, anion-cation resin, was added and the mixture kept at 5°C overnight. The resulting light yellow, isoionic solution of pH 5.11 was decanted and used without further purification.

The concentration of this solution was determined by evaporation to dryness. Four weighed aliquots, ranging from 1.0 to 2.5 ml. were evaporated in 30 mm. flat weighing bottles. They were dried at 110°C. After a few minutes cooling period, they were placed in a desiccator over P₂O₅. After equilibration, they were covered and weighed. Weighings were made daily until a constant value was obtained after six days drying time. A precision of 0.0004 gm. protein/gm. water was achieved.

* The term buoyant density (ρ_0^0) is used to describe the density of the solution at atmospheric pressure at the center of the protein distribution.

Thirty-five ml. pycnometers of the flask type with a 1 mm. capillary were used. The volumes were adjusted in a $25 \pm 0.02^\circ\text{C}$ water bath. Weighings were always made against a tare which was handled in the same manner as the filled pycnometer. All weights were corrected to vacuum.

Apparent Specific Volume of BSA in Water

The weight of the pycnometer filled first with water and then with protein solution was determined. At least two fillings and weighings were carried out for each density determination. A precision of ± 0.0003 gm. was generally achieved. The apparent specific volume, φ , was then calculated from the relation

$$\varphi = \frac{d_0 - d_1}{c' d_0 d_1} + \frac{1}{d_1}$$

where d_0 = density of the solvent, d_1 = density of the solution, and c' = concentration of solution in gm. protein/gm. solvent.

Apparent Specific Volume of BSA in 2.47 Molal CsCl Solution

The determination in CsCl solution is complicated by the two-component solvent. Satisfactory measurements were obtained by mixing exactly equal volumes (22 ml.) of water and a concentrated CsCl solution. The density of the CsCl solution was adjusted refractometrically so that addition of an equal volume of water would yield a composition

corresponding to the buoyant density. The masses corresponding to these volumes were accurately weighed in stoppered, 50 ml. flasks and the solutions carefully mixed.

The protein solution was similarly prepared. The protein concentration was used to calculate the amount of BSA solution required to again add the same mass of water to the CsCl solution. The masses were adjusted to within about 0.4 mg. in the 35-40 gm. weighings. Density measurements of these solutions yielded a value of φ for BSA in a CsCl solution.

The measurements in CsCl were conducted in duplicate on different protein solutions in which concentrations were independently determined. The results of these measurements are listed in Table II.

TABLE II

Apparent Specific Volume of BSA in Water
and in a 2.47 Molal CsCl Solution

T = 25.0°C

Solvent	c'	d_0	d_1	φ
A. H ₂ O	0.0467	0.99704	1.00908	0.7347
B. CsCl	0.01824	1.28151	1.28277	0.7361
	0.01877	1.28187	1.28318	0.7369
Average for B.				0.736

The value for φ in water agrees favorably with the

value 0.7343 reported by Dayhoff, et al (18). Cox and Schumaker (20) have recently reported values of φ in water and in 1.4 molal KCl. Interpolating their data between measurements at 29.9°C and 10°C for the measurement in salt solution gives a value of 0.739 at 25°C. Considering the precision of their data, this number may be regarded as not differing significantly from the value reported here.

The close agreement of the values for φ in water and in a concentrated CsCl solution indicates that the BMA molecule experiences approximately the same electrostriction in H₂O as in a concentrated salt solution or that there are several compensating factors. The close agreement is in accord with the present picture of this globular protein as a compact structure which is not subject to large deviations in size.

As pointed out by Edsall (21), the quantity $\partial\varphi/\partial c'$ is very small or negligible for most aqueous protein solutions. Thus, the apparent specific volumes obtained above are considered to be the partial specific volumes, \bar{v} , in the respective solvents. Since the values of \bar{v} in water and in 2.47 molal CsCl are nearly identical, the value of 0.736 will be assumed in all salt solutions subsequently discussed.

Calculations

The experimental parameters in equation 1 which must be determined are r_0 , ρ_0 , $(d\rho/dr)_0$, and σ^2 .

The center of the Gaussian band can be located on the plate to ± 0.002 cm. at the intersection of the baseline and sigmoidal protein curve. The value of r_0 in centimeters is determined by dividing the distance between band center and the top reference edge on the tracing by the magnification factor, MF, and adding the result to 5.730. The magnification factor is found by dividing the distance between the reference edges in cm. by 1.595. All other radial distances were similarly obtained.

As shown in Part II, the salt distribution is unaffected by pressure. Thus the data of Part I can be used to locate r_e , the isoconcentration point corresponding to ρ_e^0 , the initial solution density. The value of $(r_e - r_a)/(r_e' - r_a)$ was obtained from the middle curve of figure 5 of Part I. The value of r_e was found with an accuracy of about 0.003 cm.

The bands were always formed near enough to r_e so that a constant density gradient could be assumed between r_e and r_0 . The buoyant density at atmospheric pressure was computed from the approximate relation

$$\rho_0^0 = \rho_e^0 + \frac{\omega^2 r_0}{\beta^0} (r_0 - r_e) \quad (4)$$

The values of β^0 which correspond to ρ_e^0 are tabulated in Part I.

The buoyant densities thus calculated are a function only of salt composition. The buoyant density corresponding to the physical situation was next calculated as

$$\rho_o = \rho_o^o (1 + K P_o) \quad (5)$$

where K is the isothermal compressibility of the CsCl solution of this composition and P_o is the hydrostatic pressure at band center. The value of K was found from Pohl's data (22) to be $35.2 \times 10^{-6} \text{ atm.}^{-1}$. The magnitude of P_o was calculated by the procedure outlined in Part II. The pressured buoyant densities are 0.007 density units, 0.6%, higher than the values determined by means of equation 4.

The density gradient at band center was computed as the sum of the composition and compression density gradients.

$$\left(\frac{d\rho}{dr}\right)_{\text{phys},o} = \left[\left(\frac{1}{\beta^o} + K \rho^{o^2}\right) \omega^2 r\right]_{r_o} \quad (6)$$

The compression term is $9\frac{1}{2}\%$ of the composition term for this system.

The above treatment neglects any interactions due to the presence of the macromolecule. Such effects are the compressibility of the polymer, selective solvation of the polymer, etc. The effects of some of these interactions are considered in Section D. They can contribute as much as 10-15% to the effective density gradient.

The standard deviation σ is the most difficult quantity to obtain with satisfactory precision. A variety of procedures are available for its evaluation based on the Gaussian concentration relation, equation 7. All are based on the fact that $n - n_0 = K \times c$ and hence $(dn/dr) - (dn_0/dr) = K dc/dr$. The refractive index increment K is assumed to be constant in the concentration range under investigation.* In the foregoing, n and n_0 are the refractive indices of the protein solution and the baseline solution respectively. None of the methods used require a knowledge of the refractive index increment.

$$c = c_0 \exp \left[-\frac{(r - r_0)^2}{2\sigma^2} \right] \quad (7)$$

The simplest procedure for evaluating σ and the only one not requiring a numerical integration is to replot the two lobes of the protein gradient curve after subtraction of the baseline. The distance from the center of this concentration distribution to each maximum is equal to σ . This is readily seen by differentiating equation 7 twice and equating the result to zero. While this method is rapid, it yields only an approximate value of σ because the maxima are

* The validity of this assumption is examined in the Appendix. A variation of the refractive index increment of the form $(dn/dc) = (dn/dc)_0 (1 - k\epsilon)$ was assumed. The quantity k is a positive constant and ϵ is the distance from band center. The analysis indicates that this effect causes a shift in band position and alters the shape of the (dn/dr) distribution. Both effects are negligible.

broad. A precision of ± 0.005 cm. can be obtained. This corresponds to the precision found by Cox and Schumaker (8) who used absorption optics.

Another procedure which also suffers the disadvantage of being an evaluation made at just one point in the distribution is to numerically integrate the curve described above and to obtain the concentration distribution shown in figure 5. Measurement of the half-width of this curve at an elevation of $0.609 K(n-n_0)_{r_0}$ yields the value of σ . A plot of $1/n \cdot dn/dr$ versus $(r-r_0)$ should be linear of slope $-1/\sigma^2$. However, this procedure is very sensitive to errors at the ends of the CsCl column. Badly skewed curves were obtained at both ends of the cell, the plots being linear only near the center of the cell.

The best procedure found and the one used in all of the experiments reported below was the logarithmic plot. A plot of $\ln K(n-n_0)$ versus $(r-r_0)^2$ is linear for a Gaussian concentration distribution with slope inversely proportional to σ^2 . The running subtotals of the numerical integration were plotted as the ordinate values and the values of $(r-r_0)^2$ in cm. on the tracing as abscissa values on semi-log graph paper. The slope of this straight line multiplied by the square of the magnification factor is equal to $-1/2 \sigma^2$.

A protocol sheet was developed to facilitate the computations described above. This converts a sometimes perplexing calculation into a routine procedure and also

provides a convenient way to file the raw data and the results. A sample copy is included in the Appendix.

The third portion of the Appendix is an examination for this system of the magnitude of an approximation made in the derivation of equation 1. It was necessary to neglect terms of order higher than $(r-r_0)^2$ in the original formulation. It is shown that this is a good approximation even for BMA in a CsCl solution where $\sigma = 1$ mm.

The amount of hydration was computed by the two methods discussed in the introduction to this section. The value of \bar{v}_3 in equation 2 from which Γ'_a was calculated was the previously measured value for the anhydrous protein in CsCl, namely 0.736 ml./gm.

2. Concentration plot	Top	0.111	0.110
	Bottom	0.109	0.106
	Average	0.110	0.106

Results and Discussion and 0.001 cm. respectively. A comparison of the four methods of evaluating σ is presented in Table III. Measurements were made on photographs taken at 55° and 85° bar angles. The standard deviations are uniformly higher than those from the bottom side of the distribution.

TABLE III

The density, density gradient, and refractive gradient Standard Deviations Evaluated by Various Methods (Expt. no. 2; 0.11% BMA in 2.47 molal CsCl solution)

Distribution was obtained by the computer program outlined in Part I. The composition density gradient distribution photograph similar to that shown in figure 1. The concentration distribution evaluated from experiment is shown in figure 2. The distribution is seen to be similar to that shown in figure 3. The distribution is seen to be similar to that shown in figure 4.

Method	Type of σ	55° (cm.)	85° (cm.)
1. Sigmoidal plot	Top*	0.099	0.107
	Bottom	0.106	0.104
	Average	0.103	0.106
2. Concentration plot	Top	0.111	0.110
	Bottom	0.109	0.106
	Average	0.110	0.108
3. $(dn/dr)/n$ vs. $(r-r_0)$ plot	Average	0.108	0.108
4. Logarithmic plot	Top	0.113	0.109
	Bottom	0.109	0.107
	Average	0.111	0.108
Average		0.110	0.108

* Top is used in this and in all subsequent graphs and tables to indicate that this result was derived from the less dense region of the band closest to the center of rotation. Bottom stands for the other half of the band.

The average deviations of all the values in Table III

for the 55° and 85° analyses are 0.002 cm. and 0.001 cm. respectively. These deviations correspond to 4% and 2% in the molecular weights. It is to be noted that the values of σ determined from the top side of the band are uniformly higher than those from the bottom side of the distribution.

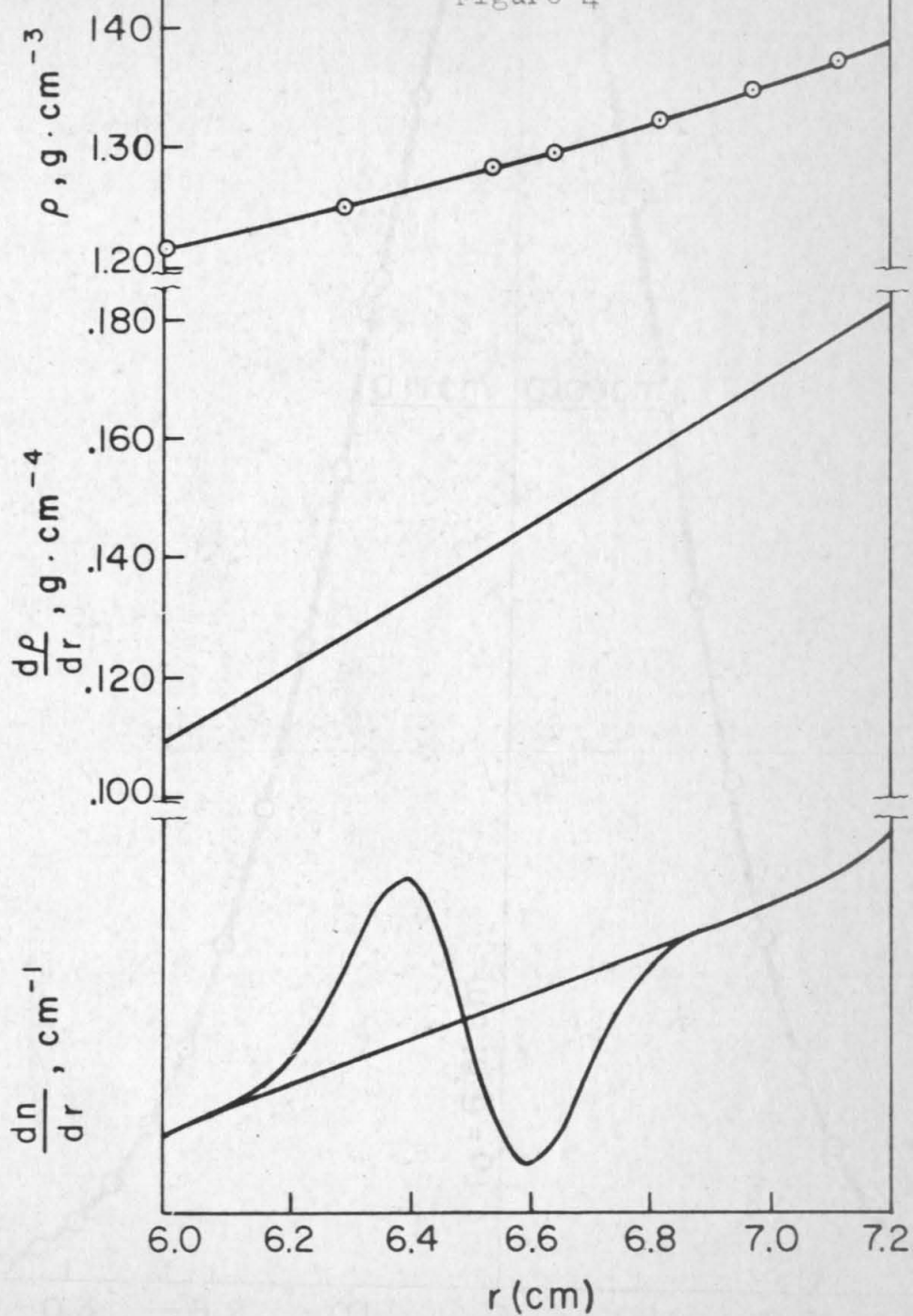
The density, density gradient, and refractive gradient of experiment no. 2 is given in figure 4. The density distribution was obtained by the computer program outlined in Part I. The composition density gradient was then calculated from this data for $\rho(r)$ using the $\beta(\rho)$ data of Part I. The bottom plot is a tracing of the equilibrium photograph similar to that shown in figure 3. The ordinate of this plot is in arbitrary units and hence is not expected to be superimposable on the middle plot of $d\rho/dr$.

The concentration distribution evaluated from experiment no 2. is shown in figure 5. The distribution is seen to be slightly skewed to the light side. Otherwise the data points fall on a reasonably smooth and symmetrical curve out as far as elevations could be measured. The ordinate is in arbitrary units of $K(n-n_0)$.

A typical logarithmic plot is presented in figure 6. This is the data obtained from a tracing of a 75° photograph. The behavior noted here is typical of almost all the experiments performed. The data from the top half are usually linear out to about 2σ and then curve downward. The data from the bottom half however are seldom linear

Density, Density Gradient and
Refractive Index Gradient;
0.1% Mercaptalbumin in 31.08% CsCl

Figure 4



DISTRIBUTION OF MERCAPTALBUMIN CONCENTRATION
IN A DENSITY GRADIENT AT
SEDIMENTATION EQUILIBRIUM

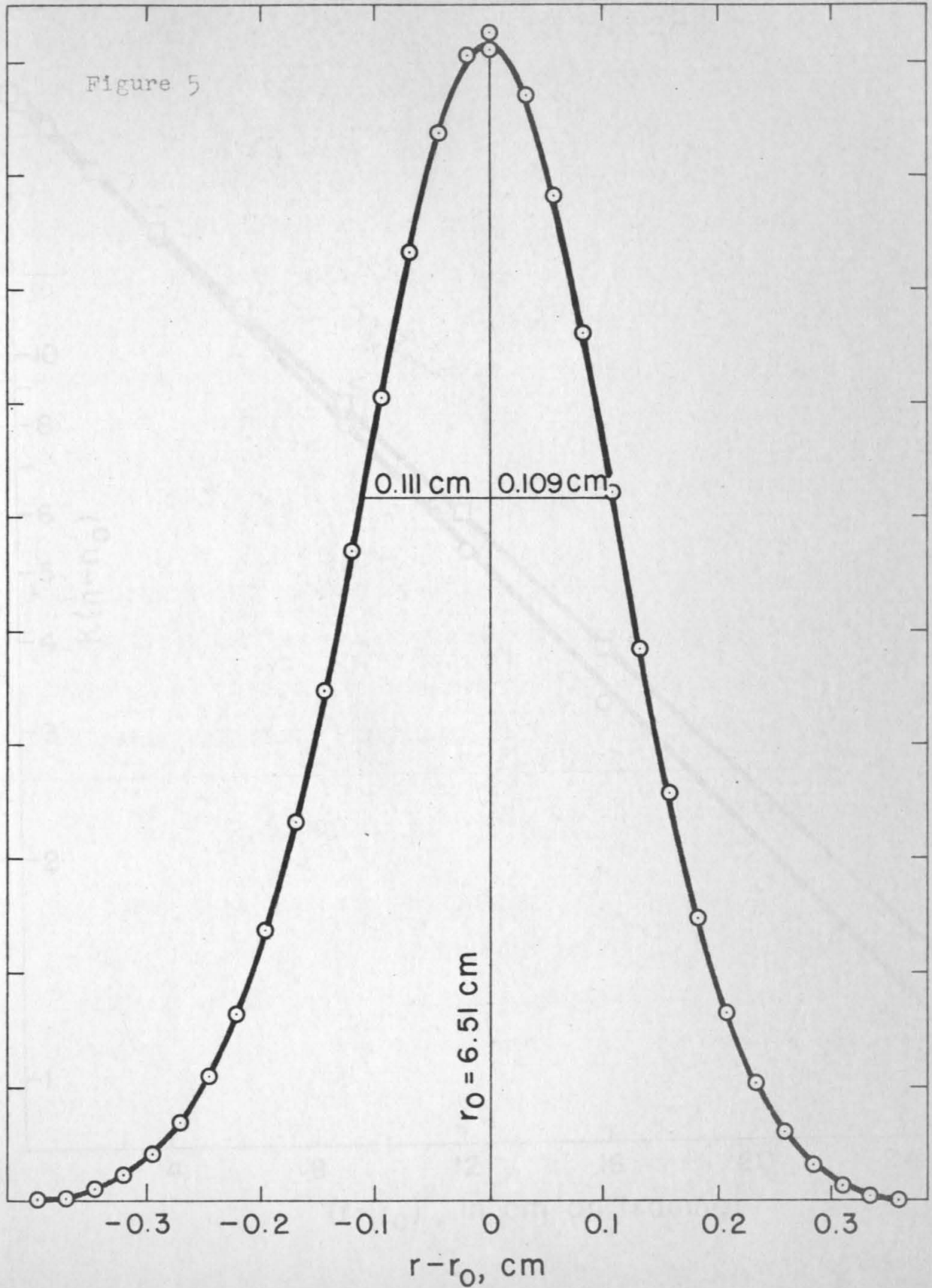
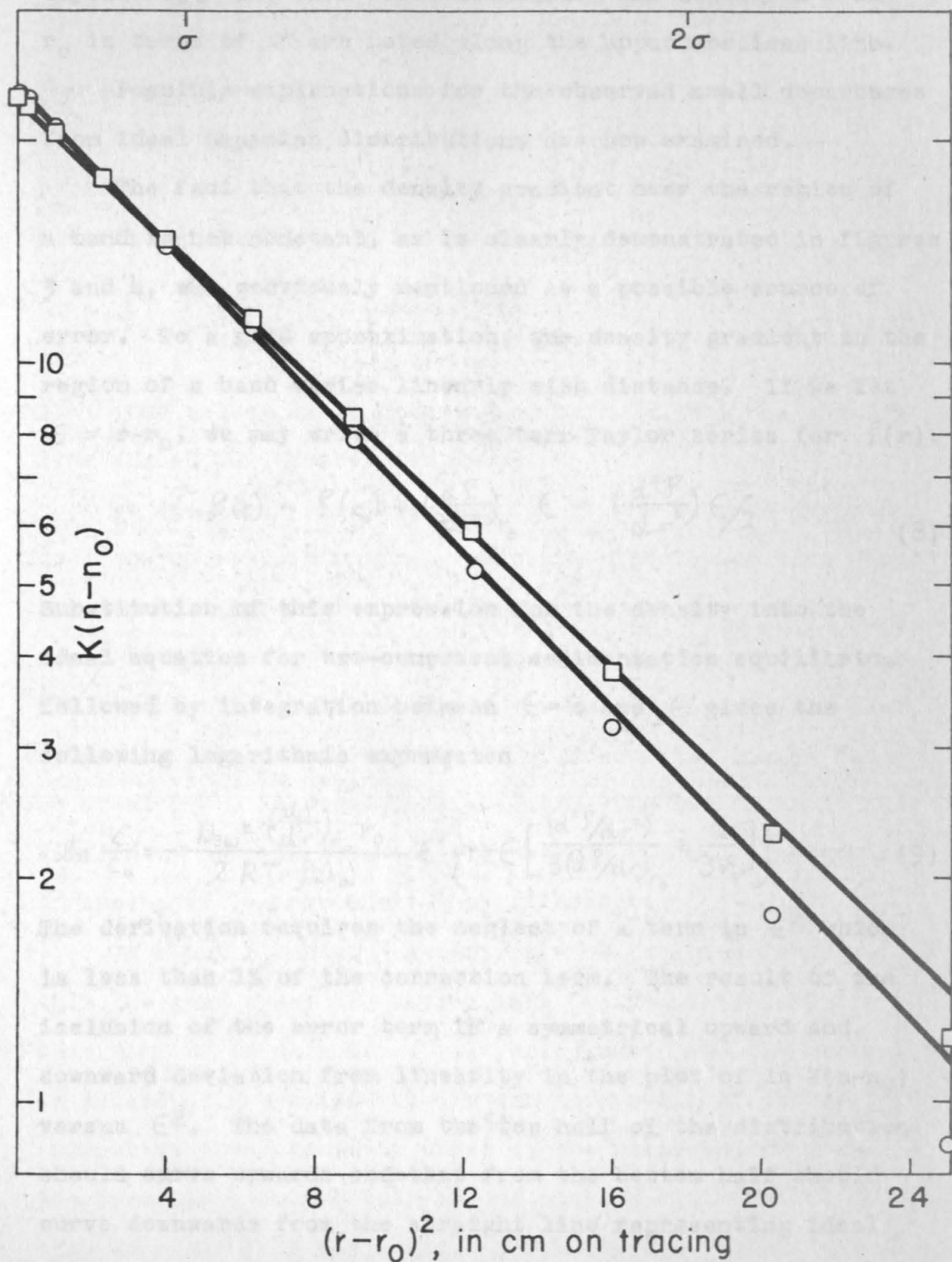


Figure 6 - Logarithmic Plot of Experiment No. 6,
0.10% BMA in 2.47 Molal CsCl



beyond 1.5σ and then curve downward. The distances from r_0 in terms of σ are noted along the upper abscissa line.

Possible explanations for the observed small departures from ideal Gaussian distributions are now examined.

The fact that the density gradient over the region of a band is not constant, as is clearly demonstrated in figures 3 and 4, was previously mentioned as a possible source of error. To a good approximation, the density gradient in the region of a band varies linearly with distance. If we let $\epsilon = r - r_0$, we may write a three term Taylor series for $\rho(r)$.

$$\rho(r) = \rho(r_0) + \left(\frac{d\rho}{dr}\right)_{r_0} \epsilon + \left(\frac{d^2\rho}{dr^2}\right) \frac{\epsilon^2}{2} \quad (8)$$

Substitution of this expression for the density into the ideal equation for two-component sedimentation equilibrium followed by integration between $\epsilon = 0$ and ϵ gives the following logarithmic expression

$$\ln \frac{c}{c_0} = - \frac{M w^2 \left(\frac{d\rho}{dr}\right)_{r_0} r_0}{2 RT \rho(r_0)} \epsilon^2 \left\{ 1 + \epsilon \left[\frac{(d^2\rho/dr^2)}{3(d\rho/dr)_{r_0}} + \frac{2}{3r_0} \right] \right\} \quad (9)$$

The derivation requires the neglect of a term in ϵ^4 which is less than 1% of the correction term. The result of the inclusion of the error term is a symmetrical upward and downward deviation from linearity in the plot of $\ln K(n-n_0)$ versus ϵ^2 . The data from the top half of the distribution should curve upwards and that from the bottom half should curve downwards from the straight line representing ideal

behavior.

The magnitude of this deviation can be readily evaluated. The slope of the almost linear $d\beta/dr$ versus r plot in figure 4 is $0.060 \text{ gm./cm.}^{-5}$. Combination of this value with typical values of r_0 and $(d\beta/dr)_{r_0}$ for these experimental conditions allows us to write equation 9 as

$$\ln c/c_0 = -\frac{1}{2\sigma^2} \epsilon^2 (1 + 0.25 \epsilon) \quad (10)$$

At σ the values of $\ln c/c_0$ differ by 2.5% from the straight line and at 2σ they differ by 5%.

As stated in the discussion of figure 6, this deviation does not correspond entirely with the majority of data which has been obtained. The data from the lower half of the distribution deviate downward to about the expected amount. The top portion of the data however apparently never curves upward but instead curves downward after being linear out to about 2σ . A possible explanation may lie in the difficulty in extrapolating the protein and baseline curves in the outer regions where they intersect.

In about 4 out of 5 experiments it has been found that the area under the bottom lobe is from 1-3% larger than that of the top lobe. Let us assume that this error is caused by a consistently incorrect drawing of the protein refractive index gradient curve at the intersection with the baseline near the tail end of the top distribution such that an area δ is neglected. Comparing the log plot of

this distribution with that of the correct one, we can express the measured distribution for distances less than 2σ from band center as

$$\ln \frac{c + \delta}{c_0 + \delta} \cong \ln \frac{c}{c_0} \left(1 - \frac{\delta}{c_0}\right) \left(1 + \frac{\delta}{c}\right) \quad (11)$$

or

$$\ln \frac{c}{c_0} = \ln \frac{c + \delta}{c_0 + \delta} - \frac{\delta}{c_0} \left(\frac{c_0}{c} - 1\right) \quad (12)$$

Because δ is negative, each point on the log plot for the data of the top half must be elevated to obtain the correct plot. The magnitude of this effect is surprisingly large. Suppose $\delta = 0.01$; the measured total area of the top lobe corresponding to c_0 is 1% low. At 2σ , this error amounts to 3% of $\ln c/c_0$. For larger values of δ , the error is correspondingly larger. Thus we have found that the effect of the non-constant gradient can be overcome by a very small error in the numerical integration. It is difficult to quantitatively analyze the situation because neither area is known absolutely. Nevertheless, the above calculation qualitatively explains the majority of the results obtained.

Taking the antilog of equation 10, we can express the concentration of BMA in a non-constant gradient.

$$c = c_0 \exp \left[-\frac{1}{2\sigma^2} \epsilon^2 (1 + 0.25 \epsilon) \right] \quad (13)$$

This equation predicts the correct shape for the concentration distribution given in figure 5. The curve is wider for the top half than it is for the bottom half of the plot.

Both the concentration plot and logarithmic plot should yield higher values for σ for the upper half of the plot than for the lower. As shown in Tables III and IV, this trend is generally followed.

In conclusion, the best procedure and the one that was followed is to draw straight lines through the linear portion of the data starting at $\epsilon = 0$. The value selected for σ was the average of the two values found for each lobe. This procedure should yield the correct value of σ to within 0 to +2%.

The results of a number of density gradient experiments with BMA in CsCl solutions conducted and analyzed as described above are presented in Table IV.

Apart from the one high value for ρ_0 , it appears that the buoyant density at the pressures in the rotating liquid column can be determined with a precision of ± 0.001 gm./ml. The buoyant density of BMA in a CsCl gradient is 1.282 gm./ml.

Averages should not be taken for the density gradients or the standard deviations. Whereas the ρ_0 's are all essentially identical, the r_0 's varied somewhat and this is reflected in a higher or lower density gradient. The σ 's

should vary in a corresponding inverse relation but the precision in the σ values is not good enough to observe this. Again it can clearly be seen however that the values derived from the top half are larger than those derived from the bottom half.

TABLE IV

Results of Density Gradient Experiments
with 0.1% BMA in CsCl Solutions**

Expt. No.	ρ_0	$(\frac{d\rho}{dr})_{\text{phys},0}$	σ_{top}	σ_{bot}	$M_{\text{app},0}$ Top Bottom	Γ'_a	Γ'_b
1†	1.282	0.153	0.109	0.105	75,500 81,700	0.200	0.115
2	1.282	0.151	0.109	0.107	78,800 82,400	0.200	0.143
3*	1.287	0.153	0.106	0.106	81,000 80,700	0.184	0.146
4	1.282	0.153	0.105	0.104	82,800 83,600	0.200	0.180
5	1.281	0.154	0.108	0.105	77,400 81,300	0.204	0.126
6	1.282	0.154	0.108	0.105	76,300 81,100	0.200	0.116
Ave	1.282				78,600 81,600	0.198	0.138

** Columns 2, 4, and 5 are physically measured quantities. All other quantities are based on assumptions stated in the text.

† Non-grooved double-sector centerpiece, 0.15% BMA

* Non-grooved double-sector centerpiece, 0.20% BMA

This variation in σ is reflected directly in the apparent molecular weights presented because all other parameters are fixed for a given experiment. Although deviations as large as 8% between the two molecular weights evaluated for a single experiment are observed, several

generalizations can be made. The standard deviations of the values for M_{top} and M_{bot} are ± 2800 and ± 1100 respectively or about 2-3%. At present no statement can be made as to why there is more scatter in the M_{top} values. The molecular weights evaluated from the top half of the distribution are lower by an average of about 4% than the values obtained from the upper half. Finally it is clear that we are not measuring the molecular weight of the anhydrous species. The results presented in Table IV for the number average molecular weights are 10,000 higher than the z-average values given earlier.

The precision of the Γ'_a numbers reflects the accuracy with which the buoyant density can be determined. The values of Γ'_b were derived from the average of the two molecular weights obtained for one experiment. The average deviation of 0.023, ca. 17%, reflects the wide fluctuations in the molecular weight values.

The Γ'_a values measure only the net amount of water bound. However, the Γ'_b reflect the total amount of material bound, both water and salt, and hence the numbers should indicate that $\Gamma'_b \geq \Gamma'_a$. Despite the lack of precision in the Γ'_b values, it is significant to note that the average of the Γ'_b values is considerably lower than the Γ'_a average. Because this is the inverse of the expected behavior, the result shows that one or perhaps both of these quantities does not represent the physical situation.

SECTION B

THE BUOYANT BEHAVIOR OF BOVINE SERUM
MERCAPTALBUMIN IN VARIOUS SALT SOLUTIONS

Serum albumin is an unusual protein because of its ability to bind large numbers of anions (23, 24). In order to determine the effect of such binding on the previous results and in an attempt to clarify the ambiguities arising from the differences in the two methods of calculating Γ' observed in section A, an investigation of BMA in a variety of salt solutions was conducted. It was expected that information concerning solvation and binding would be obtained. Also, the problems associated with conducting density gradient experiments with proteins in solvents of both higher and lower density gradients were examined.

The salts used in this investigation were selected so that the effects of both an anion and a cation series could be determined. The salts chosen for this purpose were CsCl, CsBr and CsI, and KBr, RbBr and CsBr. Other salts investigated to determine the effects of dissimilar anions were Cs_2SO_4 and CsAc.

The Cs_2SO_4 and CsI Experimental were those prepared by
Materials. The albumin used in these experiments was the BMA sample described in Section A.

The sources of the salts and the properties of the stock solutions are given below. The optical densities at 260 $m\mu$ of the stock solutions are included to indicate the presence of unknown impurities.

The three bromide salts were used as supplied by the manufacturer. The KBr was the reagent grade material supplied by the Baker Chemical Company. It contained 0.12% chloride. The stock solution had a density of 1.358 and an $OD^{260} = 0.036$. The RbBr was produced by the De Rewal International Rare Metals Company. The stated purity was 99.6%. The properties of the RbBr stock solution were: $\rho = 1.665$, $pH = 8.02$, and $OD^{260} = 0.608$. The CsBr was obtained from A. D. Mackay Incorporated and was stated to be 99.8% pure. No stock solution was prepared as all preparations with this salt were made up to give approximately the desired density by weighing the dry salt into the appropriate quantity of water assuming the partial specific volume of the salt to be the reciprocal of the crystal density.

The CsI was supplied by Penn Rare Metals Incorporated. The stock solution of $\rho = 1.536$ was purified by sedimentation of insoluble dark particles in the Spinco Model L preparative centrifuge at 20,000 rpm for 20 minutes.

The Cs_2SO_4 and CsAc solutions were those prepared by Dr. J. Hearst (14). They were carried out in most respects as described above for CaCl solutions. Because the composition

Procedures. Density gradient experiments in each of these salt solutions were carried out in most respects as described above for CsCl solutions. Because the composition density gradients were available for KBr and RbBr solutions, the procedures followed were identical to those with CsCl. Four experiments in each solvent were conducted. With the other salt solutions, and as a check with a RbBr solution, the following procedures were used.

As is the case when any macromolecule is banded in a particular solvent for the first time, several runs at differing initial densities were required before the albumin was banded near the center of the cell. A single-sector run was performed first using an original density arrived at by extrapolating from buoyant densities obtained in other salts. If one lobe of the protein distribution curve was available on the photograph, a rough estimate of the density gradient could be obtained. If the molecular weight of the species is the same in this buoyant salt solution as in a solution in which the density gradient is known and if the radial banding positions are the same, the quantity $\sigma^2(d\rho/dr)_0/\rho_0$ is identical for both solutions. Upon inserting the known gradient, in say a CsCl solution, and the values of σ and ρ_0 in each solution into this equation, an approximate value for the density gradient in the new salt solution is obtained. Successively better approximations were obtained in the two or three experiments required

to determine ρ_0 .

When ρ_0 was known with suitable precision, the buoyancy density gradient defined by equation 21 was evaluated in all cases, except KBr and CsCl by performing a double-cell experiment. The densities of two solutions were adjusted so as to bracket the buoyant density. These solutions and the corresponding baseline solutions were placed in cells equipped with grooved double-sector centerpieces and a combination of wedges. Some pertinent primary data for the double-cell experiments are given in Table V. The equilibrium distributions were analyzed as before.

TABLE V
Double-Cell Experiments

Salt	ρ_0	$\rho_{e,2} - \rho_{e,1}$	Wedges (degrees)	Conc. BMA (gm./ml.%)
RbBr	1.302	0.053	0, -1	0.10
CsBr	1.306	0.084	-1, -2	0.05
CsI	1.331	0.111	-3, -4	0.03
Cs ₂ SO ₄	1.237	0.111	-1, -2	0.05

The equilibrium photograph of the double-cell experiment with Cs₂SO₄ is shown in figure 7. The two menisci are plainly visible. The cell bottom is fuzzy because the refractive index gradient of the upper distribution near the bottom of the cell is so great that light is bent out of the optical path. The vertical stripe due to the refer-

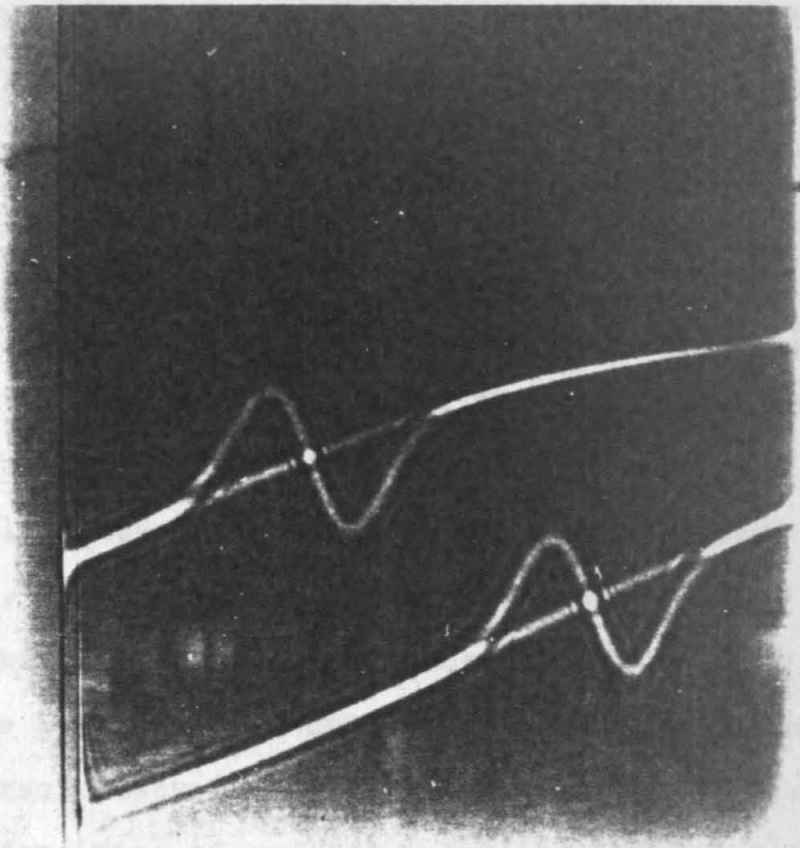


Figure 7 - Equilibrium distributions of 0.05 % BMA in Cs_2SO_4 solutions and of baselines, $\rho_{e,1} = 1.190$ and $\rho_{e,2} = 1.301$, 56,100 rpm, 25.0° C, pH 5.5

ence hole in the rotor does not show on this reproduction. It is faintly visible on the original plate and was used for spatial orientation.

The solutions were prepared in the same way as described in Section A. For convenience in preparing solutions, the relation between refractive index and density at 25°C for each salt in the concentration range of interest was obtained. Data for $n_D^{25^\circ\text{C}}$ and $\rho^{25^\circ\text{C}}$ for KBr were found in Landolt-Börnstein (25). The remaining n versus ρ relations were obtained experimentally. The relation for RbBr was obtained with considerable precision. An analytical balance was used to weigh a glass bob immersed in successively diluted RbBr solutions. The densities of these solutions could then be computed with a precision of about ± 0.0002 gm./ml. The refractive index of each solution was measured with the Zeiss refractometer.

The densities of several solutions each of CsBr, CsI, and Cs_2SO_4 were determined by weighing a calibrated 300 μ micropipette filled with solution. The refractive index of each solution was measured. Measurements were not made on CsAc solutions.

Calculations about half as large as the isothermal compressibility coefficients \mathcal{K} for each salt at the concentration corresponding to the buoyant density of BMA were obtained. The data of Gibson (26) for \mathcal{K} versus weight fraction of KBr was plotted and the value of \mathcal{K} determined directly.

Extrapolations were required for the remaining solutions. Gibson's data for KCl and KI were plotted on the same graph with the KBr data. Pohl (22) presents data for CsCl and RbCl. The values of \mathcal{K} for CsBr, CsI, and RbBr were obtained by interpolation between the two sets of data. For instance, the difference in the compressibility of a KCl and a KBr solution at a density of 1.3 was assumed to be the same as the difference between a CsCl and CsBr solution at the same concentration. The temperatures at which the compressibility coefficients are insensitive to concentration were assumed to be valid at 25°C.

Gibson (27) presents data for Cs_2SO_4 solutions only in terms of the compression as a function of weight fraction. His data for Cs_2SO_4 , KBr, and KCl were plotted on the same graph. The values for Cs_2SO_4 closely paralleled those for KBr. The value for \mathcal{K} in Cs_2SO_4 was obtained by a short interpolation between the KBr and KCl curves.

The values for \mathcal{K} for each salt are given in Table VI. These values are accurate to about $\pm 2 \times 10^{-6}$.

The buoyant densities and physical density gradients were calculated as before for the single sector KBr and RbBr experiments. It should be noted that the density

gradients in KBr solutions are only about half as large as those in CsCl and RbBr solutions (cf. β^0 values given in Table I of Part I). The compression density gradient is 18% of the composition density gradient for KBr.

TABLE VI

Isothermal Compressibilities of
Salt Solutions of Buoyant Composition*

Salt	$K \times 10^6$ (atm. ⁻¹)	Salt	$K \times 10^6$ (atm. ⁻¹)
CsCl	35.2	CsBr	40.5
KBr	33.4	CsI	43.4
RbBr	37.3	Cs ₂ SO ₄	34.0

* The temperatures at which the compressibility coefficients were determined varied from 13.8° to 25°C. Because the isothermal compressibility is an insensitive function of temperature, the values were assumed to be valid at 25°C.

The compressibility coefficients of the remaining salts were necessary only to compute the buoyant densities at the pressures in the rotating liquid column.

As mentioned above, a density gradient, which we will designate as the buoyancy density gradient, can be obtained from banding a macromolecule in two cells containing solutions of slightly different composition. The properties of this gradient can be evaluated in the following way.

Writing equation 13 of Part II for each solution, we have

$$\rho_{o,1}^{\circ} = \frac{1}{\bar{v}_{s,o}^{\circ}} (1 - \Psi_1 P_{o,1}) + \omega^2 \rho_{o,2}^{\circ} \quad (14)$$

Because $\bar{v}_{s,o}^{\circ}$ is a constant, and making the reasonable assumption that Ψ is the same in each solution, we may combine these equations.

$$(\rho_{o,2}^{\circ} - \rho_{o,1}^{\circ}) = -\frac{1}{\bar{v}_{s,o}^{\circ}} \Psi (P_{o,2} - P_{o,1}) \quad (15)$$

The pressure difference can be closely approximated as

$$\left(\frac{dP}{dr}\right)_{\bar{r}_o} P_{o,2} - P_{o,1} = \rho_o^{\circ} \omega^2 (r_{o,2} - r_{o,1}) \bar{r}_o \quad (16)$$

where $\bar{r}_o = (r_{o,1} + r_{o,2})/2$ and ρ_o° can be considered to be the average of the two buoyant densities.

These buoyant densities are composition variables and we can therefore express them as

$$\rho_{o,1}^{\circ} = \rho_{e,1}^{\circ} + \int_{r_{e,1}}^{r_{o,1}} \left(\frac{\omega^2 r}{\beta_1^{\circ}}\right) dr = \rho_{e,1}^{\circ} + \frac{\omega^2 \bar{r}_1}{\beta_1^{\circ}} (r_{o,1} - r_{e,1}) \quad (17)$$

where $\bar{r}_1 = (r_{o,1} + r_{e,1})/2$ and β_1° corresponds to the density at the radial distance \bar{r}_1 . A similar equation can be written for $\rho_{o,2}^{\circ}$. Combining the two expressions yields

$$(\rho_{o,2}^{\circ} - \rho_{o,1}^{\circ}) = (\rho_{e,2}^{\circ} - \rho_{e,1}^{\circ}) + \omega^2 \left[\frac{\bar{r}_2}{\beta_2^{\circ}} (r_{o,2} - r_{e,2}) - \frac{\bar{r}_1}{\beta_1^{\circ}} (r_{o,1} - r_{e,1}) \right] \quad (18)$$

For the case that $r_{e,1} = r_{e,2}$, this expression can be simplified with negligible error:

$$(\rho_{o,2}^{\circ} - \rho_{o,1}^{\circ}) = (\rho_{e,2}^{\circ} - \rho_{e,1}^{\circ}) + \omega^2 \left[\frac{\bar{r}_o}{\bar{\beta}^{\circ}} (r_{o,2} - r_{o,1}) \right] \quad (19)$$

where $\bar{r}_o = (r_{o,1} + r_{o,2})/2$ and $\bar{\beta}^{\circ}$ is evaluated at ρ_o° .

We can now combine equations 15, 16 and 19.

$$-\frac{1}{\bar{v}_{s,o}} \psi \rho_o^{\circ} \omega^2 (r_{o,2} - r_{o,1}) \bar{r}_o = (\rho_{e,2}^{\circ} - \rho_{e,1}^{\circ}) + \omega^2 \left[\frac{\bar{r}_o}{\bar{\beta}^{\circ}} (r_{o,2} - r_{o,1}) \right] \quad (20)$$

Noting that $1/\bar{v}_{s,o}$ closely approximates ρ_o° , this equation can be simplified by dividing by $(r_{o,2} - r_{o,1})$ and rearranging.

$$\left(\frac{d\rho}{dr} \right)_{\text{buoy},o} = \frac{\rho_{e,2}^{\circ} - \rho_{e,1}^{\circ}}{r_{o,2} - r_{o,1}} = \left[\frac{1}{\bar{\beta}^{\circ}} + \psi \rho_o^{\circ 2} \right] \omega^2 \bar{r}_o \quad (21)$$

This expression is defined as the buoyancy density gradient.

That this expression is reasonable can be seen by considering the physical situation involved in this measurement and by comparing equation 21 with equation 24 in reference 28 for the effective density gradient. Each band is formed at essentially identical salt composition but at different pressures. Thus the change in hydration with distance is the same in each band and therefore this measurement should not reflect solvation effects except insofar as these effects depend on pressure. We find that the multiplicative factor $(1 - \alpha)$ contained in the effective density gradient expression is missing in the equation for $(d\rho/dr)_{\text{buoy},o}$. This is the predominant factor expressing the effects of solvation.

The primary difference in the environment of the two bands is hydrostatic pressure. This effect is correctly included in the buoyancy density gradient expression in the Ψ term because Ψ is determined by the difference in compressibilities of the solution and of the solvated macromolecule.

The standard deviations of the top and bottom lobe of each band were determined as before. Because the buoyancy density gradient is evaluated at \bar{r}_0 , a position midway between the two bands, the average of the four values of σ was used. This is the correct value of σ for \bar{r}_0 to within 0.2% providing that $r_{0,1} \sigma_1 = r_{0,2} \sigma_2$. These products were found to agree to within 2% for the four salts examined. This provides evidence that the effects of pressure on solvation are small.

Molecular weights were calculated with whichever gradients were available for the particular salt solution. Values of \bar{r}' by the two methods were again evaluated.

Now that hydration data are available for BMA in a number of solvents, it is of interest to determine whether or not there is a correlation between hydration and the activity of water in the solvent as was found by Hearst and Vinograd (14). Water activities, a_w , were computed for each salt at the molality of the buoyant solution. Data for the molal osmotic coefficient at different molalities were available in Robinson and Stokes (29) for each

of the salt solutions studied in the concentration range of interest. The osmotic coefficient was found to be a slowly varying function of molality so that linear interpolations could be used. Only four for the remaining salts. The

Results

The data for refractive index and density were plotted for each salt. Five points were available for the KBr and RbBr solutions and only four for the remaining salts. The equations for the straight line through these points are given in Table VII. Due to the larger number of points and the greater precision of the densities, the equations for KBr and RbBr can be expected to yield densities accurate to ± 0.001 gm./ml. while the precision for the remaining salts is only ± 0.002 gm./ml.

TABLE VII

Density versus Refractive Index Relations
for Various Aqueous Salt Solutions

Solvent	%	$\left(\frac{d\rho}{dn}\right)_{25^\circ\text{C}}$	σ_{ave}	M_{ave}	Γ_a	Γ_b
RbBr	1.310	0.278	0.071	102,000	0.225	0.301
CsBr	1.315	0.278	0.071	102,000	0.225	0.301
CsI	1.347	0.278	0.071	102,000	0.225	0.301
Cs ₂ SO ₄	1.241	0.278	0.071	102,000	0.225	0.301
KBr		6.4786		7.6431	1.10	1.35
RbBr		9.1750		11.2410	1.15	1.65
CsBr		9.9667		12.2876	1.25	1.35
CsI		8.8757		10.8381	1.20	1.55
Cs ₂ SO ₄		12.1200		15.1662	1.15	1.40

The results of the density gradient experiments in the various salt solutions are presented in Tables VIII-a and VIII-b.

The results of the density gradient experiments in the various salt solutions are presented in Tables VIII-a and VIII-b.

Section A. The σ_{ave} of TABLE VIII-a of the standard

deviations Calculation of Solvation Parameters and of the
Molecular Weights in Various Salt Solutions
distribution using the Physical Density Gradient are values

selected from typical experiments and the precision of each
is ± 0.002 gm./ml. respectively.

Solvent	ρ_0	$(\frac{d\rho}{dr})_{phys,0}$	σ_{ave}	MW _{ave}	Γ'_a	Γ'_b
CsCl	1.282	0.154	0.106	80,200	0.200	0.138
KBr	1.302	0.083	0.147	78,900	0.138	0.119
RbBr	1.310	0.157	0.103	84,700	0.115	0.202
CsAc	1.291				0.171	

TABLE VIII-b

the standard deviations were calculated from the two-cell
experiment. The values in the lower table may deviate by
gm. cm.⁻³. The σ_{ave} values are the arithmetic mean of the
four values obtained in the experiment. Each solvent.

Calculation of Solvation Parameters and
Molecular Weights in Various Salt Solutions
using the Buoyancy Density Gradient

Solvent	ρ_0	$(\frac{d\rho}{dr})_{buoy,0}$	σ_{ave}	MW _{ave}	Γ'_a	Γ'_b
RbBr	1.310	0.138	0.106	91,700	0.115	0.301
CsBr	1.315	0.220	0.084	91,300	0.102	0.295
CsI	1.347	0.274	0.071	102,000	0.025	0.447
Cs ₂ SO ₄	1.241	0.247	0.071	108,000	0.359	0.532

The data presented in Table VIII-a was obtained and
The precision of the molecular weights in Table VIII-a is
calculated in exactly the same manner as described in Section
about ± 0.005 . The values in the lower table may deviate by
A. The buoyant densities for CsCl, KBr, and RbBr are the
as much as 0.01. The precision of the Γ'_a values corresponds
averages of the results of a number of single-sector experi-
to that of the ρ_0 values while the precision of the Γ'_b
ments. Their precision is ± 0.001 gm./ml. Only one experi-
ment was conducted in CsAc. The value given for CsAc is
probably accurate to ± 0.005 gm./ml. The density gradients
result of these experiments. The values for ρ_0 and σ_{ave}
presented are physical density gradients as defined in

Section A. The σ_{ave} are the averages of the standard deviations evaluated from the upper and lower half of the distribution. The gradients and the band widths are values selected from typical experiments and the precision of each is ± 0.002 gm. cm.⁻⁴ and cm. respectively.

The information obtained from the two-cell experiments is given in Table VIII-b. The buoyant densities were determined by one or two single-cell experiments and one double-cell experiment. The precision of the values listed is ± 0.002 density units. The buoyancy density gradients and the standard deviations were evaluated from the two-cell experiment. The expected error for the gradients is ± 0.005 gm. cm.⁻⁴. The σ_{ave} values are the arithmetic mean of the four values obtained from the one experiment in each solvent. The average deviations about this value were 0.004 cm. for RbBr and CsBr and 0.002 cm. for CsI and Cs₂SO₄.

The molecular weights and hydration parameters in each table were calculated from equations 1, 2, and 3 from the data in columns 2-4 and the usual experimental parameters. The precision of the molecular weights in Table VIII-a is about ± 2000 . The values in the lower table may deviate by as much as 4-6%. The precision of the Γ'_a values corresponds to that of the ρ_0 values while the precision of the Γ'_b numbers depends on that of the molecular weights.

Let us consider what conclusions can be reached as a result of these experiments. The values for ρ_0 and σ_{ave}

are the only numbers which are free of any assumptions. Only the qualitative statement that the standard deviation of the Gaussian distribution decreases with increasing molecular weight of the salt can be made from the σ_{ave} values presented. The gradients in the solutions of heavier salts are expected to be higher and the band widths correspondingly narrower.

The values of ρ_0 provide additional information. The large range of values observed provides a clear demonstration that there are significant interactions between the albumin molecule and one or both components of the solvent and that these interactions depend on the nature of the salt solution. As shown in figure 10 later, the variation is seen to follow a Hofmeister series for both the cation and anion series examined. The buoyant density is seen to be a very sensitive function of the type of anion present and a somewhat less sensitive function of the nature of the cation.

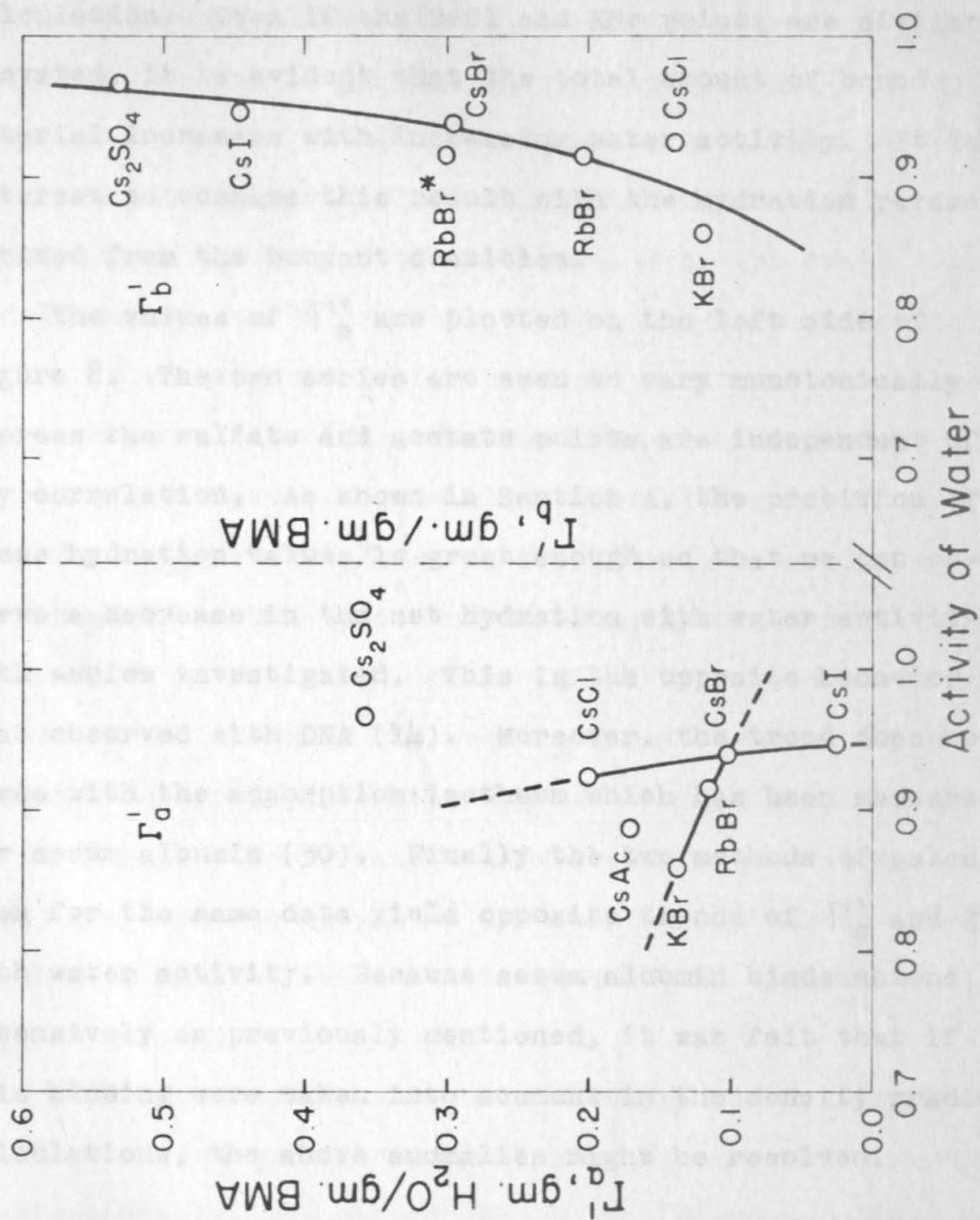
Before any comparison of the molecular weights or Γ'_b values can be made between the two tables, it is necessary to examine the results obtained for RbBr by the two methods. The fact that $(d\rho/dr)_{buoy}$ is 12% less than $(d\rho/dr)_{phys}$ is the most significant point to be noted. All density gradient expressions include the factor $1/\beta^0$ for the composition density gradient as the leading term. As seen by a comparison of equations 6 and 21, the physical density gradient differs from the buoyancy density gradient by the

factors involved in the second term of each expression. Only the compressibility of the solution enters in the physical density gradient expression whereas the compressibility of the solution and of the solvated polymer and pressure dependent solvation effects are included in the Ψ of the buoyancy density gradient. In order for these two values for the density gradient in RbBr to be reconciled, the compressibility of the solvated species must be almost as large as that of the solution and pressure dependent solvation effect must be small. This point will be considered further in the last section.

The molecular weights listed for RbBr differ by 7,000. This difference is regarded as significant and arises from the differences in the density gradients. To compare all the data in Tables VIII-a and VIII-b, the molecular weights and also the Γ'_b values for CsCl and KBr must be increased by perhaps 10-15%. Bearing in mind the error limits and the two methods of calculation, we can reach a tentative conclusion from this portion of the data. The species being measured in the different salt solutions are not the same. The molecular weights and the Γ'_b , the total amount of material bound to the anhydrous protein molecule, are seen to increase roughly in the order of listing, the molecular weights by about 25% and the Γ'_b by a factor of 2 or 3.

An interesting aspect of this dependence is seen in figure 8 which plots Γ'_b versus the activity of water in

Figure 8 - Binding Parameters of BMA by Two Methods



each solution. The two values listed for RbBr are a result of the two methods of calculation. The point marked with an asterisk was obtained from the buoyancy density gradient calculation. Even if the CsCl and KBr points are similarly elevated, it is evident that the total amount of bound material increases with increasing water activity. It is of interest to compare this result with the hydration parameters derived from the buoyant densities. The values of Γ'_a are plotted on the left side of figure 8. The two series are seen to vary monotonically whereas the sulfate and acetate points are independent of any correlation. As shown in Section A, the precision of these hydration values is great enough so that we can observe a decrease in the net hydration with water activity in both series investigated. This is the opposite behavior to that observed with DNA (14). Moreover, the trend does not agree with the adsorption isotherm which has been measured for serum albumin (30). Finally, the two methods of calculation for the same data yield opposite trends of Γ'_a and Γ'_b with water activity. Because serum albumin binds anions extensively as previously mentioned, it was felt that if this binding were taken into account in the density gradient calculations, the above anomalies might be resolved.

SECTION C
DETERMINATION OF ANION BINDING BY BMA

The inconsistency of the centrifuge results presented so far clearly indicates the necessity of introducing an additional factor or factors in order to account for the behavior observed. Because serum albumin is known to bind large numbers of anions (23, 24, 31) such as chloride, bromide, and iodide and because these ions are present in concentrations up to 4 molal, it was felt that an investigation of the extent of this binding in each of the solvents employed and of its effect on the hydration parameters obtained might clarify the density gradient results.

The only investigation in the literature reporting measurements on BMA in concentrated salt solutions is the recent work of Scatchard, et al (32). Using osmotic pressure methods, they extended the region of salt concentration examined in previous studies (33) to 6 molal NaCl. However, no other anions pertinent to this research were studied. Thus, a method was sought of determining the amount of anion binding in each of the solvents used in the density gradient experiments.

After considering several methods available for the study of ion binding, equilibrium dialysis, electromotive force and electrophoresis, the method used by Scatchard and Black (34) was selected for this study. The method consists of measuring the pH of an isoionic protein solution in water and the

pH of the protein in a salt solution of the salt concentration of interest, in this case, that corresponding to the buoyant density. The shift in pH observed is due to the change in the electrostatic free energy of the protein molecule which is caused by the introduction of some 50-70 negative charges onto the molecule. A bold extension of the Debye-Hückel theory yields a relation between ΔpH and $\bar{\nu}$, the average increase in negative charge per molecule. he mercury dimer

Procedures. Experimental for the pH measurement

Materials. The protein used in the majority of these measurements was mercaptalbumin obtained from the Pentex Corp. The material was Lot No. MB 52. A sedimentation velocity experiment showed two symmetrical schlieren peaks of approximately the same concentration corresponding to material of $S_{20,w}$ equal to 4.45 S and 6.84 S. These values indicate that the material supplied was the mercury dimer which partially dissociates in water. The mercury was removed and the monomer prepared by crystallizing the material twice followed by passing a 5% solution over an ion-exchange bed prepared by the method of Dintzis (11). The isoionic solution was light yellow, had a pH of 5.18, and was stored as described in Section A. A sedimentation velocity experiment was performed as described in Section A. Again a symmetrical sedimenting peak was observed with a slightly larger amount of fast material than shown in figure 3. Several experiments were conducted using the BMA described in Section A. The stock salt solutions were those used in the density gradient experiments. Other chemicals used were reagent grade. An identical pH shift in the 1% and 2% protein solution was observed indicating no detectable de-

Procedures. The solutions used for the pH measurement study were prepared as before. Aqueous solutions containing 1% isoionic BMA and salt of concentration corresponding closely to the buoyant density were prepared. The densities of these solutions were not adjusted exactly to that corresponding to the buoyant density. Scatchard's data (32) indicates that the extent of binding is not sensitive enough to differences in composition corresponding to the maximum density differences of 0.010 gm./ml. to warrant such an adjustment. Most of the measurements were done with the purified Pentex BMA. One measurement with the BMA supplied by Dr. Ridgeway was carried out in each salt solution.

Two experimental checks were performed. The pH of the slightly basic KBr stock solution was adjusted to pH 4.2 with dilute HBr and KOH and the protein experiment repeated using this stock solution. Within experimental error, the pH shift observed was the same as that found for the basic stock solution. This indicates that there was no buffer in the stock solution which would have caused high pH readings. Also the protein concentration was doubled in one of the RbBr measurements. An identical pH shift in the 1% and 2% protein solution was observed indicating no detectable dependence of the number of anions bound on protein concentration in the concentration region of interest.

Measurements were made with a Beckmann Model G pH meter. Standard glass and calomel reference electrodes were used.

As is generally the case when measuring the pH of a concentrated protein solution with a glass electrode, the instrument response was slow. Final readings were made only after frequent stirring and after the electrodes had been in contact with the solutions for 10-15 minutes. After three or four measurements or when the meter response became extremely slow, the protein coat was removed from the glass electrode by alternate immersion in 0.1 N HCl, 0.1 N NaOH, and 0.1 N HCl for about one minute in each solution. The precision of the measurements was about 0.05 pH units.

The density of each solution was determined refractometrically.

The acetate binding could not be investigated by this method due to its buffering action in the region of measurement.

The precision of 0.05 pH units corresponds to an uncertainty

Calculations

The change in charge on each protein molecule was computed using the relation given by Scatchard and Black (34). They treated the protein as a spherical ion of radius 30 Å. The distance of closest approach of the anion was considered to be 2.5 Å for an anion series similar to the one investigated here. The value of the electrostatic free energy term* is given by

$$w = 0.1190 \left(\frac{1 + 0.581\sqrt{I}}{1 + 8.125\sqrt{I}} \right) \quad (22)$$

where I is the double ionic strength, $\sum_i m_i z_i^2$. The change in pH is related to the number of anions bound by

$$\bar{v} = \frac{2.303}{2w} \Delta\text{pH} \quad (23)$$

The precision of ± 0.05 pH unit corresponds to an uncertainty of 4-5 ions per mole protein.

* The formula for w given by Edsall and Wyman (35) on page 603 is incorrect and does not agree with the equation apparently used by Scatchard and Black. The value of

Results and Discussion

The results of these measurements and calculations are given in Table IX. The values for RbBr and CsBr are uncertain. Two sets of pH readings differing by about 0.2 pH units were obtained in each case. The value selected for CsBr was that given by 3 out of 5 measurements. The value selected for RbBr was that which gave results consistent with the other two bromides. This is reasonable because Scatchard (34) has shown that the nature of the alkali cation has little effect on the extent of anion binding. The densities listed in Table IX agree within 0.010 gm./ml. with the buoyant densities.

TABLE IX

Also, in the same paper and in a previous publication as well (33), Isoionic Protein Solutions

Salt	ρ	\sqrt{I}	w	ΔpH	\bar{v}	No. of anions bound
CsCl	1.278	2.22	0.0153	0.71	53	53
KBr	1.306	2.98	0.0138	0.81	67	67
RbBr	1.315	2.40	0.0149	0.85	66	66
CsBr	1.306	2.04	0.0158	0.96	70	70
CsI	1.331	1.93	0.0162	1.10	78	78
Cs ₂ SO ₄	1.237	2.31	0.0151	0.64	49	25

As noted in the experimental section, the isoionic points of the two BMA samples were different. The value of

the isoionic pH of each sample was used in the calculation of pH. The difference in pH of the isoionic protein in salt and in water was found to be the same within experimental error for both samples in each salt solution.

Although the calculation of \bar{v} involves a flagrant use of the Debye-Hückel theory, there are several pieces of confirming evidence. The value of \bar{v} in 2.47 molal NaCl is determined by Scatchard by the osmotic pressure method is 52. The agreement with the number 53 in 2.47 molal CsCl is not to be construed as a measure of the precision of the two techniques as is evidenced by his long interpolation and by the precision of the present data. But it does permit some confidence to be placed in the results of the pH measurements.

Also, in the same paper and in a previous publication as well (33), Scatchard has plotted pH versus $2\bar{v}_w/2.303$ using the values of \bar{v} determined by electromotive force and osmotic pressure measurements in the former and latter papers respectively. He has drawn lines with unit slope and intercept corresponding to the pH of the isoionic protein through these points. The data points fall within 0.05 pH units of the straight line for solutions of thiocyanate and chloride ion.

The third indication of the validity of this method is the consistency of the results obtained below.

SECTION D

EFFECT OF ANION BINDING ON THE RESULTS OF DENSITY GRADIENT EXPERIMENTS

The pH measurements show that the albumin molecule in 2-3 molal salt solutions binds some 50-70 anions and carries the corresponding negative charge. The question now presented is, what is the molecular species that is banded in a density gradient experiment?

The negatively charged albumin molecules cannot segregate in a band with no charge compensation. There must be approximately the same number of cations present as anions in a close secondary layer. Because the forces involved in separating a sphere with a net charge of -60 from a cluster of 60 positive cations are much larger than any other forces present, the unit which responds to the centrifugal and diffusional forces must be the albumin molecule plus the number of neutral salt molecules equal to the number of anions bound. Therefore we must recalculate the results of the density gradient experiments taking into account the effect of this binding.

Because we know the amount of bound salt and the solvent density, we may compute

The Net Hydration of the BMA-Salt Complex

The values of Γ'_a obtained in Sections A and B correctly represent the net hydration of the salt-free protein. In molecular terms, the net hydration is the minimum amount of water bound by the protein. This is the amount of water per gram of protein that is in excess of water which we associate with the total salt in the solvate to provide a composition corresponding to the buoyant density. The total salt associated with the protein may be considered to be in two states. These are the salt measured in the anion binding experiments and an unknown additional amount of salt in the solvate if this solvate, neglecting bound salt, is not pure water.

Another quantity which may be computed is the net hydration of the protein-salt complex. This hydration is designated as Γ'_* . It is the amount of water in excess of the quantity of water assigned to the salt in the solvate, exclusive of the bound salt, in order that the ratio of salt to water be the same as in the bulk solution. The units of Γ'_* again are gm. water/gm. protein. Because we know the amount of bound salt and the buoyant density, we may compute the value of Γ'_* from equation 24.

$$\rho_0 = \frac{1 + Z_{XY} + \Gamma'_*}{\bar{V}_3 + Z_{XY}\bar{V}_{XY} + \Gamma'_*\bar{V}_{H_2O}} \quad (24)$$

The quantities z_{XY} and \bar{v}_{XY} are the weight fraction in gm./gm. dry protein and the partial specific volume in the solvate layer of the salt, XY, respectively.

The buoyant densities at the pressure at band center are tabulated in Tables VIII-a and b. The partial specific volume of BMA, \bar{v}_3 , was taken as 0.736 in all salt solutions. It is necessary to introduce the anhydrous molecular weight of BMA in order to determine z_{XY} because the anion binding as determined by the pH measurements yields moles anions bound per mole of albumin. The values of z_{XY} are calculated as $v_{XY} M_{XY} / M_a$ where M_a is the anhydrous molecular weight of BMA which we take as 70,500. The partial specific volume of water in the solvate is set equal to 1.00.

Values for the partial specific volume of the salts at infinite dilution were obtained from the recent tabulation of Mukerjee (36). The values used here are those based on $\bar{v}_{O,H^+} = -4.5$ ml./mole. The partial specific volumes were obtained by dividing the sum of the partial molar volumes of the anion and cation by the molecular weight of the salt. That these values are reasonable approximations is seen by a comparison with the value of \bar{v} for CsCl at the lowest density calculated in Part I. The value of \bar{v} at $\rho = 1.13$ is 0.252 ml./gm. This is to be compared with the value of 0.233 given in Table X.

The hydration parameters Γ'_* were calculated for each salt solution. These results are tabulated with the values these hydration values represent the hydration of the salt-

of z_{XY} and \bar{v}_{XY} in Table X. The uncertainty in z_{XY} produces expected deviations of about 5% in the Γ'_* values. In Table X, all of the column headings have been defined in the text except $\rho_{0,*}$ which will be defined later.

TABLE X

Net Hydrations of BMA-Salt Complex
and Derived Buoyant Densities

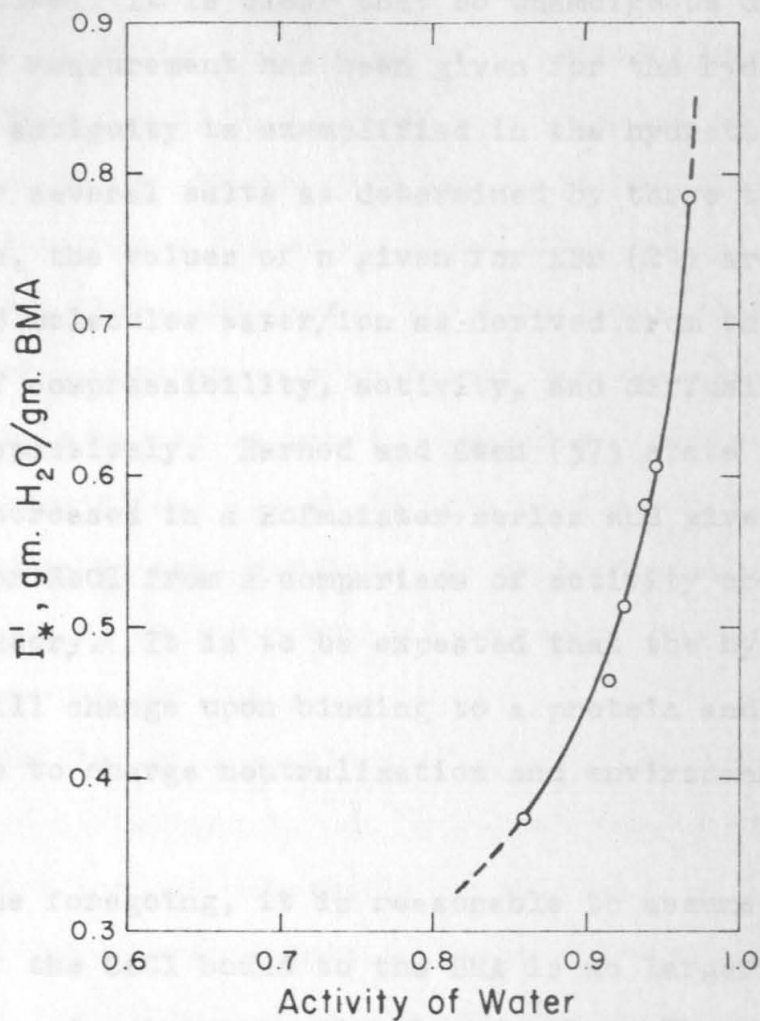
Salt	ρ_0	z_{XY}	\bar{v}_{XY}	Γ'_*	$\rho_{0,*}$
KBr	1.302	0.113	0.283	0.37	1.24
RbBr	1.310	0.155	0.234	0.46	1.22
CsCl	1.282	0.127	0.233	0.51	1.21
CsBr	1.315	0.211	0.217	0.58	1.20
CsI	1.347	0.288	0.222	0.61	1.20
Cs ₂ SO ₄	1.241	0.128	0.162	0.78	1.17

It is now of considerable interest to examine whether or not these values of Γ'_* increase monotonically with water activity. Figure 9 demonstrates that an excellent correlation now exists. The six points given on this figure represent data obtained in the salt solutions listed in order of increasing water activity in Table X.

Let us now consider the physical significance of this relationship between hydration and water activity. The values of Γ'_* give the hydration both of the protein and of the bound salt. We must therefore inquire as to how closely these hydration values represent the hydration of the salt-

Figure 9

Adsorption Isotherm of BMA



free protein molecule.

The hydration of ions is a difficult subject to assay. Robinson and Stokes (29) have discussed the numerous experimental techniques and theoretical considerations involved in this problem. It is clear that no unambiguous definition or method of measurement has been given for the hydration of ions. This ambiguity is exemplified in the hydration numbers, n , given for several salts as determined by three techniques. For instance, the values of n given for KBr (29) are 6-7, 2.1, and 0.3 molecules water/ion as derived from the interpretations of compressibility, activity, and diffusion measurements respectively. Harned and Owen (37) state that the hydration decreases in a Hofmeister series and give a value of $n=1.2$ for RbCl from a comparison of activity coefficient data with theory. It is to be expected that the hydration of a salt will change upon binding to a protein and will decrease due to charge neutralization and environmental changes.

From the foregoing, it is reasonable to assume that the hydration of the CsCl bound to the BMA is no larger than 2-3 molecules of water per molecule of salt. The measured binding of CsCl to BMA is 53. Thus, 100-150 moles of water/mole BMA may be attributed to the salt. It is therefore surprising that there is such a good correlation between Γ^* and a_w noted in figure 9 because both the number and nature of the bound anions change appreciably. However, it

is necessary to consider the magnitude of this hydration in relation to the total number of moles of water bound. For CsCl, $\Gamma'_* = 0.51$ which corresponds to a hydration of about 2000 moles water/mole albumin. Therefore, the maximum hydration attributable to the salt represents at most 6-8% of the total hydration. The number of anions bound varies roughly between 50 and 75 or about a 50% variation. The hydration for the salts employed varies perhaps between 1 and 5. Approximately the same number of salt molecules are bound for KBr, RbBr, and CsBr. The ionic hydration decreases in this order. However, a significant increase in the Γ'_* values for this series is noted. Therefore, ionic hydration is not the predominant factor in determining the net hydration of the BMA-salt complex. We conclude that the maximum variation in the amount of hydration due to the salt is between 5 and 10%.

The precision of the values of Γ'_* is $\pm 5\%$. Thus, it is unlikely that deviations in net hydration due to differences in ionic hydration are detectable by this method. We conclude that figure 9 represents to first order the actual hydration of the albumin molecule and that these values may be 5-10% high.

Therefore, figure 9 may be regarded as an adsorption isotherm at relatively high water activities. We should compare this data with adsorption isotherms previously obtained and with other hydration data available for serum

albumin. Bull. (30) has measured the water adsorption isotherms of a great number of proteins including horse serum albumin. He measured the adsorption by the air-dried protein up to relative water vapor pressures of 0.95. His values at 0.90 and 0.95 relative vapor pressures are 0.29 and 0.36 as compared with the values taken from figure 9 of 0.45 and 0.63. Several factors may contribute to this discrepancy. The proteins are not identical. His material was horse serum albumin which contained fatty acid whereas the material used in the present study was bovine serum mercaptalbumin which had been freed of fatty acid. It is apparent from Bull's data for egg albumin that the extent of hydration is markedly decreased if the protein is denatured. No data concerning the state of the albumin was given. Finally, it is not clear that the amount of hydration in the solid will be the same as the hydration of the protein in solution. There are interactions between molecules in the solid state which are not present in solution. These interactions will lead to lower values for solvation than those obtained in solution. Recently, low angle x-ray scattering has been used to determine the physical-chemical properties of proteins. Anderegg, et al (38) have measured the radius of gyration of the serum albumin molecule and from this quantity and the molecular weight, axial ratios were determined. Some

ambiguities arose when the results of the low angle studies were compared with the extended scattering curve. The axial ratio in correspondence with the extended scattering curve yielded a value for the internal hydration of serum albumin of 0.37 gm. water/gm. protein. By combining the known frictional ratio with the latter value of the axial ratio, they obtained a value for the total hydration of BSA of 0.48 gm. water/gm. protein. It is to be noted that the authors of this work present these results with reservations.

Of the several studies which have been made to determine the net hydration of BSA in solution, the work of Adair and Adair (39) has yielded the most accurate results. They measured the densities of concentrated (10-40%) solutions of bovine serum albumin and the dialysates of these solutions. They defined the density increment as the difference between these two densities divided by the protein concentration. The increment is found experimentally to be independent of protein concentration. The non-solvent volume which corresponds to the net hydration of the BSA can be calculated by measuring this increment at two buffer concentrations. It can be shown that this hydration is identical to that calculated as \bar{v}'_a in this paper. A value of 0.44 gm. water/ gm. dry protein is reported for a protein solution which has been dialyzed against a 1 M sodium phosphate buffer. Unfortunately no data for the binding of phosphate by BSA is available and therefore no direct comparison can be made.

Since the experiments reported in this thesis were completed, Cox and Schumaker (8,20) published two studies dealing with the hydration of BSA. In the first study, the sedimentation velocity of BSA was measured as a function of salt concentration. An extrapolation of a plot of the product of the sedimentation coefficient and the viscosity of the solution against S to zero sedimentation rate presumably yielded values of the buoyant density. From these densities, values of 0.19 and 0.26 gm. water/gm. BSA for NaCl and KCl solutions respectively were obtained. Again these values correspond to the \bar{v}'_a reported here, the net hydration of the salt-free protein. Although these values compare favorably with the value of 0.20 determined for a CsCl solution by the density gradient work reported above, several serious problems limit the usefulness of the sedimentation velocity method. The concentration of salt is varied between a few tenths molar to saturation. Because the chloride binding and the hydration both change significantly with concentration, the sedimenting species is changing as the density of the solution is increased. Furthermore, a dubious extrapolation over a distance equal to the range of $S\eta$ values that could be measured was necessary.

In a second paper (20), they studied the behavior of BSA in several density gradient systems and obtained a buoyant density at atmospheric pressure at 25°C in CsCl of 1.295 ± 0.005 gm./ml. using absorption optics. The unpressured

buoyant density, ρ_0^0 , corresponding to the pressured buoyant density given on page 68 of this thesis is 1.275 ± 0.001 gm./ml. Because of the relatively large error involved in their measurements and because they used BSA and not mercaptalbumin, this difference need not be regarded as significant.

A problem of greater concern is their value of ρ_0^0 for BSA in 3.6 molal $(\text{NH}_4)_2\text{SO}_4$ of 1.175 ± 0.005 gm./ml. This corresponds to a hydration of 0.79 ± 0.05 . The water activity of this solution is 0.88. If sulfate binding were taken into account, the value of Γ'_* thus obtained would be even larger than the value reported for Γ'_a . This is very much higher than the result predicted from figure 9. The reason for this discrepancy is not known. It may have to do with the fact that the bovine albumin is banded at a composition only slightly less than that required for precipitation and that some transition in the albumin molecule has occurred.

We conclude that the density gradient method as reported here is one of the most satisfactory methods of determining the net hydration of the salt-free protein. None of the methods reported here including the present one, by themselves yield the net hydration of the protein-salt complex. Separate measurements of anion binding are additionally required.

It would be interesting to examine the buoyant behavior of BMA in solvents having much lower water activities to determine whether the sigmoidal character of the usual ad-

sorption isotherm is obtained. Low molecular weight salts such as LiBr and LiCl should be examined as possible banding media.

$$P_{0.2} = \frac{1.7 \times 10^4}{0.2 \times 10^4}$$

(25)

The Derived Buoyant Density

A derived buoyant density can be defined by equation

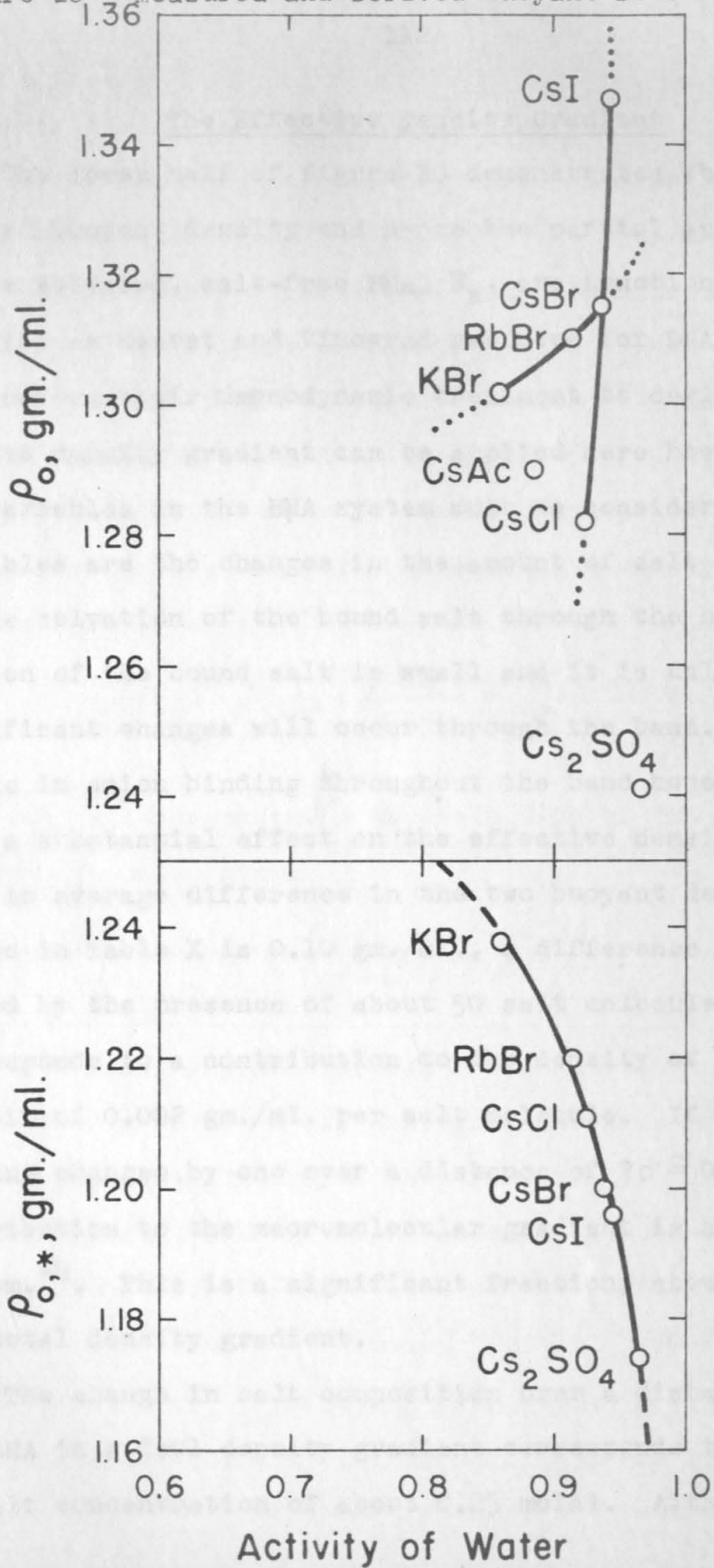
25.

$$\rho_{0,*} = \frac{1 + \Gamma'_*}{\bar{V}_3 + \Gamma'_* \bar{V}_{H_2O}} \quad (25)$$

This is the buoyant density that is to be expected if no salt were bound and if the amount of hydration is independent of the bound salt. The assumptions involved in the calculation of Γ'_* are apparent upon inspection of equation 24. If the values of Γ'_* are 5-10% too high because of ion hydration of the bound salt, the derived buoyant densities will be about 5% at most lower than that corresponding to the hydrated, salt-free protein.

The results of this calculation are given in column 6 of Table X and plotted in the lower half of figure 10 against the water activities previously calculated. Figure 10 indicates the correlation which exists between these values of $\rho_{0,*}$ and water activity as opposed to the lack of correlation in the measured buoyant densities which are plotted in the upper half of the figure.

Figure 10. Measured and Derived Buoyant Densities of BMA



The Effective Density Gradient

The lower half of figure 10 demonstrates that the derived buoyant density and hence the partial specific volume of the solvated, salt-free BMA, \bar{v}_s , are functions of water activity as Hearst and Vinograd reported for DNA (14).

Before their thermodynamic treatment to derive the effective density gradient can be applied here however, some new variables in the BMA system must be considered. These variables are the changes in the amount of salt bound and in the solvation of the bound salt through the band. The hydration of the bound salt is small and it is unlikely that significant changes will occur through the band. A small change in anion binding throughout the band however may have a substantial effect on the effective density gradient.

An average difference in the two buoyant densities reported in Table X is 0.10 gm./ml., a difference in density caused by the presence of about 50 salt molecules. This corresponds to a contribution to the density of the hydrated protein of 0.002 gm./ml. per salt molecule. If the anion binding changes by one over a distance of $2\sigma \approx 0.2$ cm., the contribution to the macromolecular gradient is about 0.010 gm. cm.⁻⁴. This is a significant fraction, about 7%, of the total density gradient.

The change in salt composition over a distance of 2σ for BMA in a CsCl density gradient corresponds to a change in salt concentration of about 0.25 molal. Although this

concentration difference may be large enough to cause a shift in the anion binding of one, its effect cannot be quantitatively assayed at present because of the lack of precise anion binding data at these high salt concentrations. The result of such a change in binding is to lower the effective density gradient which in turn increases the value of the solvated molecular weight.

We now calculate the effective density gradient for each salt solution using the expression given by Hearst and Vinograd (28),

$$\left(\frac{d\rho}{dr}\right)_{\text{eff}} = \left[\frac{1}{\beta^0} + \frac{\kappa - \kappa_s}{1 - \alpha} \rho^{0^2} \right] (1 - \alpha) \omega^2 r \quad (26)$$

where κ_s is an apparent compressibility of the solvated protein and α is given by

$$\alpha = \left(\frac{\partial \rho^0}{\partial a_w^0} \right)_P \left(\frac{da_w^0}{d\rho^0} \right) \quad (27)$$

Effective density gradients can be calculated not only for the salts for which β^0 is available but also from the density gradients determined experimentally. The buoyancy density gradient differs from the effective density gradient only by the factor $(1 - \alpha)$ which we now proceed to calculate. The first factor of α , $(\partial \rho^0 / \partial a_w^0)_P$, was computed from the slope of the ρ^0 versus a_w^0 plot in the bottom of figure 10 at the water activity corresponding to the measured buoyant density. This gives a value of $(d\rho/dr)_{\text{eff}} = 0.127$.

Water activities for each salt solution at several densities both above and below the buoyant density were calculated from the molal osmotic coefficients given by Robinson and Stokes (29) at various molalities. The results of these calculations are shown in figure 11. The values of the second factor of α , $(da_w^0/d\rho^0)$, were computed as the inverse of the slope at the buoyant densities.

The values of these slopes and the values of α are listed in Table XI-a and XI-b. Both slopes could be determined with a precision of 0.05. However, the accuracy of the curve drawn through the derived buoyant density data is unknown. We estimate the values of α to be good to about 20%.

Effective density gradients could now be calculated for each buoyant solution. As indicated above, the effective density gradients given in Table XI-b were computed by multiplying the experimentally determined buoyancy density gradients listed in column 3 of Table VIII-b by $(1-\alpha)$.

Values of β^0 , K , and α are available for the three salts listed in Table XI-a. A reasonable value of K_s was obtained as follows. Jacobson (40) has measured the compressibility of horse serum albumin in dilute salt solutions. This value is not the apparent compressibility of the solvated polymer but since values of K_s are not available we shall consider the results of using this value. Insertion of this number and the values of β^0 and K for CsCl into equation 26 gives a value of $(d\rho/dr)_{\text{eff}} = 0.127$.

Figure 11 - Water Activities of Various Salt Solutions

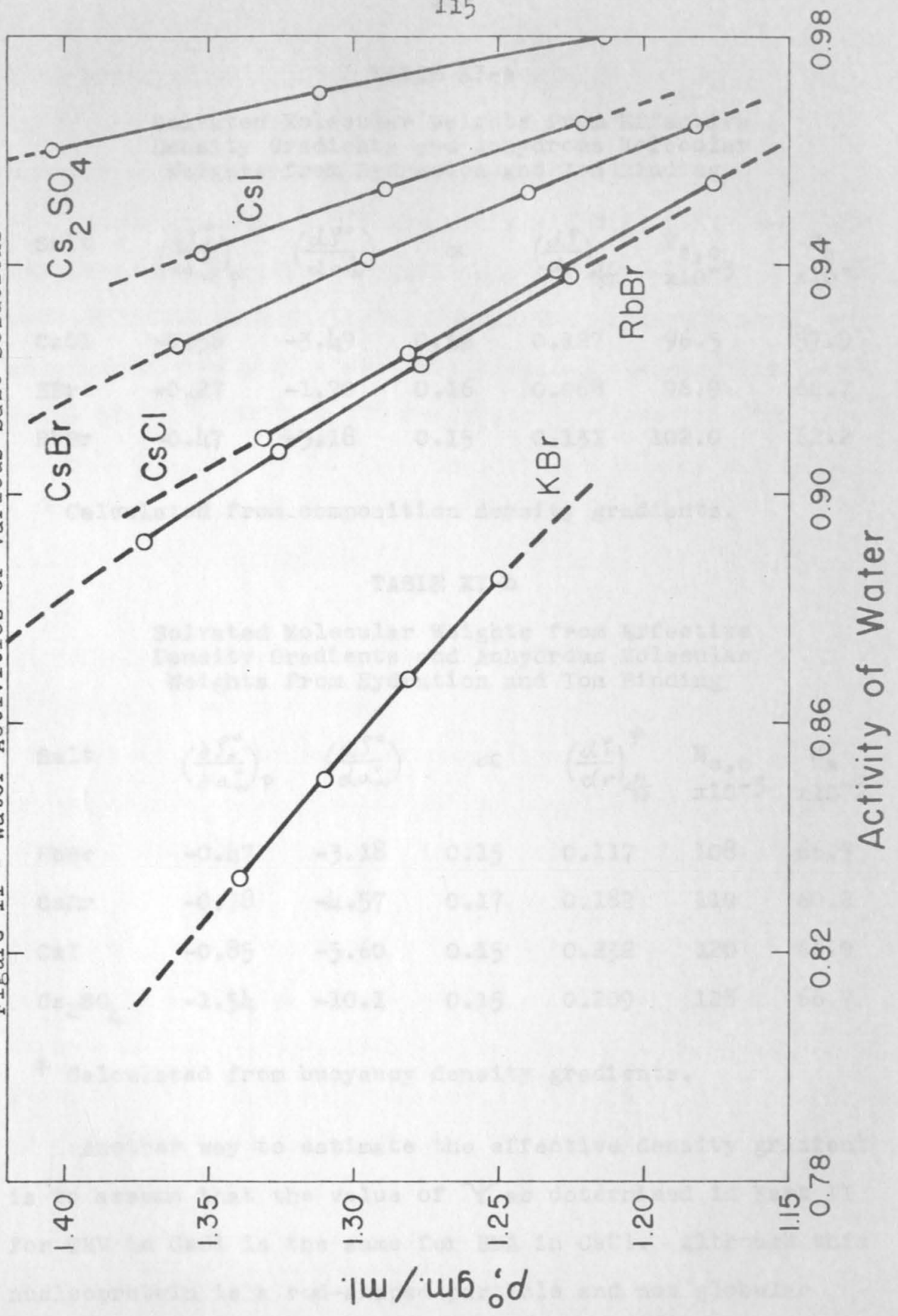


TABLE XI-a

Solvated Molecular Weights from Effective Density Gradients and Anhydrous Molecular Weights from Hydration and Ion Binding

Salt	$\left(\frac{\partial \rho_0^\circ}{\partial a_w^\circ}\right)_p$	$\left(\frac{d\rho_0^\circ}{da_w^\circ}\right)$	α	$\left(\frac{d\rho}{dr}\right)_{eff}^\dagger$	$M_{s,0} \times 10^{-3}$	$M_a \times 10^{-3}$
CsCl	-0.56	-3.49	0.16	0.127	96.5	57.9
KBr	-0.27	-1.70	0.16	0.068	96.9	64.7
RbBr	-0.47	-3.18	0.15	0.131	102.0	62.2

[†] Calculated from composition density gradients.

TABLE XI-b

Solvated Molecular Weights from Effective Density Gradients and Anhydrous Molecular Weights from Hydration and Ion Binding

Salt	$\left(\frac{\partial \rho_0^\circ}{\partial a_w^\circ}\right)_p$	$\left(\frac{d\rho_0^\circ}{da_w^\circ}\right)$	α	$\left(\frac{d\rho}{dr}\right)_{eff}^\ddagger$	$M_{s,0} \times 10^{-3}$	$M_a \times 10^{-3}$
RbBr	-0.47	-3.18	0.15	0.117	108	66.3
CsBr	-0.78	-4.57	0.17	0.182	110	60.2
CsI	-0.85	-5.60	0.15	0.232	120	62.0
Cs ₂ SO ₄	-1.54	-10.1	0.15	0.209	128	66.7

[‡] Calculated from buoyancy density gradients.

Another way to estimate the effective density gradient is to assume that the value of Ψ as determined in Part II for TMV in CsCl is the same for BMA in CsCl. Although this nucleoprotein is a rod-shaped particle and not globular

like serum albumin, it is 94% protein. Use of this value of ψ and the values of β^0 and K for CsCl gives a value of 0.125 for the effective density gradient. Because values of ψ are not available in KBr and RbBr solutions and because the gradients obtained by the two methods are substantially the same, the gradients given in column 5 of Table XI-a were all computed assuming Jacobson's value of $9.1 \times 10^{-6} \text{ atm.}^{-1}$ for k_s .

Calculation of Solvated and Anhydrous Molecular Weights

Now that effective density gradients are available for all the salt solutions investigated, solvated molecular weights which should include the mass of bound salt can be calculated employing equation 1. These values of $M_{s,0}$ are listed in column 6 of Tables XI-a and b. Finally, we should inquire as to whether this value is consistent with the anhydrous molecular weight and the known amount of water and salt binding. We do this by calculating M_a .

$$M_a = \frac{M_{s,0} - \nu_{XY} M_{XY}}{1 + \Gamma'_*} \quad (28)$$

The resulting molecular weights are tabulated in column 7 of Tables XI-a and b. An examination of the results given in Table XI is now necessary. One interesting and unexpected result is that the α 's obtained in a variety of salt solutions are identical within experimental error. Although the values of each factor which make up α vary by a factor of 6, $\alpha = 0.16 \pm 0.01$ in all cases. No satisfactory explanation of this behavior has been found. A qualitative observation can be made from an examination of figures 10 and 11. Because all the curves in figure 11 must extrapolate to a water activity of 1 at a density of 0.997, the slopes of these curves must increase as we proceed from left to right on the figure. This order is seen to be exactly that for the values of $\rho_{0,*}$ given in

figure 10. Here the slope of the curve increases with increasing water activity. Thus, the trend of the two slopes used to compute α is such that the values of α should tend to be constant. However, it is not certain that a straight line through the lower 5 points for $\rho_{0,*}$ in figure 10 and a sharp bend between the KBr and RbBr points might not be the correct interpretation. In this case the values of α will reflect only the slope of the ρ^0 versus a_w^0 plot and will vary by a factor of 3. Therefore, the constancy of α must be regarded at the present time as being fortuitous.

The most disturbing data listed in Tables XI-a and b are the two values given for the effective density gradient of RbBr solutions evaluated by two methods. The 10% difference however almost lies within the experimental error limits involved in each measurement. Although the value of α may be in error, it enters in the same way in the calculation of the effective density gradient by the two methods except for the weak dependence in the Ψ term. The errors in β^0 and in K_s may cause the value of $(d\rho/dr)_{\text{eff}}$ evaluated from the composition density gradient to be in error by 5%. The expected error in the value derived from the buoyancy density gradient due to the uncertainties in determining the density difference alone is 4%. Therefore, the wide error limits for each value of the effective density gradient preclude any conclusion as to the significance of the observed difference. α is increased by about 3%. The dependence is even more

The solvated molecular weights again roughly increase in the order of listing. This is due to the increasing amounts of solvation and ion binding. given in Table 33-4

The values of the anhydrous molecular weights provide additional information. Excluding the low CsCl value, the molecular weights are seen to agree within 10%. Considering the experimental errors involved in determining ν_{XY} , $(d\rho/dr)_{\text{buoy},0}$, α , and σ and the additional theoretical uncertainty in assigning values to \bar{v}_{XY} and \bar{v}_{H_2O} , this agreement is considered to be as good as can be expected at present. Refinements in anion binding measurements in particular should reduce this deviation to about 5%. It can be said that the two sets of values of M_a given in the separate tables do not differ in a non-random way. This indicates that the two methods of evaluating the effective density gradient are substantially in agreement. The fact that all of the molecular weights are below the 70,500 weight average value obtained previously is attributed primarily to the failure to take into account the change in ion binding across the protein band.

Also, it must be remembered that the calculation of M_a and the Γ'_* values given earlier are prejudiced by the assumption of a value for M_a in order to determine z_{XY} . If the anhydrous molecular weight were taken as 65,000 instead of 70,500, all of the Γ'_* values reported here would be increased by about 5%. The dependence is even more

insensitive in the determination of M_a from equation 28. A similar error in the selection of M_a needed to calculate z_{XY} would make all of the values of M_a given in Table XI-a and b about 2% too high.

Conclusions

The technique of sedimentation equilibrium in a density gradient in the ultracentrifuge is a satisfactory and accurate method for determining the net hydration of proteins expressed as gm. water/gm. salt-free protein. Only 50 λ of a 1% solution is required. This determination of net hydration is independent of bound salt and is calculated directly from the buoyant density and the partial specific volume of the anhydrous protein.

Because of the difficulties involved in determining the effective density gradient, the density gradient method is not recommended if only molecular weights are sought. Other techniques such as two component sedimentation equilibrium in the ultracentrifuge or osmotic pressure give more accurate results and require less effort. If for some reason an investigation in a high salt concentration is desired such as a study of the dissociation of hemoglobin in concentrated salt solutions, the density gradient method should be employed.

Concentration. Differential
Appendix

1. The Effect of a Non-Constant (dn/dc) on the Refractive Index Increment

Following this substitution, rearrangement yields

In general, analyses performed with the schlieren optical technique assume the relation

$$n_c = K \times c \quad (1)$$

where $K = (dn/dc)$, the refractive index increment, and n_c is the refractive index contribution of the protein; i.e., the difference in refraction between the protein solution and the reference solution. We now consider the case for which (dn/dc) varies throughout the protein band due to the changing CsCl concentration. Differentiation of equation 1 yields

$$\frac{dn_c}{dr} = \frac{dc}{dr} \left(\frac{dn}{dc} \right) + c \times \frac{d(dn/dc)}{dr} \quad (2)$$

We assume that (dn/dc) varies linearly.

$$(dn/dc) = (dn/dc)_0 (1 - k\epsilon) \quad (3)$$

where $(dn/dc)_0$ is the refractive index increment at $\epsilon=0$ and ϵ is the distance from band center. Substitution of equation 3 into 2 yields

$$\left(\frac{dn_c}{dr} \right) = \left(\frac{dn}{dc} \right)_0 \left[\frac{dc}{dr} - k \left(c + \epsilon \frac{dc}{dr} \right) \right] \quad (4)$$

Equation 4 can be recast in more readily available terms by substitution of the derivative of the Gaussian

concentration distribution, namely $(dc/dr) = -c\epsilon/\sigma^2$.

Following this substitution, rearrangement yields

$$\left(\frac{dn_c}{dr}\right) = -\frac{c}{\sigma^2} \left(\frac{dn}{dc}\right)_0 \left[\epsilon - k(\epsilon^2 - \sigma^2)\right] \quad (5)$$

Alternatively, we may rearrange equation 5 to examine the behavior of (dn/dr) at positions in the band other than band center. At band center, equation 5 reduces to

$$\left(\frac{dn_c}{dr}\right) = -\frac{c\epsilon}{\sigma^2} \left(\frac{dn}{dc}\right)_0 \left[1 - k\left(\frac{\epsilon^2 - \sigma^2}{\epsilon}\right)\right] = \left(\frac{dn}{dr}\right)_{ideal} \left[1 - k\left(\frac{\epsilon^2 - \sigma^2}{\epsilon}\right)\right] \quad (6)$$

Equations 5 and 6 now permit an examination of the effect on band shape and position caused by a non-constant refractive index increment provided we have estimates of the quantities involved.

The constant k is given by $\frac{1}{(dn/dc)_{r_0}} \left(\frac{d(dn/dc)}{dr}\right)_{r_0}$. We can obtain a rough estimate of this quantity by making a bold extrapolation of the specific refractive increment of BSA, 0.001901 (39), which is the difference in refractive index between a 1% albumin solution and water. Addition of 100 times this quantity to $n_{H_2O} = 1.3325$ yields a rough value of $n_{BSA} = 1.523$. Subtraction of the refractive index of the CsCl solution at band center, which is generally about 1.360, from n_{BSA} and division by 100 yields an estimate of $(\Delta n/\Delta c) = 0.00163$. We can estimate the same quantity at a distance 1σ (0.1 cm.) from band center. The difference in refractive index between band center and 1σ is given by:

with increasing distance from the center of the band.

however, $\Delta n = \Delta r \times \frac{\Delta f}{\Delta r} \times \frac{\Delta n}{\Delta f} = \frac{0.1 \times 0.15}{10.86} = 0.0014$ out beyond 3σ so that the contribution to the total area under

Addition of 0.001 to n_{r_0} followed by the same procedure

as above yields 0.00162 for the refractive increment at

1σ . Thus $k \cong \frac{1 \times 10^{-5}}{1.9 \times 10^{-3} \times 1 \times 10^{-1}} = 0.05$.

At band center, equation 5 reduces to

$$\frac{dn_c}{dr} = -k_c \left(\frac{dn}{dc} \right)_0$$

The magnitude of this shift is so small as to not affect

The concentration at band center in a typical BSA experiment the value of r_0 or σ .

is 0.5%. The gradient of refraction at band center is

$$\left(\frac{dn}{dr} \right)_{\epsilon=0} = -0.05 \times 0.5 \times 0.95 \times 10^{-3} \cong -2.4 \times 10^{-5}$$

This is to be compared with the inflection point of (dn_c/dr)

which occurs at 1σ where $(dn_c/dr) \cong (dn_c/dr)_{ideal} = -c\epsilon/\sigma^2$

$(dn/dc)_0 = \pm 0.02$. The shift in the refractive index gradient

at $\epsilon=0$ is 0.1% of the maximum gradient in the distribution.

We may also determine the radial shift in the point of intersection of the sigmoidal curve with the baseline for the actual and the ideal cases. This shift is calculated by setting equation 5 equal to zero and solving the quadratic expression for ϵ using the parameters given above. The shift is -0.0005 cm. which is beyond the precision either obtainable or needed in this technique.

Examination of equation 6 reveals that there is no correction at $\epsilon=\sigma$. At 2σ , the correction term is $0.05 \left(\frac{(2\sigma)^2 - \sigma^2}{2\sigma} \right) \cong 0.0075$. The correction term becomes larger

Log-Plate-Frame No. 1535-1-3

Name

J. J. ...

with increasing distance from the center of the band.

Material

Date

4/7/60

However, there is less than 0.2% of the material out beyond 3σ so that the contribution to the total area under the curve is negligible.

A plot of the points determined above, combined with an examination of the sign of the correction in intermediate regions indicates that the entire refractive index gradient distribution is shifted towards the center of rotation while the sigmoidal shape, to first order, remains unchanged. The magnitude of this shift is so small as to not affect the value of r_0 or σ .

orig. coin. density
 Δr : Algebraic difference
 Rotation Point (obtain from plot at r_0)

2. Density Gradient Molecular Weight Evaluation

Log-Plate-Frame No. 1555-1-3Name Jim IfftMaterial BMA in C₃ClDate 4/7/60

Notation

I. Distances

A. In cell in cm.

 r_0 : Band center r_e : Pt. corresponding to orig. soln. density Δr : Algebraic difference of ($r_0 - r_e$)

B. Related distance quantities

 $\frac{r_e - r_a}{r'_e - r_a}$ = Normalized Isoconcentration Point (obtain from plot at ρ_e)

M.F. = magnification factor from cell to tracing

C. On tracing in cm.

 R_T : Top reference edge R_a : Meniscus R_0 : Band center R_b : Bottom of cell R_B : Bottom reference edge

II. Densities and density gradient

 ρ_0 : Density at r_0 , gm. cm.⁻³ ρ_e : Density at r_e , original solution density $\Delta \rho$: Algebraic difference of ($\rho_0 - \rho_e$) $(d\rho/dr)$: Physical density gradient at r_0 , gm. cm.⁻⁴ β : Density gradient proportionality constant (obtain from β vs. ρ plot), egs.

III. Other experimental parameters

 σ^2 : (standard deviation)², cm.² ω^2 : (radians/sec.)², sec.⁻²

T: Absolute temperature

K: Isothermal compressibility coefficient of salt solution at ρ_e

Calculations

I. Absolute temperature: 298.2 °K

II. Angular velocity

Odometer readings:

Elapsed time:

At t_2 : 479,532

$$t_2 - t_1 = (1440 \cdot x \text{ days} + 60 \cdot y \text{ hrs} + z \text{ min}) 60 \text{ sec}$$

At t_1 : 468,288

$$= (1440 \cdot 0 + 60 \cdot 21 + 23) 60 \text{ sec}$$

Total rev = 11,244 x 6400 =

$$\frac{7.1962 \times 10^7 \text{ rev.}}{7.698 \times 10^4 \text{ sec}} = \frac{7.698 \times 10^4 \text{ sec}}{7.698 \times 10^4 \text{ sec}}$$

$$\omega^2 = \left(\frac{\text{total rev.} \times 2\pi}{\text{elapsed time (sec)}} \right)^2 = \left(\frac{7.1962 \times 10^7 \times 6.2832}{7.698 \times 10^4} \right)^2 = 34.50 \times 10^6 \text{ sec}^{-2}$$

III. Distances

$$\text{M.F.} = \frac{R_B - R_T}{\text{dist. between reference edges}} = \frac{34.83}{1.595} = 21.84$$

$$r_o = 5.730 + \frac{(R_o - R_T)}{\text{M.F.}} = 5.730 + \left(\frac{17.32}{21.84} \right) = 6.523 \text{ cm.}$$

$$r_a = 5.730 + \frac{(R_a - R_T)}{\text{M.F.}} = 5.730 + \left(\frac{6.43}{21.84} \right) = 6.024 \text{ cm.}$$

$$r_\alpha = \sqrt{(r_o^2 + r_a^2)/2} = 6.278 \text{ cm.}$$

$$r_b = 5.730 + \frac{(R_b - R_T)}{\text{M.F.}} = 5.730 + \left(\frac{32.66}{21.84} \right) = 7.225 \text{ cm.}$$

$$r'_e = \sqrt{(r_a^2 + r_b^2)/2} = 6.652 \text{ cm.}$$

$$\frac{r_e - r_a}{r'_e - r_a} = 1.0325 \quad (\text{evaluated at } \rho_e \text{ given below})$$

$$r_e = r_a + (r_e - r_a)/(r'_e - r_a) \cdot (r'_e - r_a) = 6.672 \text{ cm.}$$

$$\Delta r = (r_o - r_e) = -0.149 \text{ cm.}$$

IV. Density Parameters

$$\rho_e^0 = 10.8601 (n_D^{25^\circ\text{C}}) - 13.4974 = 1.298 \text{ d.u.}$$

$$\beta_e^0 = 1.57 \times 10^9 \text{ cgs.}$$

$$(d\rho/dr)_e = \omega^2 r_e / \beta_e^0 = \frac{34.50 \times 10^6 \times 6.670}{1.57 \times 10^9} = 0.147 \text{ d.u./cm.}$$

$$\Delta \rho^0 = \Delta r (d\rho/dr)_e = -0.149 \times 0.147 = -0.022 \text{ d.u.}$$

$$\rho_0^0 = \rho_e^0 + \Delta \rho^0 = 1.298 - 0.022 = 1.276 \text{ d.u.}$$

$$\beta_0^0 = 1.63 \times 10^9 \text{ cgs.}$$

V. Pressure Corrections

$$\rho_\alpha^0 = \rho_e^0 + (d\rho/dr)_e (r_\alpha - r_e) = 1.240 \text{ d.u.}$$

$$P_{r_0} = \frac{\rho_\alpha \times \omega^2}{2.026 \times 10^6} (r_0^2 - r_a^2) = 132.2 \text{ atm.}$$

$$\rho_0 = \rho_0^0 (1 + K P_{r_0}) = 1.282 \text{ d.u.}$$

$$(d\rho/dr)_{\text{phys},0} = \left(1/\beta_0^0 + \frac{K \rho_0^{02}}{1.013 \times 10^6} \right) \omega^2 r_0 = 0.151 \text{ d.u./cm.}$$

VI. Standard Deviations

Numerically integrate schlieren curve from center of band outwards in 5 mm. intervals.

Plot $\ln c$ vs. $(r-r_0)^2$ using $(r-r_0)$ in terms of cm. on schlieren tracing.

$$\text{Slope} = \frac{(\ln c)_1 - (\ln c)_2}{(r-r_0)_1^2 - (r-r_0)_2^2} \times \text{M.F.}^2 \text{ cm.}^{-2}$$

$$\sigma^2 = - \frac{1}{2 \times \text{slope}} \text{ cm.}^2$$

	Top	Bottom
Slope:	-42.88 cm. ⁻²	-45.43 cm. ⁻²

σ^2 :	0.01166 cm. ²	0.01101 cm. ²
--------------	--------------------------	--------------------------

σ :	0.108 cm.	0.105 cm.
------------	-----------	-----------

VII. Apparent Molecular Weights

$$M_{\text{app.},0} = \frac{RT \rho_0}{\sigma^2 \omega^2 r_0 (d\rho/dr)_{\text{phys.},0}}$$

Top: 87,500 gms./mole

Bottom: 92,700 gms./mole

3. Effect of Neglecting Cubic Term in Derivation of Density Gradient Expression

In the original derivation of equation 1 in the text, terms of the order of $(r-r_0)^3$ were neglected because the band widths were very narrow. In the case of protein analyses however, the band extends over a significant region of the cell, as seen in figure 3, in which case this term may not be negligible. The validity of this assumption was examined.

The concentration distribution was obtained by assuming a Boltzman distribution of particles. The energies of the particles are determined as the negative of the distance integral of the force F on each particle.

$$F = v(\rho_p - \rho_s) \omega^2 r$$

The quantity v is the volume of one particle, ρ_p is its density, and ρ_s is the density of the solution at the radial position r. As before ρ_s is assumed to vary linearly with distance. The resulting expression for the mass distribution is:

$$\ln \frac{m(r)}{m(r_0)} = - \frac{M\bar{v} \left(\frac{d\rho}{dr} \right)_{r_0} \omega^2}{RT} \left[\frac{r_0 (r-r_0)^2}{2} + \frac{(r-r_0)^3}{3} \right]$$

This ratio was computed for one experiment in which a skewed concentration distribution had been obtained. Also, the ideal Gaussian distribution given by the first term was calculated. The three distributions thus obtained were all

normalized to one and plotted on the same graph. The cubic term does shift the concentration curve in the direction experimentally found. However, the magnitude of this shift is so slight as compared with the observed displacement that the error introduced by neglecting the cubic term can be considered as negligible.

References

6. Cox, D. J., and V. N. Schussler, J. Am. Chem. Soc. 71, 2120 (1949).

19. Schachman, H. G., in *References Enzymology*, (1957), edited by S. P. Colowick and T. P. Kaplan, Academic Press, New York, 1957, p. 265-283
1. Meselson, M., F. W. Stahl, and J. Vinograd, *Proc. Natl. Acad. Sci.*, (1957), 43, 581
20. Cox, D. J., and V. N. Schumaker, *J. Am. Chem. Soc.*, (1961), 83, 2439
2. Meselson, M., and F. W. Stahl, *Proc. Natl. Acad. Sci. U. S.*, (1958), 44, 671
21. Rolfe, R., in *The Proteins*, (1958), edited by H. Frazer and T. P. S. Casey, Academic Press, New York, 1958, pp. 265-283
3. Rolfe, R., and M. Meselson, *Proc. Natl. Acad. Sci. U. S.*, (1959), 45, 1039
4. Marmur, J., and D. Lane, *Proc. Natl. Acad. Sci. U. S.*, (1960), 46, 453
5. Williams, R. C., S. J. Kass, and C. A. Knight, *Virology*, (1960), 12, 48
6. Smith, J. D., G. Freeman, M. Vogt, and R. Dulbecco, *Virology*, (1960), 12, 185
7. McCrea, J. F., R. S. Epstein, and W. H. Barry, *Nature*, (1961), 189, 220
8. Cox, D. J., and V. N. Schumaker, *J. Am. Chem. Soc.*, (1961), 83, 2439
9. Siegel, A., and W. Hudson, *Biochim. Biophys. Acta*, (1959), 34, 254
26. Wilson, R. E., *J. Am. Chem. Soc.*, (1955), 77, 266
10. Bock, R. M. (private communication)
27. Wilson, R. E., *ibid.*, (1955), 77, 266
11. Dintzis, H. M., Ph. D. Thesis, (1952), Harvard University
28. Hearst, J. E., and J. Vinograd, *Proc. Natl. Acad. Sci. U. S.*, (1961), (in press), paper no. 2
12. Baldwin, R. L., *Proc. Natl. Acad. Sci. U. S.*, (1959), 45, 939
29. Robinson, R. A., and R. S. Stokes, *Electrolyte Solutions*, Butterworths, London, 1959, p. 172
13. Williams, J. W., K. E. Van Holde, R. L. Baldwin, and H. Fujita, *Chem. Rev.*, (1958), 58, 715
30. Bull, R. B., *J. Am. Chem. Soc.*, (1944), 66, 1637
14. Hearst, J. E., and J. Vinograd, *Proc. Natl. Acad. Sci. U. S.*, (1961), (in press), paper no. 2
31. *ibid.*, (1961), 47, 535
15. Baldwin, R. L., *Biochem. J.*, (1957), 65, 503
32. Sothard, G., Y. V. Wu, A. L. Shen, *ibid.*, (1959), 81, 103
16. Van Holde, K. E., and R. L. Baldwin, *J. Phys. Chem.*, (1958), 62, 734
33. Sothard, G., J. B. Coleman, A. L. Shen, *ibid.*, (1957), 61, 103
17. Trautman, R., *Biochim. et Biophys. Acta*, (1958), 28, 417
18. Dayhoff, M. O., G. E. Pearlmann, and D. A. MacInnes, *J. Am. Chem. Soc.*, (1952), 74, 2515

19. Schachman, H. K., in Methods in Enzymology, (1957), edited by S. P. Colowick and N. O. Kaplan, Academic Press, New York, N. Y., vol. IV, pp. 65-71
20. Cox, D. J., and V. N. Schumaker, J. Am. Chem. Soc., (1961) 83, 2433
21. Edsall, J. T., in The Proteins, (1953), edited by H. Neurath and K. Bailey, Academic Press, New York, N. Y., p. 564
22. Pohl, F., Dissertation, (1906), Rheinische Friedrich-Wilhelms Universität, Bonn, Germany
23. Carr, C. W., in Electrochemistry in Biology and Medicine, (1955), edited by T. Shedlovsky, John Wiley & Sons, Inc., New York, N. Y., pp. 266-283
24. Scatchard, G., W. L. Hughes, F. R. N. Gurd, and R. E. Wilcox in Chemical Specificity in Biological Systems, (1954), edited by F. R. N. Gurd, Academic Press, New York, N. Y., pp. 193-219
25. Roth, W. A., and K. Scheel, Landolt-Börnstein Physikalisch-Chemische Tabellen, (1935), fünfte Auflage, dritter Ergänzungsband, zweiter Teil, Julius Springer, Berlin, Germany, p. 1700
26. Gibson, R. E., J. Am. Chem. Soc., (1935), 57, 284
27. Gibson, R. E., ibid., (1934), 56, 4
28. Hearst, J. E., and J. Vinograd, Proc. Natl. Acad. Sci. U.S., (1961), (in press), paper no. 1
29. Robinson, R. A., and R. H. Stokes, Electrolyte Solutions, (1955), Academic Press, New York, N. Y., pp. 469-70, 473
30. Bull, H. B., J. Am. Chem. Soc., (1944), 66, 1499
31. Scatchard, G., I. H. Scheinberg, and S. H. Armstrong, Jr., ibid., (1950), 72, 535
32. Scatchard, G., Y. V. Wu, A. L. Shen, ibid., (1959), 81, 6104
33. Scatchard, G., J. S. Coleman, A. L. Shen, ibid., (1957), 79, 12
34. Scatchard, G., and E. S. Black, J. Phys. and Colloid Chem., (1949), 53, 88

35. Edsall, J. T., and J. Wyman, Biophysical Chemistry, (1958), Academic Press, New York, N. Y., p. 603
36. Mukerjee, P., J. Phys. Chem., (1961), 65, 740
37. Harned, H. S., and B. B. Owen, The Physical Chemistry of Electrolytic Solutions, (1950), Reinhold Pub. Corp., New York, N. Y., p. 409
38. Anderegg, J. W., W. W. Beeman, S. Shulman, and P. Kaesberg, J. Am. Chem. Soc., (1955), 77, 2927
39. Adair, G. S., and M. F. Adair, Proc. Roy. Soc., (1947), A190, 341
40. Jacobson, B., Arkiv För Kemi, (1950), 2, 177
41. Perlmann, G. E., and L. G. Longworth, J. Am. Chem. Soc., (1948), 70, 2719

Propositions

relaxation Propositions technique
desaf

Proposition 1

A Simple Method for the Approximate Evaluation of the Effective Density Gradient

A method, based on only one ultracentrifuge experiment, is proposed for the determination of an approximate value of the effective density gradient which is required for the evaluation of molecular weights from density gradient experiments. The method requires an accurate evaluation of the difference in density of two salt solutions, each containing the macromolecule of interest. An interferometric technique is proposed.

Since the development of the technique of sedimentation equilibrium in a density gradient, attempts have been made to utilize this method for the determination of molecular weights. The work of Hearst and Vinograd (1) and the comparison of effective density gradients with physical density gradients given in Part III of this thesis show that the effective density gradient for the macromolecule of interest in a particular salt solution must be obtained if molecular weights are sought. Methods are given in Parts I, II, and III of this thesis for the evaluation of the quantities needed to determine the effective density gradient. However, a minimum of about 10 ultracentrifuge experiments is needed for the determination of the quantities α and ψ in equation 24 of reference 1. Thus, the density gradient method will not appear to be an attractive technique if only molecular weights are to be obtained. A method is proposed for the

approximate evaluation of $(d\rho/dr)_{\text{eff}}$ which requires only one ultracentrifuge experiment.

As shown in Part III of this thesis, the buoyancy density gradient (equation 21) can be obtained by simultaneously running two cells which contain the macromolecule in salt solutions of slightly different densities which bracket the buoyant density. If the buoyancy density gradient, $(d\rho/dr)_{\text{buoy}}$ can be obtained with sufficient accuracy, the pressure-dependent term ψ can be calculated from the measured value of $(d\rho/dr)_{\text{buoy}}$ and the value of β^0 which in general can be readily calculated if the function $\beta^0(\rho)$ has not already been tabulated for this salt solution. If a reasonable estimate of the apparent compressibility of the solvated species K_s is available, the solvation parameter α can be calculated from the values K_s , ψ , and K , the compressibility of the salt solution. Thus, all of the quantities needed to calculate $(d\rho/dr)_{\text{eff}}$ could be determined with just one centrifuge experiment.

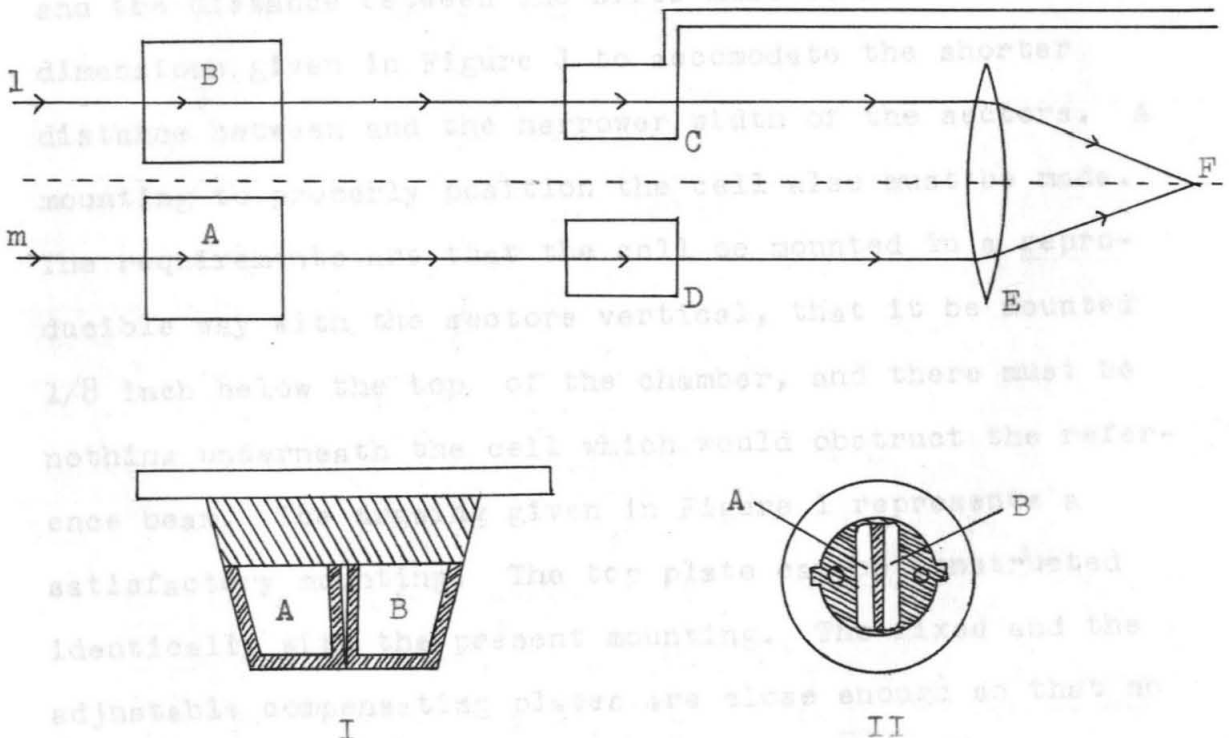
This procedure is not feasible using the techniques which are currently employed. The most serious difficulty encountered in the determination of $(d\rho/dr)_{\text{buoy}}$ is the accurate evaluation of the difference in density between the two solutions. If β^0 is essentially constant over the density range used and if the density gradient is sufficiently large, density differences as large as 0.100 gm./ml. may be employed. However, especially in protein investigations, β^0 varies significantly over such a density range and a $\Delta\rho$ of 0.02 to 0.04 gm./ml. must be used to obtain accurate values of $(d\rho/dr)_{\text{buoy}}$. The technique of measuring the refractive

index of each solution which is currently employed gives errors of from 5% to 10% in the buoyancy density gradient. Also there now exists some doubt as to whether such solutions can be prepared, inserted into the centrifuge cell, and run to equilibrium with no change in density in either solution. Because the pressure dependent term ψ is only 10-15% of $(d\rho/dr)_{\text{buoy}}$, the value of ψ and hence the solvation parameter α cannot be obtained with satisfactory accuracy using this procedure. It is proposed that the experiment described above be conducted with a cell equipped with a double sector center-piece and the difference in density between the two salt solutions in the two sectors be determined by interferometry. This would permit the value of $\Delta\rho$ to be determined after the cell had been filled and sealed. Also, this method permits an evaluation of the difference in density after the run has been completed. The cell is thoroughly shaken to make the solution homogenous again and the Δn remeasured.

Interferometry is an excellent method for determining differences in refractive index with great accuracy. Because $(\Delta\rho/\Delta n)$ is accurately known for a number of salt solutions, this method provides the difference in density of two solutions with great accuracy. One problem which must be considered in the conversion of the measurement of Δn to $\Delta\rho$ is whether the refractive index increment of the protein is identical in the two salt solutions. Perlmann and Longworth (2) have measured the refractive index increments of BSA and egg

albumin in NaCl solutions. A reasonable extrapolation of their data for the case of an albumin in a CsCl gradient indicates that the largest error in Δn caused by the non-constant refractive index increment is less than 1×10^{-5} . This is a negligible error.

In order for this proposition to be of practical value, it was felt that the modification of an existing instrument would be necessary. The reason for the suggested modifications and the principle involved in interferometric measurements are shown in the following diagrams.



Parallel light rays (l and m) that are in phase pass through the cells A and B which contain the solutions of interest. The optical paths between the common light source and the point F at which the rays are brought back together to pro-

Figure 1 - Modifications of Zeiss Interferometer

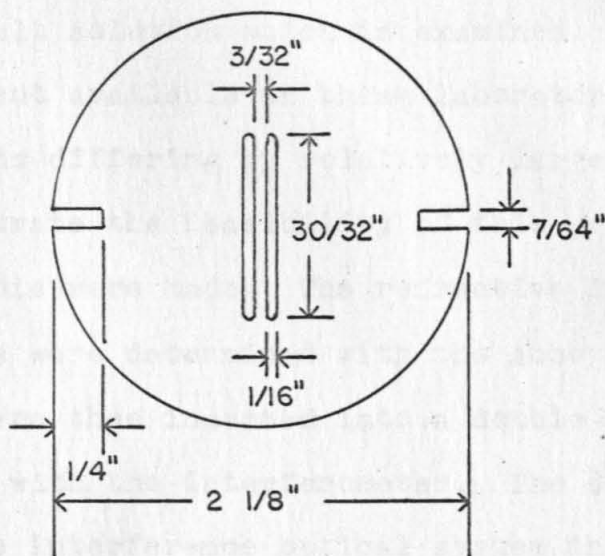
duce the interference fringes are equalized by the adjustable compensator C. The measured angle of the compensating plate is proportional to Δn . The liquid cell of the Rayleigh interferometer made by the Zeiss Company is shown in actual size as diagram I. The proposal is to substitute the double sector cell illustrated as II for the present cell. The diagrams point out the two changes which are necessary for the modification of the interferometer for use with a double-sector ultracentrifuge cell.

A new double slit mask must be made. The slit width and the distance between the slits must be reduced to the dimensions given in Figure 1 to accommodate the shorter distance between and the narrower width of the sectors. A mounting to properly position the cell also must be made. The requirements are that the cell be mounted in a reproducible way with the sectors vertical, that it be mounted $1/8$ inch below the top of the chamber, and there must be nothing underneath the cell which would obstruct the reference beam. The drawing given in Figure 1 represents a satisfactory mounting. The top plate can be constructed identically with the present mounting. The fixed and the adjustable compensating plates are close enough so that no further modifications are needed.

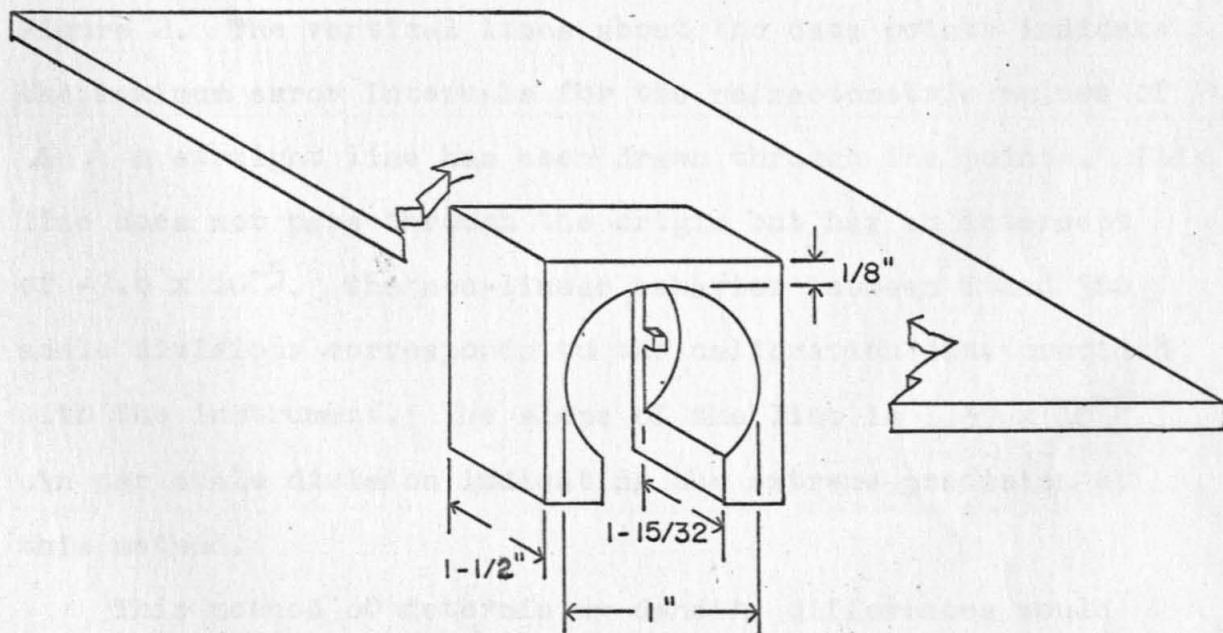
Cells must be filled and mounted in such a way that the dense solution is on the right hand side of the instrument. Cells should be assembled with wide cups, and pre-

Figure 1 - Modifications of Zeiss Interferometer
for Use with Double-Sector Ultracentrifuge Cells

Double Slit Mask



Cell Mount

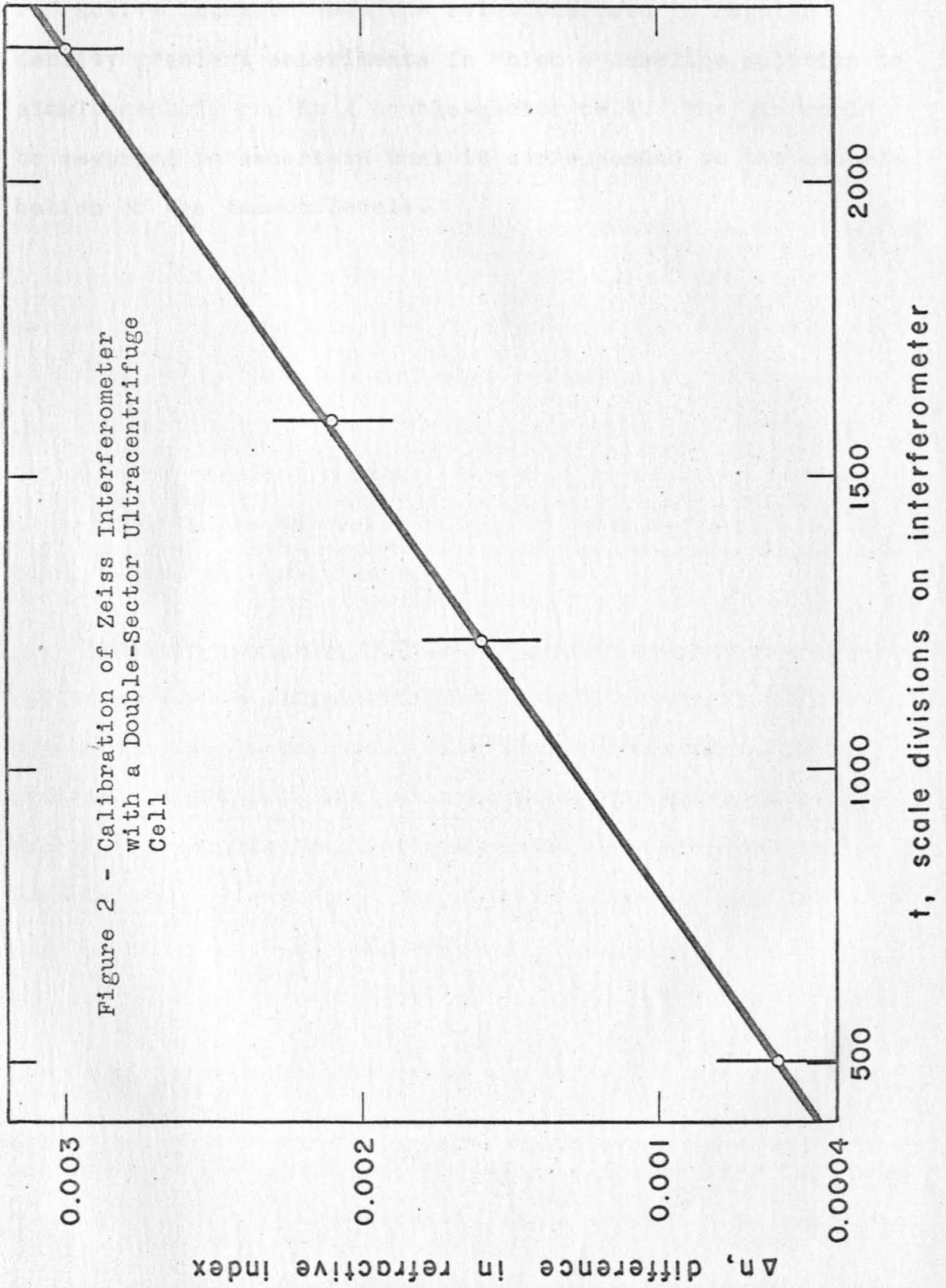


Scale: actual size

ferably with a black centerpiece and black window cups to reduce reflections.

Because white light is used, the system must be calibrated for each salt solution which is examined. To calibrate the Zeiss instrument available in these laboratories for use with CsCl solutions differing by relatively large values of Δn and to demonstrate the feasibility of this proposal, several measurements were made. The refractive indices of two CsCl solutions were determined with the Abbé refractometer. These solutions were then inserted into a double sector cell and readings made with the interferometer. The double slit mask used with the interference optical system in the ultracentrifuge and a laboratory clamp were used for the two necessary modifications. Several such solutions were prepared and measured. The results of this calibration are given in Figure 2. The vertical lines about the data points indicate the maximum error intervals for the refractometric values of Δn . A straight line has been drawn through the points. This line does not pass through the origin but has an intercept of -9.8×10^{-5} . The non-linear behavior between 0 and 500 scale divisions corresponds to the calibration data provided with the instrument. The slope of the line is 1.39×10^{-6} Δn per scale division indicating the extreme precision of this method.

This method of determining density differences would also be useful as a routine check on the difference in



refractive index between the solutions used in regular density gradient experiments in which a baseline solution is simultaneously run in a double-sector cell. The Δn could be measured to ascertain that it corresponded to the contribution of the macromolecule.

It is pointed out that a recent study of the hydration of bovine hemoglobin by a freezing-point depression technique which apparently showed that bovine hemoglobin is not hydrated

equivalent to Proposition 2. The Hydration of Bovine Hemoglobin

It is proposed that a recent study of the hydration of bovine hemoglobin by a freezing point depression technique which apparently showed that bovine hemoglobin is not hydrated in an aqueous solution is in error both as to use of this method for the determination of the hydration of proteins in solution and as to the conclusion reached. It is proposed that the net hydration of bovine hemoglobin be measured by the density gradient method. A method is proposed for the evaluation of the molecular weight of bovine hemoglobin in concentrated salt solutions.

Olmstead and Stone (3) have recently studied the solvation of bovine hemoglobin (Hb) in salt solutions of physiological composition. They used a freezing point depression technique. The per cent water, W, which is available for dissolving salts was computed from the empirical formula

$$W = \frac{C_2 - C_1}{R_2 - R_1} \times 100$$

The quantities in the numerator are the effective concentrations of two buffer solutions containing NaCl, KCl, K_2HPO_4 and KH_2PO_4 whose molal concentrations differed by a factor of two. The effective concentrations are expressed as mosmoles.

A mosmole is defined as that amount of electrolyte which is equivalent in osmotic pressure to that of a one molal solution of an ideal, non-ionized solute. The R's are the mosmolar concentrations of 30-60% hemoglobin solutions in the same two buffers. After the freezing point depression measurement on the hemoglobin solution of higher salt concentration, this solution was dried and the total per cent water calculated.

Six protein solutions of concentration ranging from 35 to 62 gms. Hb/100 ml. solution were measured by this method. The per cent water by desiccation varied between 74 and 63%. In all cases, the values of W agreed with the values obtained by desiccation within 1%. The authors conclude that "crystalline bovine hemoglobin does not 'bind' water in solutions in the sense that this water is made unavailable as a solvent for salts."

This result is not in agreement with that obtained in other studies. Drabkin (4) succeeded in growing macro-crystals of bovine hemoglobin. He analyzed the crystals gravimetrically and spectrophotometrically for the amounts of water, phosphate salt, and hemoglobin. A comparison of the ratio of the concentration of buffer in the crystal to that of the mother liquor revealed a bound water content of 0.339 gm. water/gm. hemoglobin. Ritland, et al (5) used low angle x-ray scattering to determine the shape and hydration of bovine hemoglobin in dilute salt solutions. They found a hydration of 0.20 gm. water/gm. hemoglobin with an uncertainty

of 40-50%. Therefore, the results of Olmstead and Stone are not in agreement with results of two independent measurements using two different techniques. It is proposed that the freezing-point technique as employed by them is not a satisfactory method for determining net hydration and that their conclusion regarding the lack of hydration of bovine hemoglobin is in error. The following sources of error are proposed as the reasons for the apparent agreement of the percentages of water as determined by the two methods used by Olmstead and Stone.

1. The most serious error in their procedure appears to be comparing the values of W which are expressed as ml. water/ml. solution with the values obtained by desiccation which are in units of gm. water/gm. solution. The authors do not report density measurements or taking this factor into account in the comparison of the two percentages. The density of even the 35% hemoglobin solution is about 1.1 gm./ml. This means that the values of W should be decreased at least 10% corresponding to a significant net hydration. However, even if the values of W are divided by the density, several problems with this method remain which cannot be resolved so easily.

2. The activity coefficients of the salts are changing appreciably over the concentration range employed. The ratio

of $C_2/C_1 = 1.91$ and not 2.00. If we consider all the salt to be K_2HPO_4 (which is present in largest amount), we can obtain an estimate of the magnitude of the error incurred by this variation.

The solutions yielding the values of R_1 and C_1 are at nearly the same salt concentration and hence comparable osmolar values are to be expected. However, the molarity of the salt solution used to measure C_2 was about 0.5 and that for R_2 , 0.7 M. The activity coefficient of a 0.7 M Na_2HPO_4 solution is 10% lower than that of a 0.5 M solution. Therefore, the values of R_2 must be increased to be comparable to C_2 . This would lead to a lower value of W , hence a net hydration.

3. A second problem that was not considered in this investigation is that both the solvation and the salt binding are changing as the hemoglobin is placed in the two different salt solutions. It is to be expected that the hydration will be lower in the more concentrated salt solution. It can be analytically shown that the same values of W would have been observed if x ml. H_2O were bound in solution 1 and y ml. H_2O in solution 2 where $y > x$ and if x and y obeyed the relation

$$\left(1 + \frac{A}{1,000}\right)x - \frac{A}{1,000}y = \frac{xy}{A}$$

The quantity A is the volume of water in a liter of Hb solution if no hydration occurs. There is at least one set of values for x and y which satisfy this equation other than

$x = y = 0$. A similar relation could be written for the salt binding. Cejka (6) has reported that Hb binds about half as many Cl^- ions as serum albumin. According to the data of Scatchard and Black (7), this corresponds to a Cl^- binding of 3 and 6 in the two Hb salt solutions. That this effect is large is seen by noting that the hemoglobin concentration in the 62% solution is 0.009 M. The concentration of bound chloride therefore should change from 0.027 to 0.054. Because the total chloride concentration is only 0.053 M, the $[\text{Cl}^-]$ changes from half its original value to zero.

4. The authors dried the concentrated Hb solutions for only 24 hours at 105°C . I have observed that even 5% solutions of BSA in water do not reach a constant weight in 3 days drying at 105°C . It is very likely that the Hb samples were not thoroughly dry in which case the per cent water reported by desiccation would be too low. This would also lead to the spurious conclusion that there is no net hydration.

It is proposed that the net hydration of salt-free bovine hemoglobin be measured by the density gradient method in order to clarify the results of Olmstead and Stone. Satisfactory conditions for this experiment would be the following: $[\text{Hb}] = 0.1\%$ in CsCl solution of $\rho_e = 1.245$ gm./ml. containing phosphate buffer at pH 6.8; angular velocity = 56,100 rpm; 25°C ; no wedge is required. The investigation could be extended to a number of other salt solutions to obtain in-

formation as to the dependence of hydration on water activity.

There is one aspect of this proposal that will be a complicating factor in the comparison of the density gradient results with those obtained by the above workers. Although the resolution of this difficulty will require additional work, it may provide some very interesting information. The difficulty alluded to is the recent report by Benhamou, et al (8) that hemoglobin dissociates in concentrated salt solutions. It must be established whether the hydration of the dimer or the tetramer is being measured before a direct comparison with the results of Olmstead and Stone can be made because the hydration of these units may be significantly different. The density gradient method would be an excellent technique for determining the molecular weight of hemoglobin in concentrated salt solutions. This would be an interesting fact to establish in light of the current interest in the hybridization of hemoglobin.

Some preliminary confirming evidence for Benhamou's result has been obtained in this laboratory.* Human hemoglobin (HbA) was run in a CsCl density gradient at pH 6.8. Buoyant densities corresponding to a net hydration of salt-free protein of 0.27 gm. water/gm. HbA were obtained. The hydration of bovine hemoglobin is not expected to differ significantly from this value for human hemoglobin. A rough calculation of the anhydrous molecular weight of HbA from

* I would like to thank Mrs. Janet Morris for assistance in conducting and analyzing these experiments.

the data of the above experiments assuming the value of ψ obtained for TMV and the value of α determined for BMA in this thesis yielded a value of 43,000. This is significantly closer to the molecular weight of the half molecules, 33,000, than to that of the tetramer.

In order to quantitatively establish the anhydrous molecular weight of bovine hemoglobin in a concentrated salt solution, the following experimental procedures are proposed. A double-sector experiment, as described in Proposition 1, using the experimental conditions given above should be performed to determine the buoyancy density gradient. An entirely different method is proposed to determine the value of α which is necessary to calculate the effective density gradient.

The Adairs' density increment method (9) provides a means of determining the factor $(\partial \rho^0 / \partial a_w^0)_P$, which is proportional to α , using solutions of only one salt. The density gradient method requires that solutions of several salts be used because only one buoyant composition exists for each salt solution. This requires the assumption that the only change in going from one salt solution to another is water activity. Using the density increment method, hydration values expressed as gm. water/gm. hemoglobin could be obtained at several water activities both greater and less than buoyant composition by dialysis against solutions of differing CsCl concentration. From these values, density values corre-

sponding to buoyant densities ρ_0 could be calculated. The net hydration of the protein-salt complex could then be computed from the values of ρ_0 and the amount of chloride binding which Cejka is currently measuring (6). Finally, this value could be used to compute the derived buoyant density which should be a sensible function of water activity. The appropriate slope would yield the value of $(\partial \rho_0^0 / \partial a_w^0)_P$.

water and anion binding by proteins. Specific proteins, chemical modifications of these proteins, and methods of detection and binding are proposed for this study.

Proteins perform a variety of diverse functions in biological systems. The functional groups in the polar amino acid residues are probably responsible for the hydration of proteins and for the reaction of proteins with anions. However, relatively little is known about the sites involved in the binding of water and essentially nothing is known about the active sites in anion binding (10) despite our extensive knowledge for some proteins of the number of anion binding sites and the dissociation constants of each class of sites.

Perling (11) has demonstrated a linear correlation between the first layer of water adsorbed on various proteins as calculated from water adsorption isotherms (12) and the transfer-Enoch-Yeller equation, and the number of polar amino acids. Kallou, et al (13) have measured the water adsorption

isotherms of adsorption. Proposition 3

Determination of the Sites of Water and Anion Binding in Proteins

A comparison of the solvation and anion binding of native proteins with that of proteins which have been chemically modified so as to selectively block certain functional groups is proposed as a means of locating the active sites in water and anion binding by proteins. Specific proteins, chemical modifications of these proteins, and methods of determining binding are proposed for this study.

The tentative conclusion can be drawn that the extent of hydration decreases as the total number of charged groups is increased. It is proposed that measurements be made of the binding of water and anions by proteins which have been modified such that certain functional groups have been selectively blocked by chemical reaction. By successively blocking different functional groups and measuring the amount of binding of each modification in relation, the extent of binding due to particular functional groups could be determined. The following sites.

Pauling (11) has demonstrated a 1:1 correlation between the first layer of water adsorbed on various proteins as calculated from water adsorption isotherms (12) and the Brunauer-Emmett-Teller equation, and the number of polar amino acids. Mellon, et al (13) have measured the water adsorption native BSA has been determined.

isotherms of chemically modified dry casein and wool. The extent of hydration of casein was substantially decreased after selective benzylation of the amino groups. There was no decrease in the water adsorption of wool after reduction of the disulfide bonds. In addition, Cox and Schumaker (14) have recently measured the sedimentation velocity of BSA in KCl solutions. They found that the buoyant density increased as the pH was raised from 4.7 to 9.2. Over at least part of this range (up to pH 7), Scatchard, et al (15) have shown that the amount of chloride binding remains constant. Thus, the tentative conclusion can be drawn that the extent of hydration decreases as the total number of charged groups is decreased.

It is proposed that measurements be made of the binding of water and anions by proteins which have been modified such that certain functional groups have been selectively blocked by chemical reaction. By successively blocking different functional groups and measuring the amount of binding of each modified protein in solution, the extent of binding due to particular functional groups could be determined. The following system and procedures are proposed for this study.

Bovine insulin and bovine serum mercaptalbumin (BMA) would be interesting proteins for this investigation. Both proteins bind anions extensively (7, 16), both are susceptible to selective chemical modification, and the hydration of native BMA has been determined.

The osmotic pressure method developed by Scatchard, et al (10) is suggested as the most satisfactory method for determining anion binding, especially in concentrated salt solutions. The density gradient method as described in this thesis is recommended for determining the net hydration of the chemically modified proteins.

The following requirements as to the chemical modifications must be met in order for this procedure to be informative. The nature of the chemically modified site must be substantially different in charge, steric availability or polarization from the original functional group. The chemical reaction must not denature the protein. Only one group or class of functional groups must be affected by a particular reagent. Such specific reactions are the reaction of mineral acid and methanol with insulin to completely and exclusively esterify the carboxyl groups (17) and the iodination of the tyrosyl groups of serum albumin (18). Although specificity has not been determined for insulin and mercaptalbumin, the reaction of acetic anhydride with available amino groups and the reaction of carboxyl groups with diazoacetamide should prove to be interesting modifications for this study because of the large number of these functional groups present in each protein.

As indicated above, perhaps the most selective chemical modification of any protein occurs on varying the pH. The net charge on the protein increases on either side of the

isoelectric point. However, the number of charged groups, which is probably the chief determinant in binding, decreases. Thus, a study of the extent of both types of binding at pH's larger than 4 coupled with a knowledge of the titration curve of each protein and the amino acid composition would yield information as to the binding sites. Solutions more acid than pH 4 must be avoided because of the swelling of the albumin molecule which may increase the number of binding sites and because of the dissociation of the insulin molecule.

Proposition 4

The Chemical Nature of Molybdenum Blue

An experimental method is proposed to determine whether a complete homologous series of molybdenum blue compounds exists. It is proposed that this method will demonstrate that all of the compositions of molybdenum blue that have been reported can be obtained by a stepwise reduction of sexipositive molybdenum compounds. A revision of the one structure that has been given for a molybdenum blue is proposed.

In their book, Molybdenum Compounds, Killeffer and Linz (19) state that "the great molybdenum puzzle is a phenomenon called Molybdenum Blue." They describe molybdenum blue as a phenomenon rather than a chemical compound because neither the structure nor the chemical composition of this compound or group of compounds has been satisfactorily elucidated. In 1951, Glemser and Lutz (20) listed all of the molybdenum blue compounds which had been reported to that time. Their tabulation is presented below to demonstrate the variety of compositions which have been obtained. In addition, Klason (21) has reported a compound of composition $\text{Mo}_{20}\text{O}_{59}$.

Despite the diversity of the compounds which have been reported, all of these compounds have a number of physical and chemical properties in common. They are all blue colloidal compounds containing Mo and O in the proportions, $1:2.5 < \text{Mo}:0 < 1:3$. The Mo thus has an average valence be-

isometric series of Molybdenum Blue Compounds

Reduction Stages	Oxides	Crystalline hydroxides	X-ray amorphous hydroxides
MoO _{2.97}	MoO ₃ sublimate (MoO ₃ + Mo ₈ O ₂₃)		
MoO _{2.89}	Mo ₉ O ₂₆		
MoO _{2.88}	Mo ₈ O ₂₃	Mo ₈ O ₁₅ (OH) ₁₆ (Mo ₈ O ₂₃ ·8H ₂ O)	Mo ₈ O ₂₃ ·xH ₂ O
MoO _{2.83}			H[Mo ₃ O ₉] (Mo ₆ O ₁₇ ·H ₂ O)
MoO _{2.75}		Mo ₄ O ₁₀ (OH) ₂ (Mo ₄ O ₁₁ ·H ₂ O)	MoO _{2.75} ·xH ₂ O
MoO _{2.60}		MoO _{2.60} ·xH ₂ O	
MoO _{2.50}		Mo ₂ O ₄ (OH) ₂ (Mo ₂ O ₅ ·H ₂ O)	

tween 5 and 6. Molybdenum blues are formed by reduction of suspensions of MoO₃ or molybdate solutions, by careful oxidation of lower valent Mo compounds or by mixing Mo^{VI} and Mo^V solutions. A wide variety of reducing agents including HI, SnCl₂, SO₂, H₂S, N₂H₄, electric current, and several metals in finely divided form have successfully been used for the reduction of sexipositive molybdenum compounds to molybdenum blues.

Wadsley (22) has suggested an important unifying concept concerning the composition of molybdenum blues. He suggests that these compounds form a homologous, non-stoich-

determined. Widely differing and products have resulted be-

isometric series of the type, $\text{Mo}_n\text{O}_{3n-1}$. As noted in parentheses in the hydroxide columns of the above table, all of these compounds do conform to this classification. However, numerous members of such a series have not been reported. Also, one of the compounds given by Killeffer and Linz (19) does not conform to this classification. The following experiments are proposed to determine whether or not such a series exists.

It is proposed that an acid solution of Na_2MoO_4 be reduced by the dropwise addition of a dilute solution of SnCl_2 . The progress of the reaction should be followed by a continuous examination of the solution by colorimetry and measurements of the paramagnetism of the sample. An instrument would have to be constructed. A mixing chamber would be suspended between the poles of a magnet in one direction and between a light source and photoelectric cell in the other direction. Continuous stirring of the solution in an inert atmosphere would be needed. As inflections in either the intensity of the blue solution or the magnetic susceptibility were noted, samples should be withdrawn and standard chemical analyses performed to determine the ratio of Mo:O. It is proposed that the results obtained would be independent of the reducing agent used.

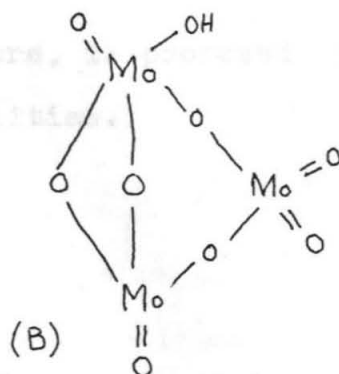
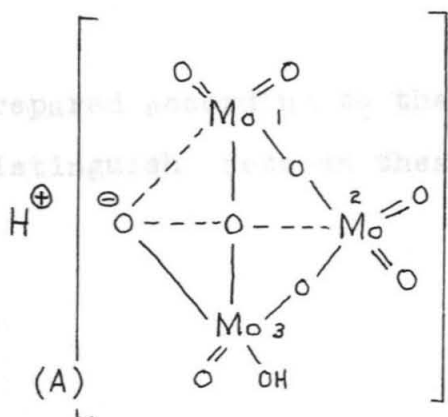
This procedure should circumvent some of the difficulties encountered in earlier work. The amount of reducing agent to add to the molybdate solution has heretofore been empirically determined. Widely differing and products have resulted be-

cause the progress of the reaction, as the sexipositive material is reduced through successive stages, has not been studied. Also, this method provides a means of studying the reaction in solution. Because of the colloidal nature of the compound, it is difficult to isolate the blue compound (23).

The paramagnetic study would be difficult but illuminating. Sacconi and Cini (24) have measured the magnetic susceptibility of a dried molybdenum blue and found a very low paramagnetism. They calculated that about 90% of the Mo^V atoms are involved in covalent bonds with other Mo^V atoms. It would be interesting to correlate any abrupt changes in the paramagnetism of the sample in the proposed experiments with changes in the intensity of the color of the solution and with the chemical composition corresponding to the molybdenum blue at that stage of the reduction.

(25) Despite numerous attempts to determine the chemical composition of molybdenum blues, few proposals for its structure have been made. Treadwell and Schaeppi (23) have proposed a structure as well as a formula on the basis of oxidimetric titrations, pH measurements, and molecular weight determinations for a molybdenum blue which they prepared. They give the formula $\frac{1}{2} \text{Mo}_2\text{O}_5 \cdot 2\text{MoO}_3$ and the (A) structure presented below.

The peroxoanion structure does not preclude the possibility that some of the six-valent Mo are present instead. A study of the magnetic susceptibility of the molybdenum blue



Glemser and Lutz (20) pointed out that the hydroxyl group on the number 3 Mo atom should be omitted, as was undoubtedly intended by Treadwell and Schaeppi. It is proposed that the formula $H[Mo_3O_9]$ and structure (B) are more in accord with the experimental evidence. The hydroxyl group can be attached to either of the 6-valent Mo atoms. If this proposal is correct, it would not fit into the homologous series suggested by Wadsley (22). It is possible that the acidic hydrogen found by Treadwell and Schaeppi was due to a bound molecule of H_2SO_4 as was recently reported by Schriever and Toussaint (25) and that the sulfate is bound so tightly that it was not detected by the addition of Ba^{+2} . If this is so and if the compound were dissociated under the conditions of the freezing point molecular weight determination, a dimer of structure (A) and of formula Mo_6O_{17} may be the correct structure and composition.

The authors assumed, as is assumed in structure (B), that the molybdenum has oxidation states of five and six. The permanganate oxidation data do not preclude the possibility that four- and six-valent Mo are present instead. A study of the magnetic susceptibility of the molybdenum blue

prepared according to their procedure, is proposed to distinguish between these possibilities.

(27) have demonstrated. Proposition 5
Hydrophobic Bonds in Proteins

It is proposed that a study of poly- α -amino acids be made in order to determine the relative strength of hydrophobic bonds in proteins. The synthetic polypeptides proposed for this investigation are block copolymers containing a small central segment of a non-polar amino acid, the remainder of the polymer consisting of amino acid residues which are soluble in water. A study of the dependence of the viscosity and light scattering properties of aqueous solutions of these copolymers on the length of the non-polar sequence is proposed.

Several proposals have recently been made regarding the principle of the minimum exposure of non-polar residues in proteins to the aqueous environment (26, 27, 28). The forces responsible for satisfying this principle are referred to as hydrophobic bonds. Two of these forces are the weak van der Waals interactions between the non-polar residues and the much stronger hydrogen bonds which can be formed in the aqueous solvent by the withdrawal of the non-polar residues into a micellar region. Kauzmann (26) has estimated the strength of hydrophobic bonds in proteins using the model of small hydrocarbons in water. He calculated a value for ΔF of +3000 to 5000 cal./mole for the transfer of one mole of hydrocarbon from a non-polar solvent to water. Tanford, et al

(27) have demonstrated by optical rotatory dispersion measurements that the configuration of β -lactoglobulin depends on the amount of water available. They suggest that hydrophobic bonds are "the most important factor in the determination of protein structure in aqueous solutions." Yanari and Bovey (28) have studied the ultraviolet difference spectra of proteins in the native and denatured states and compared these spectra with that of model compounds. They concluded that the spectral shifts observed were best explained by the rupture of hydrophobic bonds on denaturation.

The principle stated above is somewhat difficult to reconcile with the principle of maximum hydrogen bonding (29) which is an important concept in the determination of the structure of crystals of organic compounds and of proteins (30). It is proposed that the following experiments will provide further information as to the relative strengths of the forces involved in satisfying each of these two principles.

It is proposed that block copolymers such as

$$\text{---} \left[\begin{array}{c} \text{HN} - \text{CH} - \text{CO} \\ | \\ \text{R}_1 \end{array} \right]_l \text{---} \left[\begin{array}{c} \text{HN} - \text{CH} - \text{CO} \\ | \\ \text{R}_2 \end{array} \right]_m \text{---} \left[\begin{array}{c} \text{HN} - \text{CH} - \text{CO} \\ | \\ \text{R}_1 \end{array} \right]_n \text{---}$$

be prepared (31) where $l, n \gg m$ and R_1 is a residue whose polypeptide is water soluble, such as glutamic acid and R_2 is the non-polar residue of interest such as isoleucine or valine. Such copolymers would be soluble enough in water that the behavior of a sequence of non-polar amino acid residues required for the reflection point to occur would be between

could be studied in an aqueous environment.

It is proposed that a study of the viscosity and light-scattering properties of an aqueous solution of such a copolymer as a function of the length of the non-polar residue sequence will yield information as to the relative importance of hydrogen and hydrophobic bonds in proteins. Doty, et al (32) have shown that poly-L-glutamic acid exists in an α -helical form in water if the pH is below 5.4. If the length of the non-polar sequence is too short for the formation of a hydrophobic bonding region, the molecule will exist as a rigid rod and the properties of a rigid rod equal in length to the total length of the molecule will be observed in the viscosity and light scattering measurements. On the other hand, if a hydrophobic configuration is more stable than the α -helix configuration for a certain number of non-polar residues in sequence, this would create a hinge point in the rigid rod about which the α -helical end portions of the molecule would be relatively free to rotate. This configuration would behave as a small micelle with two rigid α -helical portions of the polypeptide chain emerging at various angles having lengths approximately half that of the total length of the rigid molecule. This would create an inflection point in the series of viscosity or average particle length measurements for various lengths of the non-polar region of the molecule. I estimate that the length of the non-polar sequence required for this inflection point to occur would be between

2 and 5 non-polar residues. In addition, it would be interesting to vary the polarity of the solvent or to add small amounts of a detergent such as sodium dodecyl sulfate and to repeat the above measurements. As either the polarity of the solvent or the amount of detergent was increased, the minimum length of the non-polar residue sequence required to disrupt the α -helix configuration should decrease due to the greater stability imparted to the micellar region.

References for the Propositions

10. Scatcherd, G., Y. V. Wu, and A. L. Sene, *J. Amer. Soc.*, 92, 613.

References for the Propositions

11. L. Baring, *ibid.*, (1948), 20, 755.

1. Hearst, J. E., and J. Vinograd, Proc. Natl. Acad. Sci. U. S., (1961), 47, 999
2. Perlmann, G. E., and L. G. Longworth, J. Am. Chem. Soc., (1948), 70, 2719
3. Olmstead, E. G., and R. Stone, Biochim. Biophys. Acta, (1961), 49, 265
4. Drabkin, D. L., J. Biol. Chem., (1950), 185, 231
5. Ritland, H. L., P. Kaasberg, and W. Beeman, J. Chem. Phys., (1950), 18, 1237
6. Cited in Vodrazka, Z. and J. Cejka, Biochim. Biophys. Acta, (1961), 49, 502
7. Scatchard, G. and E. S. Black, J. Phys. and Colloid Chem., (1949), 53, 88
8. Benhamou, N., M. Daune, M. Jacob, A. Luzatti and G. Weill, Biochim. Biophys. Acta, (1960), 37, 1
9. Adair, G. S., and M. F. Adair, Proc. Roy. Soc., (1947), A 190, 341
10. Scatchard, G., Y. V. Wu, and A. L. Shen, J. Amer. Chem. Soc., 81, 6104
11. L. Pauling, *ibid*, (1945), 67, 555
12. Bull, H., *ibid*, (1944), 66, 1499
13. Mellon, E. F., A. H. Korn, and S. R. Hoover, *ibid*, (1947), 69, 827; *ibid*, (1949), 71, 2761
14. Cox, D. J. and V. Schumaker, *ibid*, (1961), 83, 2433
15. Scatchard, G. A. C. Batchelder, and A. Brown, (1946), *ibid*, 68, 2320
16. Frederiq, E., Bull soc. chim. Belges, (1956), 65, 960
17. Mommaerts, W. F. H. M., and H. Neurath, J. Biol. Chem., (1950), 185, 909
18. Hughes, W. L., Jr., and R. Straessle, J. Am. Chem. Soc., (1950), 72, 452
19. Killeffer, D. H., and A. Linz, Molybdenum Compounds, (1952), Interscience Pub., New York, N. Y., pp. 42-45

20. Glemser, O., and G. Lutz, *Zeit. Anorg. Allgemeine Chem.*, (1951), 264, 17
21. Klason, P., *Ber. Dtsch. Chem. Ges.*, (1901), 34, 158
22. Wadsley, L., *Rev. Pure Appl. Chem.*, (1955), 5, 165
23. Treadwell, W. D., and Y. Schaeppi, *Helv. Chim. Acta*, (1946), 29, 771
24. Sacconi, L. and R. Cini, *Ann. Chim. (Rome)*, (1953), 42, 706
25. Schriever, K., and R. Toussaint, *Chem. Ber.*, (1958), 91, 2639
26. Kauzmann, W., in Advances in Protein Chemistry, edited by C. B. Anfinsen, Jr., K. Bailey, M. L. Anson, J. T. Edsall, (1959), 14, Academic Press Inc., New York, N. Y. p. 1
27. Tanford, C., P. K. De, and V. G. Taggart, *J. Am. Chem. Soc.*, (1960), 82, 6028
28. Yanari, S. and F. A. Bovey, *J. Biol. Chem.*, (1960), 235, 2818
29. Robertson, J. M., Organic Crystals and Molecules, (1953), Cornell University Press, Ithaca, N. Y., p. 329
30. Pauling, L., R. B. Corey, and H. R. Branson, *Proc. Natl. Acad. Sci. U. S.*, (1951), 37, 205
31. Katchalski, E. and M. Sela, in Advances in Protein Chemistry, edited by C. B. Anfinsen, J., K. Bailey, M. L. Anson, J. T. Edsall, (1958), 13, Academic Press Inc., New York, N. Y., pp. 244-492
32. Doty, P., A. Wada, J. T. Yang, and E. R. Blout, (1957), *J. Polymer Sci.*, 23, 851